

Integrating palaeoproteomics into the zooarchaeological analysis of Palaeolithic bone assemblages

Sinet-Mathiot, V.

Citation

Sinet-Mathiot, V. (2023, March 23). *Integrating palaeoproteomics into the zooarchaeological analysis of Palaeolithic bone assemblages*. Retrieved from https://hdl.handle.net/1887/3577205

Version: Publisher's Version

License: License agreement concerning inclusion of doctoral thesis in the

Institutional Repository of the University of Leiden

Downloaded from: https://hdl.handle.net/1887/3577205

Note: To cite this publication please use the final published version (if applicable).

Chapter Three

Identifying the unidentified enhances insights into hominin subsistence strategies during the Middle to Upper Palaeolithic transition

Virginie Sinet-Mathiot^{1*}, William Rendu², Teresa E. Steele³, Rosen Spasov⁴, Stéphane Madelaine^{5,6}, Sylvain Renou⁷, Marie-Cécile Soulier⁸, Naomi L. Martisius⁹, Vera Aldeias¹⁰, Elena Endarova⁴, Paul Goldberg^{10,11,12}, Shannon J.P. McPherron¹, Zeljko Rezek¹³, Dennis Sandgathe¹⁴, Nikolay Sirakov¹⁵, Svoboda Sirakova¹⁵, Marie Soressi¹⁶, Tsenka Tsanova¹⁷, Alain Turq⁵, Jean-Jacques Hublin^{13, 1}, Frido Welker^{18*}, Geoff M. Smith^{19*}

- 1 Max Planck Institute for Evolutionary Anthropology, Leipzig, Germany.
- 2 ArchaeoZOOlogy in Siberia and Central Asia ZooSCAn, CNRS IAET SB RAS International Research Laboratory, IRL 2013, Institute of Archaeology SB RAS, Novosibirsk, Russia.
- 3 Department of Anthropology, University of California, Davis, Davis, CA, USA.
- 4 Archaeology Department, New Bulgarian University, Sofia, Bulgaria.
- 5 Musée national de Préhistoire, Les Eyzies, France.
- 6 CNRS UMR 5199 PACEA, Université de Bordeaux, Pessac, France.
- 7 HADÈS Agence Atlantique, Bordeaux, France.
- 8 CNRS UMR 5608 TRACES, Université de Toulouse-Jean Jaurès, Maison de la Recherche, Toulouse, France.
- 9 Department of Anthropology, The University of Tulsa, Tulsa, OK, USA
- 10 Interdisciplinary Center for Archaeology and the Evolution of Human Behaviour, Universidade do Algarve, Campus de Gambelas, 8005-139, Faro, Portugal
- 11 School of Earth, Atmospheric and Life Sciences, University of Wollongong, Australia
- 12 Institute for Archaeological Sciences, Eberhard Karls University of Tübingen, Tübingen, Germany.
- 13 Chaire de Paléoanthropologie, CIRB (UMR 7241 U1050), Collège de France, Paris, France.
- 14 Department of Archaeology, Simon Fraser University, Burnaby, British Columbia, Canada.
- 15 National Institute of Archaeology with Museum, Bulgarian Academy of Sciences, Sofia, Bulgaria.
- 16 Faculty of Archaeology, Leiden University, The Netherlands.
- 17 Department of Chemistry G. Ciamician, Álma Mater Studiorum, University of Bologna, Via Selmi 2, Bologna, Italy
- 18 Globe institute, University of Copenhagen, Copenhagen, Denmark.
- 19 School of Anthropology and Conservation, University of Kent, Canterbury, UK.

Under review at Archaeological and Anthropological Sciences.

Abstract

Understanding Palaeolithic hominin subsistence strategies requires the comprehensive taxonomic identification of faunal remains. The high fragmentation of Late Pleistocene faunal assemblages often prevents proper taxonomic identification based on bone morphology. It has been assumed that the morphologically unidentifiable component of the faunal assemblage would reflect the taxonomic abundances of the morphologically identified portion. In this study, we analyse three faunal datasets covering the Middle to Upper Palaeolithic transition (MUPT) at Bacho Kiro Cave (Bulgaria), and Les Cottés and La Ferrassie (France) with the application of collagen type I peptide mass fingerprinting (ZooMS). Our results emphasise that the fragmented component of Palaeolithic bone assemblages can differ significantly from the morphologically identifiable component. We obtain contrasting identification rates between taxa resulting in an overrepresentation of morphologically identified reindeer (Rangifer tarandus) and an underrepresentation of aurochs/bison (Bos/Bison) and horses (Equus) at Les Cottés and La Ferrassie. Together with an increase in the relative diversity of the faunal composition, these results have implications for the interpretation of subsistence strategies during a period of possible interaction between Neanderthals and anatomically modern humans in Europe. Furthermore, shifts in faunal community composition and in carnivore activity suggest a change in the interaction between humans and carnivores across the MUPT, and indicate a possible difference in site use between Neanderthals and anatomically modern humans. The combined use of traditional and biomolecular methods allows (zoo)archaeologists to tackle some of the methodological limits commonly faced during the morphological assessment of Palaeolithic bone assemblages.

Introduction

The investigation of behavioural shifts in prey selection and hunting strategies during phases of major changes in the material record is key to understanding the relationship between human behavioural evolution, cultural variation, and population dynamics (Delagnes & Rendu, 2011; Discamps et al., 2011; Niven et al., 2012; Rendu et al., 2012; Steele, 2004). Traditionally, such behavioural patterns have been approached through the analysis of the stone tools and faunal remains recovered from excavations at Palaeolithic sites. In particular, faunal specimens provide the opportunity to identify and document behaviour developed by human populations for the exploitation of their environment (Gaudzinski & Roebroeks, 2000; Gaudzinski-Windheuser et al., 2014; Morin, 2012; Pederzani et al., 2021; Smith et al., 2021; Stiner, 1993). However, studying ancient fauna not only provides paleoenvironmental information, but when combined with the analysis of bone surface modifications related to

human activity, it can fine-tune the timing of human occupations and helps to reconstruct human diet and interactions with other groups or even species (Steele, 2015). Indeed, faunal exploitation is related to a wide range of behaviours and cognitive aspects entwined with mobility, social organisation, technological development and subsistence capacities (Marean & Assefa, 1999).

However, Late Pleistocene bone assemblages are often highly fragmented, preventing proper taxonomic identification and anatomical attribution of many specimens based on morphology alone (Lyman, 2002; Morin et al., 2017a). Several processes affect faunal remains, starting from decomposition, selective destruction in the sediment, post mortem transport and burial, to preserved bone specimens that are potentially altered during excavation, cleaning treatment, and storage (Lyman & Lyman, 1994; Marean, 1991). All these factors, geological, biological, and cultural, can lead to variability in faunal identification. Together with differential preservation, they can create a potential source of bias for the interpretation and quantification of relative abundances of taxa (Dirrigl, 2002; Marean, 1991; Marean & Kim, 1998; Morin, 2004; Morin et al., 2017a, 2017b; Pickering et al., 2006). Indeed, combined with the impact of human and carnivore activities at the site, these factors contribute to reduced proportions of taxonomically diagnostic bones resulting in a lower number of identifiable specimens. Such processes generate the potential to seriously distort various archaeological and ecological inferences (Faith, 2007; Morin et al., 2017a).

Recent developments of biomolecular methods allow us to exploit the collagen preserved in these bone fragments to taxonomically identify faunal specimens (Buckley et al., 2009). The inclusion of the analysis of highly fragmented bone through proteomic screening using zooarchaeology by mass spectrometry (ZooMS) for the taxonomic assessment of Palaeolithic faunal assemblages has already demonstrated its great potential (Berto et al., 2021; Brown, Wang, et al., 2021; Buckley et al., 2017; Pothier Bouchard et al., 2020; Ruebens et al., 2022; Sinet-Mathiot et al., 2019; Welker et al., 2015) and highlighted the necessity to use a multimethodological approach in studying human subsistence. Taxonomic identities from both the morphologically identified and the ZooMS identified components can thus be correlated with bone surface modification analysis to address specimen surface preservation and bone accumulation agents through the reconstruction of taphonomic history. The analysis of collagen protein type I provides a taxonomic identity based on the variation in protein amino acid sequence and allows the taxonomic identification of bone assemblages to be extended to the morphologically-unidentifiable component. The previous application of ZooMS as a screening tool for faunal assemblages has provided variable results in terms of the comparability of the two components. Taxonomic abundances of the morphologically unidentifiable component of a faunal assemblage may not generally differ from the morphologically identifiable component (Berto et al., 2021; Buckley et al., 2017; Welker et al.,

2016, 2017), but that does not necessarily indicate a pattern (Ruebens et al., 2022; Sinet-Mathiot et al., 2019). Moreover, such differences could reflect a specific human behavioural signature related to bone fragmentation and intensity of carcass processing (Sinet-Mathiot et al., 2019). A better understanding of the source(s) of variability will help in anticipating the potential differences that may occur within certain bone assemblages.

The zooarchaeological literature frequently contains body size class attributions of bone specimens that cannot be reliably assigned to a particular taxon or clade. It is generally assumed that these body size class attributions are reliable and reflect or contain taxonomic information about the bone assemblage as a whole. However, previous ZooMS research has highlighted that this is a potentially unreliable approach (Sinet-Mathiot et al., 2019). Here we test the fragmentary component of bone assemblages of three Late Pleistocene sites: Bacho Kiro Cave (Bulgaria), Les Cottés and La Ferrassie (France). They all show rich and wellpreserved stratigraphic sequences spanning the Middle to Upper Palaeolithic transition (MUPT). These sites offer the opportunity to discuss diachronic changes in subsistence strategies during the period of possible interaction between Neanderthal and Late Pleistocene Homo sapiens populations (Hajdinjak et al., 2021; Higham et al., 2014; Hublin, 2015; Hublin et al., 2020; Prüfer et al., 2021). This work explores the implications of incorporating the analysis of the morphologically unidentifiable bone component into the description of faunal assemblages in terms of both overall bone accumulation and aims to advance our interpretation of human subsistence strategies during the MUPT. We address methodological limits commonly faced during the morphological assessment of faunal assemblages and demonstrate how the addition of biomolecular methods, such as untargeted ZooMS screening, can complement our understanding of subsistence behaviour by providing a clearer picture of prey selection and site occupation. By including assemblages that span the MUPT in Europe, we are thereby able to demonstrate that the assessment of the fragmented component of bone assemblages through ZooMS can provide different patterns of species frequencies than previously interpreted based solely on the morphologically identifiable record.

Material and Methods

Sample selection

This study includes the ZooMS analysis of bone material from three Late Pleistocene sites (Bacho Kiro Cave, Les Cottés and La Ferrassie; SI Figure 1, SI Table 1). All the material taxonomically identified through bone morphology by zooarchaeologists will be referred to as the morphology component. Similarly, all fragmentary specimens morphologically unidentifiable and taxonomically identified through ZooMS will be referred to as the ZooMS component. All three sites were recently excavated and have provided large, well-contextualised and highly fragmented bone assemblages of individually piece-provenienced

faunal remains. Bone surface analyses of both the morphologically identified and the fragmentary unidentifiable bone assemblages were assessed using comparable zooarchaeological methods and protocols. All faunal data were derived from recent excavation campaigns, and specimens from both the morphology and ZooMS components show similar spatial distributions over the excavated areas. Fragmentary and morphologically unidentifiable piece-provenienced specimens, generally >2 cm in length, were selected for proteomic analysis. Bone material resulting from sediment sieving during the excavation of the archaeological sites are not included in this study. All morphologically unidentifiable piece-provenienced specimens from the La Ferrassie layer 6 faunal assemblage were selected for ZooMS analysis. In the case of Bacho Kiro Cave and Les Cottés, specimens were randomly selected from among the unidentifiable components of the bone assemblages defined by the zooarchaeologists.

Bacho Kiro Cave

Bacho Kiro Cave (Dryanovo, Bulgaria) is located on the northern slope of the Balkan mountain range (Stara Planina) and about 70 km south of the Danube River. Previously investigated during the 20th century (Garrod et al., 1939; Kozłowski & Ginter, 1982), the site was reopened for excavation in 2015 by the National Archaeological Institute with Museum from the Bulgarian Academy of Sciences (Sofia, Bulgaria) and the Max Planck Institute for Evolutionary Anthropology (Leipzig, Germany). The archaeological sequence spans the Middle Palaeolithic (MP) through to the Upper Palaeolithic (UP). The archaeological material recovered from two sectors (Main Sector and Niche 1) from Layers I and J was recognized as part of the Initial Upper Palaeolithic marked by the earliest occurrence of Late Pleistocene Homo sapiens in Europe (Hublin et al., 2020). This starts around 45,990 cal BP in the upper part of Layer J and considerably intensifies in Layer I which is dated to 45,040-43,280 cal BP (Fewlass et al., 2020; Pederzani et al., 2021). This material comprises the earliest and largest number of Homo sapiens bone tool and ornament assemblages in Europe, partly taxonomically identified through ZooMS (Martisius et al., 2022). The assemblage recovered from Layer K was technologically associated with the MP and was deposited between 61 ± 6,000yr and 51,000 yr BP (Fewlass et al., 2020; Pederzani et al., 2021). We investigated 1,595 faunal remains through ZooMS from Layer I (814 specimens), Layer J (438 specimens) and Layer K (343 specimens) from both the Niche 1 and the Main Sector (Hublin et al., 2020). Zooarchaeological analysis was performed on 7,013 faunal remains from Layers I, J and K from both sectors following previously described methodology (Smith et al., 2021) and including 1,453 specimens assigned to a taxonomic group (1,077 from Layer I, 232 from Layer J and 143 from Layer K).

Les Cottés

Les Cottés (Vienne, France) is a cave located in the corridor between the Parisian basin and the Poitou in west-central France. The site was discovered in 1878 and was explored through several excavation campaigns (Bastin et al., 1976; Lévêque, 1997; Pradel, 1967), but the material included in this study derive from an excavation initiated in 2006 by M. Soressi with support of the French Ministry of Culture and Communication and the Max Planck Institute for Evolutionary Anthropology (Soressi et al., 2010), Through ZooMS, we analysed 523 morphologically unidentifiable faunal specimens, which, together with the 152 presented in Welker et al. 2015 (137 undiagnostic fragments, and 15 specimens analysed in a ZooMS blind test), means 675 specimens from Les Cottés were analysed with ZooMS. Of these, 220 are from the Mousterian (US08, dated between 46.051 to 42.034 cal BP using radiocarbon and between 55 and 48 ka according to the OSL measurements (Jacobs et al., 2015)), 217 are from the Châtelperronian (US06, dated between 42,961 to 40,344 cal BP), 168 are from the Protoaurignacian (US04 lower) and 70 are from the Early Aurignacian (US04 upper). The dates for the Aurignacian layers extend from 40,372 to 36,697 cal BP (Talamo et al., 2012) in radiocarbon years, or from 43 to 36 ka in OSL years (Jacobs et al., 2015). Interpretations coming from US04 upper are considered with caution due to the low number of specimens in comparison to the other layers. Bone surface analysis was standardised over the assemblage and was previously described elsewhere (Rendu et al., 2019). Of a total of 5,169 bone remains assessed through traditional zooarchaeology, 1,922 bone and dental specimens were morphologically identified in the range of subfamily to species (397 specimens from US08, 166 from US06, 715 from US04 lower and 629 from US04 upper).

La Ferrassie

The Grand Abri of La Ferrassie (Savignac-de-Miremont, France) is in the Dordogne region of south-western France in a tributary valley to the Vézère River and was first excavated during the 20th century by Capitan and Peyrony and then by Delporte (Delporte & Delibrias, 1984; Peyrony, 1934). An excavation conducted from 2010 to 2015 by Turq and colleagues further refine the stratigraphic sequence spanning the MUPT (Guérin et al., 2015; Turq et al., 2012). The Châtelperronian layer (Layer 6) was dated to between 45,100 and 39,520 cal BP (Talamo et al., 2020) marking the earliest appearance of this lithic industry in the region. The faunal material from this layer that was morphologically identifiable to taxon is limited to 17.5% of the bone assemblage (142 specimens) and is dominated by reindeer (*Rangifer tarandus*). All piece-plotted, morphologically indeterminate specimens were processed through ZooMS (527 specimens).

ZooMS methodology

ZooMS extraction protocols employed for this study were partially described previously (Buckley et al., 2009; van Doorn et al., 2011; Welker et al., 2016). All 2,645 specimens were sampled (10-30 mg) using pliers and placed into 96-well plates. Soluble collagen was extracted through incubation in 100µl of 50mM ammonium-bicarbonate (AmBic) buffer at 65°C for one hour. In order to improve and verify the taxonomic identity obtained from soluble collagen, 440 specimens (70 for La Ferrassie, 369 for Les Cottés and 1 for Bacho Kiro Cave) (SI Table 2) were demineralised in 130µl 0.6M HCl at 4°C for 18-20 hours, neutralised to pH 7, and solubilised again in AmBic. Then 50µl of the resulting supernatant was digested using trypsin (0.5µg/µl, Promega) overnight at 37°C, acidified using trifluoroacetic acid (20% TFA), and then cleaned on Hypersep C18 96-well plates (Thermo Scientific) using a vacuum manifold. In short, a 96-well deepwell plate (Eppendorf) is placed beneath the Hypersep plate to collect the solutions. C18 filter tips from the Hypersep plate were conditioned with 200µL of 0.1% TFA in 50:50 acetonitrile and UHQ water (conditioning solution) and washed with 200µL of 0.1% TFA and UHQ water (washing solution). Peptide extracts were then vacuumed through the filters slowly to ensure optimal binding efficiency. The obtained waste solution was discarded. Filters were then washed again with 200µL of washing solution and peptides were extracted in 100µL of conditioning solution and transferred to a 96-well plate. Digested peptides were spotted in triplicate on a MALDI Bruker plate with the addition of α-cyano-4hydroxycinnamic acid (CHCA, Sigma) matrix, using a multichannel pipette (Thermo Fisher). MALDI-TOF-MS analysis was conducted at the Fraunhofer IZI in Leipzig (Germany), using an autoflex speed LRF MALDI-TOF (Bruker) in reflector mode, positive polarity, matrix suppression up to 590 Da and collected in the mass-to-charge range 700-3500 m/z. Triplicates were merged for each sample in R version 4.0.5 (R Core Team, 2021, n.d.) and MALDIquant v. 1.21 (Gibb & Strimmer, 2012). First, we smooth the intensity using a moving average and remove the baseline using the TopHat approach. Then, for each sample we align the replicate spectra using SuperSmoother and a signal to noise ratio of 3, sum the three replicates to obtain a single spectrum, and remove the baseline once more, again using TopHat. Spectra were exported as .msd files. Taxonomic identifications were made using mMass (Strohalm et al., 2010) through manual peptide marker mass identification in comparison to a database of peptide marker series for all European Pleistocene medium- to large-sized mammals (Welker et al., 2016). To assess any potential contamination by non-endogenous peptides, we performed laboratory blanks alongside the samples. These remained empty of collagenous peptides, excluding the possibility of modern laboratory or storage contamination.

Peptide marker series can be similar for some closely related species, which is the case for the species belonging to the following taxonomic groups: *Bos/Bison*, Cervid/Saiga, Equidae and Ursidae. Cervid/Saiga can be attributed to either *Cervus elaphus* (red deer), *Megaloceros*

giganteus (giant deer), Alces alces (elk) or Dama sp. (fallow deer). Equidae and Ursidae include, respectively, species from the genera Equus and Ursus, most likely Equus ferus and Equus hydruntinus or Ursus spelaeus and Ursus arctos. In order to facilitate the comparison between ZooMS and morphology components, the most common species and taxa were grouped into broader categories of: Bos/Bison (Bos primigenius, Bison priscus and Bos/Bison sp.), Cervid/Saiga (C. elaphus, D. dama, M. giganteus), Ursidae (U. arctos, U. spelaeus and Ursus sp.), Capra sp. (C. ibex and Capra sp.), and Equidae (E. ferus, E. hydruntinus and Equid sp.). At Bacho Kiro Cave, due to the high proportion of this taxonomic group, cervid specimens from the morphology component were also included into the broader group Cervid/Saiga alongside the few specimens identified as Rangifer tarandus and Capreolus capreolus. Within the ZooMS component, the few specimens identified as Cervid/Saiga, in order to allow the comparability of both components.

Suggested as an indicator of collagen preservation (Welker et al., 2017; Wilson et al., 2012), glutamine (Gln) deamidation ratios were calculated on all samples for peptide COL1α1 508-519 (Brown, Douka, et al., 2021), which is frequently observed in peptide fingerprints of collagen type I, following published protocols (van Doorn et al., 2012; Wilson et al., 2012). The deamidation ratio ranges from %Gln=1.0 with non-deamidated glutamines to %Gln=0.0 indicating a full deamidation of the glutamines. The Gln deamidation ratios obtained during routine ZooMS screening have been previously suggested to assess bone assemblage homogeneity (spatial and temporal variability within a site), to detect stratigraphic outliers (intrusive material or differential bone preservation), to inform on the preservational quality of specific peptides and specimens, or to look at the taxonomic distribution from a biomolecular perspective (Sinet-Mathiot et al., 2019; Welker et al., 2017; Wilson et al., 2012), although with varying success (Brown, Wang, et al., 2021).

Zooarchaeological methodology

All taphonomic modifications were recorded on the morphology- and ZooMS-identified specimens by the respective zooarchaeologists, consistently within and between studied sites. Bone surfaces for both the morphologically identified and unidentified components were assessed through visual inspection, using magnification when needed (up to 20x magnification) (Blumenschine et al., 1996). The maximum length of the bone specimens was measured individually with digital calipers.

Although traces of burning were recorded during taphonomic analyses using the scale proposed by Stiner and colleagues (Stiner & Kuhn, 1995) (0: Unburnt to 6: Completely calcined), these burnt remains were excluded from subsequent ZooMS analyses due to poor collagen preservation. Weathering stages were recorded for all bones and provide a qualitative scale for understanding the exposure (short/long duration) of the bones prior to

burial (Behrensmeyer, 1978). A slightly modified scheme was used on Les Cottés bone assemblages where specific modifications were recorded related to weathering (see Rendu et al., 2019). Specifically, weathering was recorded according to three variables: exfoliation (the peeling of bone surface), cracking (the emergence of longitudinal cracks on bone surface), and disintegration (the complete destruction of the bone). In addition, other recorded modifications included root etching and abrasion (expressed as a percentage of bone surface affected). The schemes range from 0% (no visible modification observed) through 100% (the whole bone surface covered; (Smith et al., 2021; Behrensmeyer, 1978; Blumenschine et al., 1996; Domínguez-Rodrigo et al., 2017; Fisher, 1995; Lee Lyman, 1994; Olsen & Shipman, 1988; Soulier & Costamagno, 2017).

For all three bone assemblages, human modifications included traces related to butchery and carcass processing (cut marks, scraping marks, chop marks, marrow bone breakage), and carnivore modifications included tooth marks, gnawing traces and damage from bone breakage and digestion as well as rodent tooth traces. The number of identified specimens (NISP) represents the number of specimens assigned to a taxon.

When it was not possible to morphologically assign fragmentary bone specimens to a specific taxon, these were assigned to a specific body size class based on previous assignments (SI Table 3; Morin, 2012). The separation of specific taxa into different body size classes was normally done on the basis of both body and skeletal size (following (Morin, 2012; Rendu et al., 2019; Smith et al., 2021)).

The combination of the ZooMS and morphology component allows for the assessment of skeletal element distributions and the possible identification of previously unrecognised skeletal elements, which has implications for our understanding of hunting strategies and carcass transport. As skeletal elements were identified, when possible, on taxonomically unidentifiable specimens, we aimed to correlate the skeletal part identifications with the ZooMS taxonomic identities in order to assess skeletal representation among both the morphology- and ZooMS-identified components. To assess skeletal element representation for the dominant taxa within each component, bone elements were categorised into body parts for each method of identification (cranial: cranium, mandible; axial: vertebrae, pelvis, rib; forelimb: humerus, radius, ulna; hindlimb: femur, tibia; distal limbs: carpals, metacarpal, tarsals, metatarsal, phalanges; LBN: long bone fragments, FBN: flat bone fragments) (based on Stiner, 1991a, 1991b). Within all three datasets, teeth and antler were categorised separately from the cranial body part, as their inclusion might bias the comparison between components. Indeed, antlers and horn cores tend to be rare and are more easily identified morphologically, reducing their representation in the ZooMS component. Anatomically unidentifiable specimens (NID) were excluded from the assessment of skeletal element representation as they did not provide substantial information.

Ecological diversity indices were calculated in order to investigate the effect of the addition of the ZooMS-identified specimens on the diversity of the faunal community of each layer and site. We used the Shannon-Wiener Index (H') (Shannon, 1948) (R package *vegan* v. 2.6-2, Oksanen et al., 2019) to quantify the taxonomic diversity of our three faunal assemblages among each component, taking into account the taxonomic richness and the distribution of their abundance. As the Shannon-Wiener index is sensitive to sample size, values should be considered with caution when the sample size is small. Along with species richness, Pielou's evenness (J') measures taxonomic diversity by giving the count of individuals of each taxonomic group among each component and reflecting the evenness of the distributed abundances between taxa. The index value ranges from 0 (no evenness) to 1 (complete evenness).

Results

ZooMS analysis

ZooMS analysis of all three datasets shows well-preserved collagen type I with a high success rate of taxonomic identification, up to the range of subfamily or genus, between 90% and 97% (SI Table 1). For 82% of the samples, the semi-destructive extraction protocol (AmBic) is sufficient to obtain a ZooMS identification. At Bacho Kiro Cave, collagen preservation is excellent (also noted by Fewlass et al., 2020) resulting in a high proportion of distinct taxonomic identities. All ZooMS samples could be extracted using only the AmBic protocol, while we extracted one specimen through acid demineralization as well to verify its taxonomic identity (*Castor fiber*). At both Les Cottés and La Ferrassie, samples were processed using both AmBic and acid demineralisation protocols to improve and optimise taxonomic identifications (SI Table 1).

<u>Deamidation between stratigraphic units and taxa:</u>

Glutamine deamidation ratios are calculated in order to detect potential intrusive material between archaeological layers or differential collagen preservation between taxa. Because the data is not normally distributed (Shapiro-Wilk normality test, p-value < 0.05), we used Wilcoxon-Mann-Whitney tests to compare the glutamine deamidation ratios between taxa and layers. At Bacho Kiro Cave, we observe that older samples from Layer K show elevated levels of deamidation with values significantly different between layers (SI Table 4, SI Figure 2). In contrast, we note overlapping deamidation values between layers at Les Cottés (SI Figure 3) with the exception of US06 which showed values significantly different from US04 Lower and US08 (SI Table 4). Glutamine deamidation ratios seem to overlap between dominant taxa which would suggest that they have undergone similar molecular diagenetic processes within each site (SI Figure 4). However, a few exceptions could be

identified. At Bacho Kiro Cave, deamidation ratios show similarities between taxa, particularly within layer K, but ursid specimens tend to have glutamine deamidation values significantly different from other taxa in layers I and J, notably in comparison with *Bos/Bison*, *Capra* sp. and Equidae (SI Table 5). At Les Cottés, all taxonomic groups show similar deamidation ratios within each layer, except for a few *Rangifer tarandus* specimens (n = 6) showing deamidation values significantly different from Equidae in US04 Lower (Wilcoxon-Mann-Whitney tests, statistic = 64, p-values = 0.013, SI Table 5). At La Ferrassie, *Rangifer tarandus* and Cervid/Saiga specimens show deamidation values significantly different from *Bos/Bison* (SI Table 5). The statistical differences observed between some of the taxonomic groups and layers could be driven by discrepancies in sample sizes, taphonomic history and site formation or butchery practices. However, further exploration is required in order to interpret these differences.

Taxonomic representation

Species representation among both ZooMS and morphology components are generally consistent within each site, but the addition of ZooMS permits the identification of taxa that were unrecognisable through morphology. At Les Cottés, ZooMS identified Felidae and Ursidae in the faunal community obtained from US06, but also resulted in the addition of Cervid/Saiga in US04 Lower (SI Table 6). At Bacho Kiro Cave, the ZooMS analysis allowed for the identification of Elephantidae in Layer J (SI Table 7). At La Ferrassie, the use of ZooMS results in a 4-fold increase of the number of taxonomically identified specimens. Consequently, the taxonomic diversity for this layer was broadened, with the addition of *Capra* sp., Rhinocerotidae, Ursidae and several carnivores (SI Table 8).

Shannon-Wiener index calculations show that the diversity of the faunal community identified on a site can significantly change with the addition of ZooMS. More specifically, we observe an increase in the faunal diversity of the combined ZooMS and morphology components in the layers under study here at La Ferrassie, at Les Cottés and at Bacho Kiro Cave (Figure 1, SI Table 9). In contrast, the lower values of the Shannon-Wiener index, after the addition of ZooMS identities to the Layer I faunal assemblage, at Bacho Kiro Cave indicate a lower taxonomic diversity. Such a pattern possibly emphasises a better identification rate within the morphology component related to a larger sample size, or highlights a higher evenness of the ZooMS component due to the repeated identification of taxa showing a low abundance among the morphology component.

The occurrence of the dominant taxa, i.e. the taxa showing the highest proportions, among both components are consistent within each site (Bacho Kiro Cave: Ursidae, Equidae, Cervid/Saiga, Capra sp. and Bos/Bison; Les Cottés: Bos/Bison, Equidae and Rangifer tarandus; La Ferrassie: Bos/Bison, Cervid/Saiga, Equidae and Rangifer tarandus), but we

observe differences in their relative contributions to the overall bone assemblage (Figure 2). At Les Cottés and La Ferrassie, the ZooMS component indicates lower proportions of reindeer, offset by higher proportions of Bos/Bison and Equidae (SI Table 6, 8 and 10). We note a 9-fold increase in the proportion of Bos/Bison at La Ferrassie. At Les Cottés, we observe an on average 2-fold increase of Bos/Bison and Equidae with the addition of ZooMS to the analysis of the faunal assemblage. At Bacho Kiro Cave, and similar to Les Cottés and La Ferrassie, Bos/Bison remains are slightly more abundant within the ZooMS component, particularly in Layers I and J. Conversely, Ursidae show a similar pattern as reindeer at La Ferrassie and Les Cottés with slightly lower proportions notably in Layers J and K. We note a large difference between methods of identification for Cervid/Saiga in Layer I, but these differences are not consistent throughout the other layers. When comparing the faunal composition between layers to assess any changes or shifts in the NISP of different taxa across the MUPT, we note at Les Cottés a progressive decrease in the proportions of Bos/Bison offset by an increase of Equidae from US08 to US04, which is particularly clear through the use of ZooMS. Despite the low number of specimens analysed through ZooMS from the Early Aurignacian layer (US04 upper) of Les Cottés, the results obtained show a continuous pattern with those from the layers below in terms of taxonomic abundances between the dominant taxa.

While the categorisation of morphologically unidentifiable specimens into body size classes remains a useful tool when no other alternative is available for the interpretation of this component of the assemblage, the correlation between taxonomic identifications provided by ZooMS with the body size classes indicates inconsistencies. Therefore, the observations made previously at Fumane Cave therefore do not seem to be an exception, but rather the norm (Martisius et al., 2020; Sinet-Mathiot et al., 2019). We observe inconsistencies between body size class attributions, which are largely based on bone size and cortical thickness, and ZooMS taxonomic assignments (SI Table 3). For example, Ursidae specimens are present in most carnivore and ungulate body size class units (Figure 3), several equid specimens are categorised among the large carnivore class, and Caprinae and Capra sp. among the large ungulate class (Figure 3). Although many zooarchaeologists are already using alternative nomenclatures (i.e. mammal classes or unknown instead of ungulate or carnivore classes (Castel, 2011)), or standardisation tools (Discamps, 2021), these results simply confirm that body size class attributions should be used with caution, especially when translating these classes to more specific taxonomic units and/or assessment of hominin subsistence strategies. When assigning bone specimens to generalised family attributions, one should cautiously avoid "taxonomic blindness" based on presumed abundance of cladistic assignments that are based on the thickness of the cortical bone.

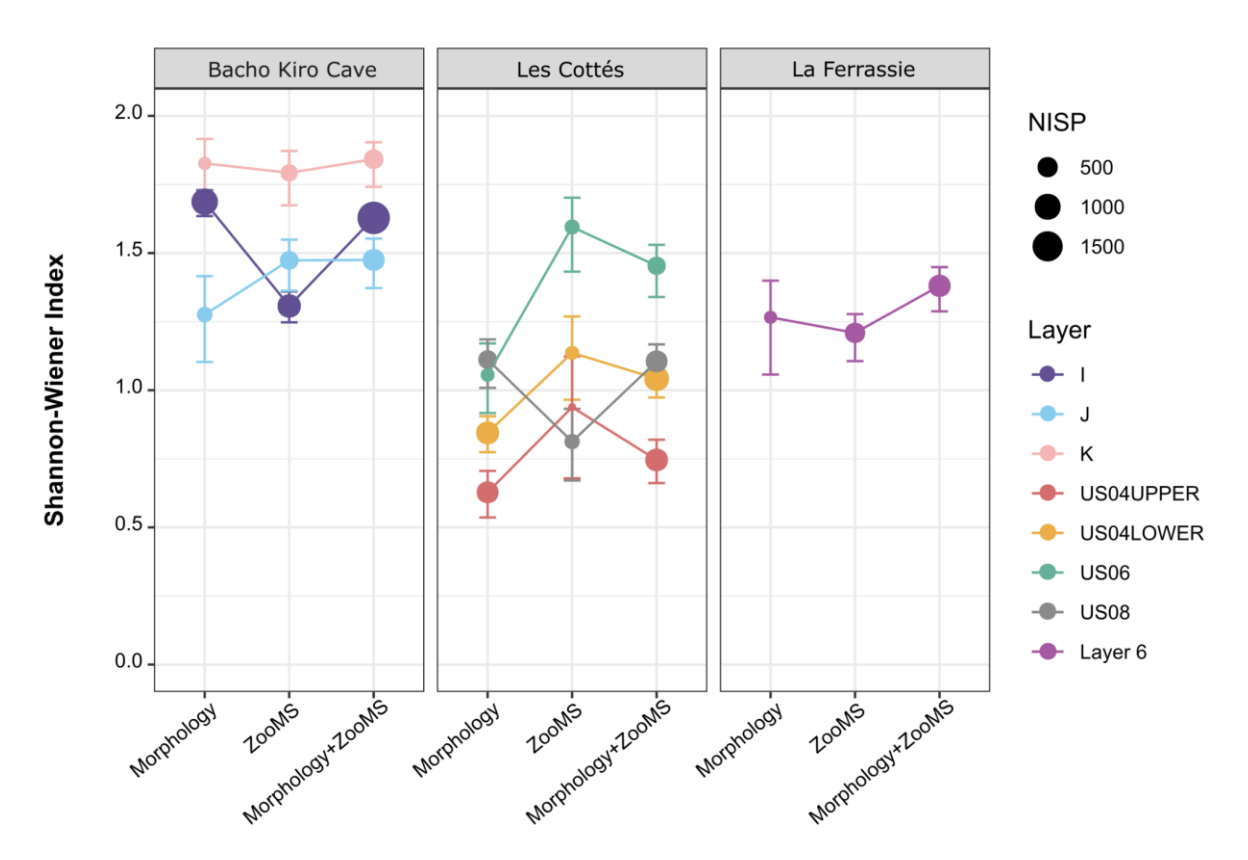


Figure 1: Shannon-Wiener Index for each studied layer of Bacho Kiro Cave, Les Cottés and La Ferrassie compared between methods of taxonomic identification (see SI Table 9 for details). Confidence intervals (2.5%-97.5%) are given for each value.

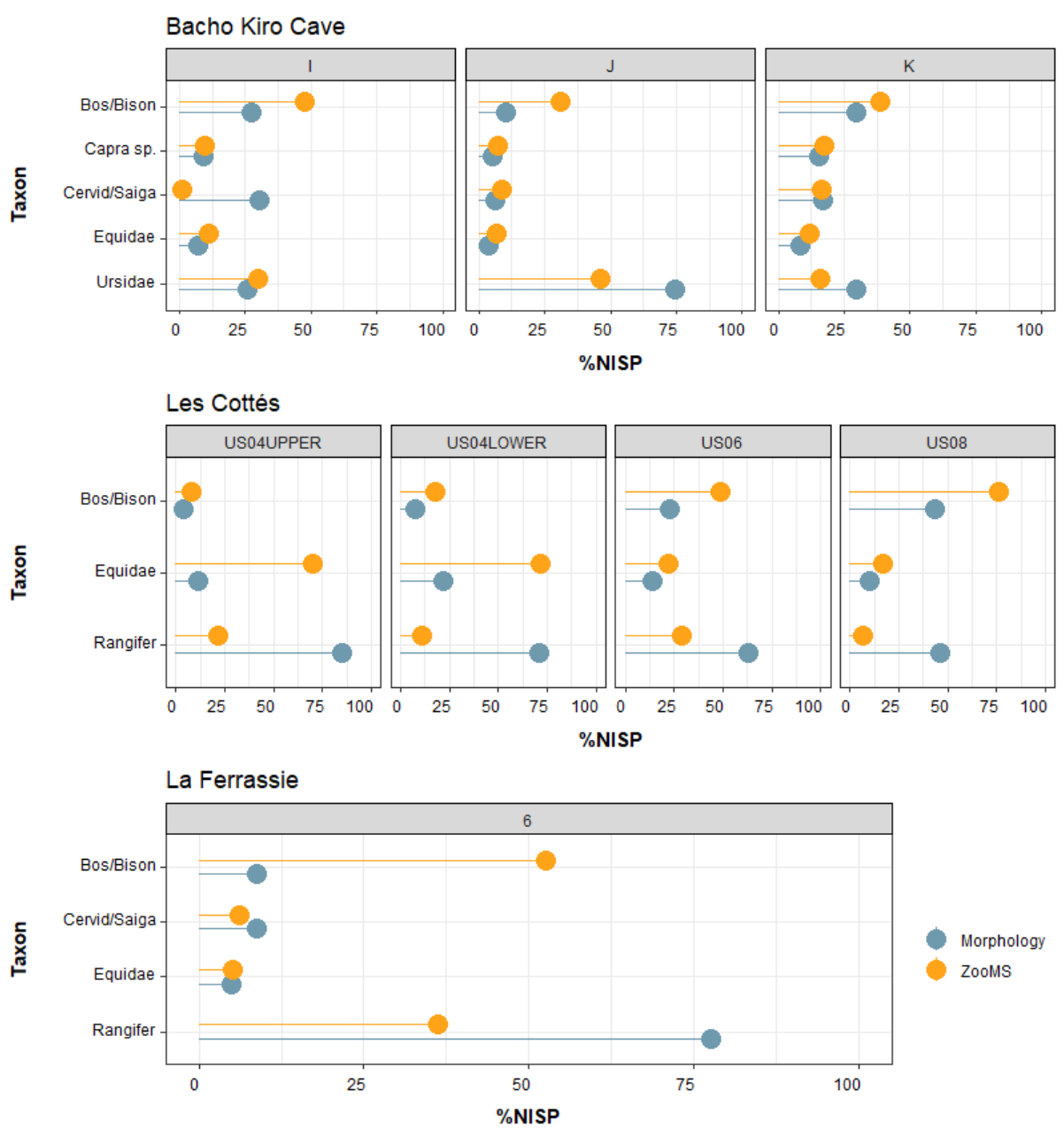


Figure 2: Percentage of the dominant taxa among both ZooMS and morphology components at Bacho Kiro Cave, Les Cottés and La Ferrassie.

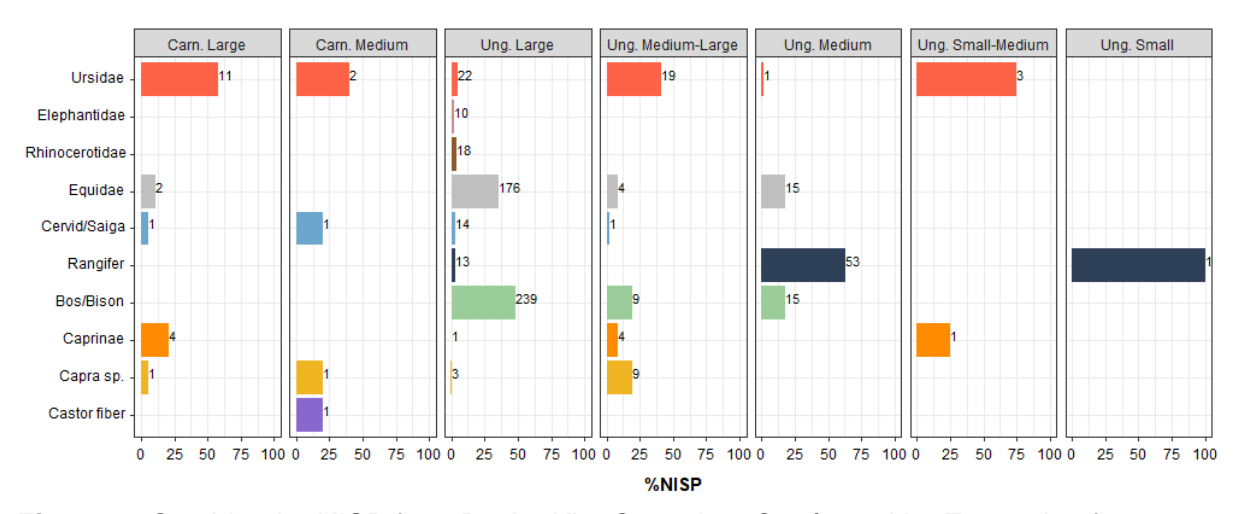


Figure 3: Combined %NISP from Bacho Kiro Cave, Les Cottés and La Ferrassie of taxa identified using ZooMS (rows) and morphology (column headings) in relation to their body size class attribution. Carn=Carnivore and Ung=Ungulate. Each taxon is assigned a colour to help the visualisation of the graph. Numbers on the bars are the NISP per category.

Bone length distribution

As expected, larger bone fragments are generally more identifiable through comparative morphology as they often preserve more morphologically distinctive features. Smaller fragments tend to be identifiable only through ZooMS (Figure 4). This pattern is particularly noticeable at Bacho Kiro Cave in Layers I and K (SI Figure 5). However, this is not the case for all taxa. We note a different specimen length distribution between both ZooMS and morphology components among dominant taxa. At Bacho Kiro Cave, Bos/Bison, Cervid/Saiga and Equidae specimens show an opposite bipolar distribution of their specimen length whereas the two distributions are more similar for Capra sp. and Ursidae. Because the data is not normally distributed (Shapiro-Wilk normality test, p-value < 0.05), we used Wilcoxon-Mann-Whitney tests to compare the bone length distribution between taxa, layers and method of identification. Bone specimens identified as Capra sp. and Ursidae through ZooMS show a fragment length distribution significantly different from other taxonomic groups particularly in layer I (SI Table 11). Likewise, observations of the bone assemblage from Les Cottés indicate a similar trend with Bos/Bison and Equidae most often exhibiting opposite distributions, compared to the similar distributions of both ZooMS and morphology components for the reindeer specimens (SI Figure 6). At Les Cottés, the bone length distribution of specimens identified morphologically as reindeer are significantly different from the Bos/Bison and of Equidae distributions in US04 and US08 (SI Table 12), but no differences are observed among the ZooMS component. When comparing the distribution between methods of identification, we also note significant differences for Bos/Bison and equid specimens in US04 and US08 (SI Table 13). The absence of metric measurements on the morphologically identified component from La Ferrassie prevents comparisons of bone length distribution between the ZooMS and morphological components. However, the ZooMS component represents 82.5% of the faunal assemblage, so a comparison of specimen length between dominant taxa for the ZooMS component is possible. Although specimens from the dominant taxa generally show similar length distributions, with a large proportion within the 2-3 cm range, equid bones tend to have fewer large fragments illustrated by a higher proportion of specimens within the smaller size classes (SI Figure 7). Equid fragments identified through ZooMS present a length distribution significantly different from *Bos/Bison*, Cervid/Saiga and reindeer (SI Table 14), most likely due to an over-representation of equid fragments of 2-3 cm counterbalanced by an under-representation of specimens of 3-4 cm. Nevertheless, it should be noted that Equidae is the taxa with the smallest sample size, which might influence these results.

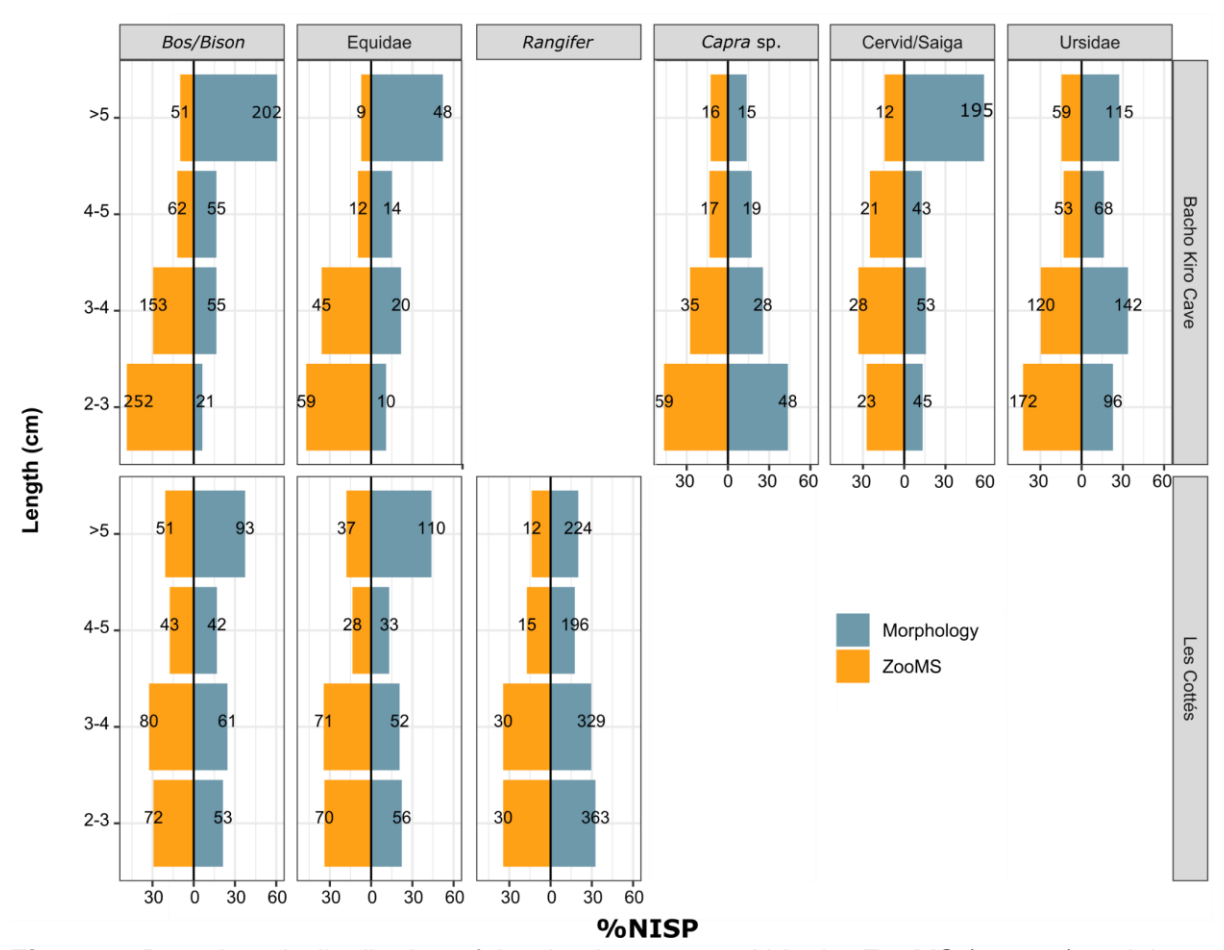


Figure 4: Bone length distribution of the dominant taxa within the ZooMS (orange) and the morphology (blue) component for all studied layers at the sites of Bacho Kiro Cave and Les Cottés. Numbers on the bars are the NISP for each size class.

Bone surface modification analysis

Bone surface preservation:

We investigated readability of the bone surfaces to rule out bone fragmentation related to environmental taphonomic factors. We find that, at Bacho Kiro Cave and La Ferrassie, the bone surfaces of specimens taxonomically identified both through ZooMS and morphology are only affected by low degrees of surface weathering, which cannot explain the differences in fragmentation between taxa and/or layers (SI Table 15 and 16).

Due to high stages of weathering at Les Cottés, many bone surfaces from the ZooMS component exhibit natural fractures. In particular, a large percentage of *Bos/Bison* fragments, from US06 and US08 and equid specimens in US04 indicate multiple types of surface damage (SI Figure 8). These patterns are also recorded on reindeer at a high percentage (>50% for US04 and US06) within the morphology component. The readability of the surfaces, which reflects how bones were affected by weathering or other factors possibly leading to fragmentation, is generally better for the reindeer specimens compared to bones from *Bos/Bison* and equids (SI Figure 9).

Bone assemblage accumulator:

We investigated bone modifications associated with carnivore and human activity to identify the accumulation agents of the bone assemblage. We find that, within all three sites, ZooMS analysis allows for improved association of taxonomic identity with taphonomic data, which in several cases provides additional behavioural information. Overall, the inclusion of ZooMS identifications within zooarchaeological analyses highlights a diverse range of taxa exhibiting bone modifications from carnivore and human activity (SI Figures 10 and 11). These results are particularly informative for Layers J and K at Bacho Kiro Cave and at La Ferrassie with the addition of three to four taxa previously unassociated with the modifying agents (carnivores and humans).

With the addition of ZooMS, carnivore modifications were identified at Bacho Kiro Cave on Cervid/Saiga (Layer J: 3% NISP, Layer K: 23% NISP) and *Capra* sp. (Layer J: 11% NISP, Layer K: 11% NISP), and on *Bos/Bison* (31% NISP) and Equidae (31% NISP) in Layer K. Carnivore modifications within the ZooMS component of Layer K affected 21% of the remains from the dominant taxa, a considerably higher percentage than previously obtained through morphology (SI Figure 12). At La Ferrassie, the proportion of carnivore activity within Layer 6 appears relatively low compared to human activity as carnivore modifications were identified on only two *Bos/Bison* specimens within the ZooMS component (SI Figure 12)., affecting all dominant taxa.

In addition to evidence of carnivore activity, anthropogenic modifications are also present on most taxa within all studied layers. Human modifications were recognised on equids (20% NISP) and Capra sp. (22% NISP) in Layer J at Bacho Kiro Cave (Figure 5) and we noted a relatively high proportion of percussion marks on Cervid/Saiga specimens from Layer J (22% NISP) (SI Figure 11 and SI Figure 15). At La Ferrassie, human activity is identified on Cervid/Saiga (4% NISP) and Bos/Bison (6% NISP) but not on equid specimens, and percussion traces occur on a higher proportion of reindeer remains (9% NISP; Figure 5 and SI Figure 13). At Les Cottés, human modifications range between 10 and 20% among dominant taxa over all studied layers and occur at higher proportions on reindeer specimens (particularly in US04 and US06), mainly represented by cut marks and percussion traces (Figure 5 and SI Figure 14). At Bacho Kiro Cave and Les Cottés, we note a progressive reduction of carnivore activity from the Late Middle Palaeolithic to the Upper Palaeolithic alongside an increase of human modifications at Bacho Kiro Cave, reinforcing patterns previously described (Rendu et al., 2019; Smith et al., 2021). In addition, we note the recurrent occurrence of anthropogenic modifications on carnivore remains (n = 93) from various taxa such as canids (Canis lupus, Vulpes vulpes), felids (Panthera leo spelaea, Panthera pardus), cave hyaenas (Crocuta crocuta spelaea), and ursids within layers I and J at Bacho Kiro Cave while layer K exhibits only two carnivores remains with human modifications (SI Table 17). At Les Cottés, only two canid specimens show human modifications, and no human modifications were observed on carnivore remains within layer 6 at La Ferrassie (SI Table 17).

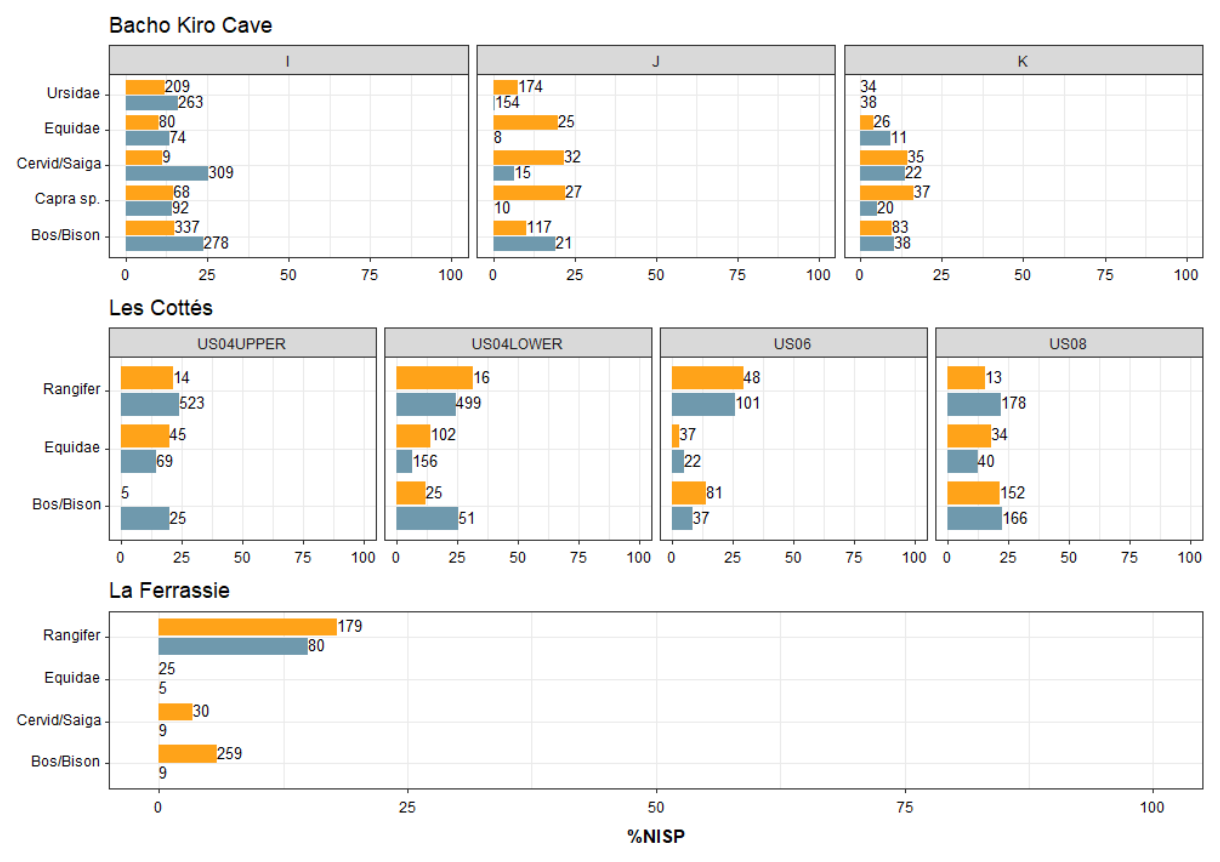


Figure 5: Percentages of anthropogenic modifications within the ZooMS (orange) and morphology (blue) components on the dominant taxa at the sites of Bacho Kiro Cave, Les Cottés and La Ferrassie. Numbers on the bars are the total NISP of specimens identified for the taxa.

Skeletal representation

Due to their morphological specificities and as they are affected differently by taphonomic processes, teeth are largely represented in the morphology component and show the highest proportions among skeletal elements, particularly illustrated by the material from Bacho Kiro Cave and Les Cottés (Figure 6 & SI Figure 16). At Bacho Kiro Cave, the skeletal composition of the ZooMS component is mostly represented by long bones (LBN), cranial and axial remains, with a higher proportion of axial elements within the ZooMS component explained by an overrepresentation of ribs (SI Table 18, Figure 6). Rib elements are difficult to taxonomically identify as they do not retain many specific morphological features relative to their size and proportion in a skeleton. Long bone fragments (LBN) correspond to unidentified bone fragments from forelimbs, hindlimbs and distal limbs (metacarpals and metatarsals). Bone specimens categorised as LBN within the ZooMS component are predominantly represented by diaphysis fragments (either from the mid-shaft or near the epiphysis of the bones) but rarely from the epiphysis, as illustrated by the example on the material of Bacho Kiro Cave (SI Figure 17). Within the morphology component at Les Cottés, we observe relatively similar proportions of limb remains between the taxa, with the exception of the absence of hindlimb and distal limb remains recorded for Bos/Bison in US06 of both

components, but higher proportions of cranial specimens from *Bos/Bison* and Equidae (SI Figure 16). At La Ferrassie, the elemental representation of the ZooMS component only contributes to a small extent to the skeletal representation of the morphology component as most of the remains were unidentifiable and had not been assigned to a body part (SI Figure 18).

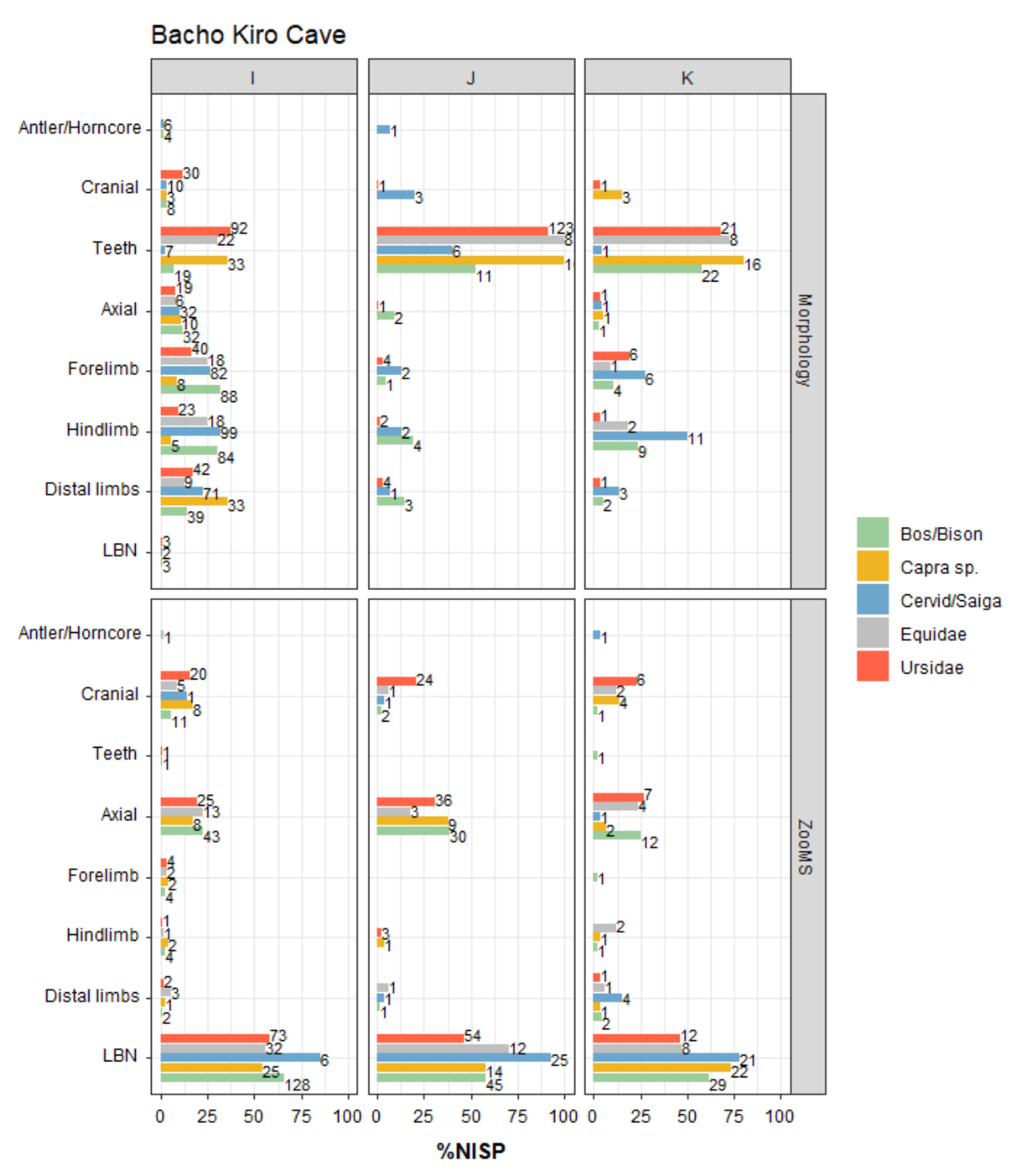


Figure 6: Skeletal distribution of the bone specimens identified through morphology (top) and ZooMS (bottom) from the dominant taxa at Bacho Kiro Cave. Numbers on the bars give the total NISP for each body part, layers and ID-method. Unidentified body parts (NID) were excluded from the plot. LBN: Long Bone fragment.

Discussion

This study represents the first combined palaeoproteomic and zooarchaeological analysis of faunal material from three datasets covering the Middle to Upper Palaeolithic transition. It aims to overcome methodological limits in taxonomic identification resulting from bone fragmentation and to address human subsistence and fauna processing behaviour during a period of possible interaction between Neanderthals and Late Pleistocene *Homo sapiens* groups in Europe. Together with a high success rate of taxonomic identification, the inclusion of ZooMS analysis of the fragmented, unidentifiable component of bone assemblages can identify species previously unrecognised through traditional morphological analysis and, furthermore, be integrated and correlated with traditional zooarchaeological, taphonomic and ecological data (Berto et al., 2021; Sinet-Mathiot et al., 2019; Welker et al., 2015). In the case of highly fragmented bone assemblages, this addition can provide highly valuable information for the interpretation of human subsistence. This is notably exemplified in our study at La Ferrassie Layer 6 with a 4-fold increase in taxonomic identification through ZooMS compared to the morphologically identified component (NISP_{Morph} = 142, NISP_{ZooMS} = 518).

Prey selection and sampling bias.

In the absence of alternative methods to address the fragmented component of Palaeolithic bone assemblages, previous studies of past human behaviour related to subsistence strategies have relied solely on morphologically identifiable fauna, excluding a vast majority of the available bone specimens. However, the fragmented component of Palaeolithic bone assemblages can differ significantly from the morphologically identifiable component, highlighted by differences in proportions of the dominant taxonomic groups between morphologically identified and ZooMS components. Our study does not reflect the pattern observed in several other ZooMS screening studies which found a similar taxonomic composition of dominant species between both components. (Berto et al., 2021; Buckley et al., 2017; Welker et al., 2016, 2017). In this study, discrepancies in taxonomic abundances between both components are seen through an overrepresentation of reindeer and an underrepresentation of Bos/Bison and equids at the sites of Les Cottés and La Ferrassie. These differences seem to be related to differential identification rates between taxa, possibly creating a reporting bias in the representation of the dominant taxa depending on their ease of identification. Thus, taxa such as reindeer or Ursidae will be overrepresented in the morphologically identified component as they are easy to differentiate even when fragmented. On the contrary, Bos/Bison and Equidae are more difficult to distinguish when fragmented and are often categorised as unidentifiable remains.

Assemblage composition and identification rates.

The uniformity in low weathering patterns on the bone material from Bacho Kiro Cave and La Ferrassie sites indicate that, throughout the stratigraphy, natural factors played a limited role in bone fragmentation. Overall, bone material was relatively quickly buried and suffered minimal re-exposure at these two sites. At Les Cottés, the degree of weathering was comparable among the dominant taxa, although reindeer showed slightly better bone surface readability. Further study is required to understand if this pattern could be explained through bone morphology or specific depositional conditions of the reindeer specimens (shorter exposition of the specimens prior to burying), especially knowing that glutamine deamidation ratios do not indicate a clear differential molecular preservation. Further, our analysis of collagen deamidation at each site does not provide a molecular diagenetic explanation for the differences in taxonomic proportion between the two bone components of each assemblage. When incorporating ZooMS identifications into the zooarchaeological analysis we should keep in mind that both components, by definition, commonly show different bone length distributions, as larger fragments tend to be more easily identifiable morphologically. However, when comparing taxa, we note that this is not the case for all taxonomic groups (Pickering et al., 2006). Certain taxa, such as reindeer at Les Cottés and Capra sp. at Bacho Kiro Cave, can show a bone length distribution significantly different from other taxonomic groups (Bos/Bison and Equidae), possibly resulting from the size of the bone fragments most likely produced during marrow extraction and a different identification rate between these taxa. Indeed, because of the low cortical thickness relative to bone diameter and their smaller body size compared to Bos/Bison and equids, reindeer fragments will cover more of the reindeer bone proportionally, which would give it a better chance of preserving identifiable features. On the other hand, breaking open the bones of larger animals such as Bos/Bison or equids will produce larger fragments on average. Fragments of bovine bone specimens are often difficult to distinguish from homologous parts of Equidae or red deer as the skeletal elements of these taxa tend to overlap in size and morphology (Morin, 2012). However, since reindeer are more easily identifiable, this results in increasing representation of this species within the morphological component alongside a limited proportion of identified Bos/Bison and equid specimens (Gobalet, 2001).

The assessment of prey skeletal part distribution is often closely related to the taxonomic identification of the bone specimens. Small long bone shaft fragments tend to be difficult to identify due to a lack of diagnostic features on the bone diaphyses in combination with their high fragmentation rate due to marrow extraction (Morin et al., 2017a). Thus, the morphologically unidentifiable component analysed through ZooMS often contains a high proportion of long bone, particularly diaphysis portions, and rib fragments challenging the evaluation of skeletal distributions. Epiphysis portions tend to retain more specific

morphological criteria facilitating the taxonomic identification of the remains. However, their representation within the long bone fraction of the ZooMS component do not strongly differ from the morphology component at Bacho Kiro Cave. Thus, an underrepresentation of epiphyses can also result from selective destruction due to various factors such as differential preservation and bone density, carnivore activity, specific butchering practices like extraction of bone grease, and post-depositional or sampling bias during the archaeological excavation (Binford, 1981; Grayson & Delpech, 2008; Morin, 2010, 2020; Yravedra & Domínguez-Rodrigo, 2009). Behavioural inferences such as carcass processing and the selected transport of different body parts are often made based on skeletal part representation and abundance (Bartram et al., 1999; Binford, 1981; Klein et al., 1999; Marean & Assefa, 1999). The integration of skeletal representation with the taxonomic identification obtained through ZooMS has the potential to add elements to the inventory of the faunal record, contributing to our understanding of the transport of articulated remains to the site.

Subsistence during the Middle to Upper Palaeolithic transition.

The addition, through peptide mass fingerprinting, of taxonomically identified bone specimens to faunal assemblages spanning a transitional phase during human evolution, contribute to our understanding of patterns of shifts observed during the MUPT. Our results contribute further detail to the general picture that, over this period, the hominin diet was dominated by a range of medium and large herbivores (Discamps et al., 2011; Gaudzinski-Windheuser & Niven, 2009; Gaudzinski-Windheuser & Roebroeks, 2011; Jaouen et al., 2019; Niven et al., 2012; Rendu et al., 2019; Richards et al., 2008; Smith, 2015). Our work highlights the exploitation of a more diverse range of taxa by both hominins and carnivores, permitting the correlation of certain taxa with particular agents that were contributing to the bone accumulation on site, notably at Bacho Kiro Cave. Across dominant taxa, human modifications mainly consist of cut marks, with a low occurrence of percussion traces from marrow extraction, thus providing no suitable explanation for the difference in proportions between the components. The ZooMS analysis emphasises and refines shifts of proportions of taxa throughout the stratigraphy at Les Cottés, particularly between equids and Bos/Bison specimens (Rendu et al., 2019). These shifts in the faunal composition could represent either a slow change in the prey availability in the environment around the site or human selection strategies paralleling the expansion of Late Pleistocene Homo sapiens over Europe. Nonetheless, while the morphologically identified fauna suggests a more specialised focus on hunting reindeer (Rendu et al., 2019), our results suggest this underestimates the exploitation of other species; in particular, Equidae. These results are particularly of interest within the framework of the debate about reindeer hunting specialisation (Grayson & Delpech, 2002; Mellars, 2004). Although the progressive increase of reindeer remains through the MUPT

transition correlates with a progressive climatic degradation during MIS3 and can be explained by an adaptation of the human groups to environmental fluctuations (Banks et al., 2013; Discamps et al., 2011), the role of large ungulates in the human diet throughout the MUPT might have been under-represented due to differential identification rates.

The incidence of carnivore modifications during late Neanderthal occupation of the sites suggests a context where both humans and carnivores were important in faunal accumulation and modification, still indicating frequent human occupation of the cave and sporadic carnivore visits, but the latter possibly more frequent than previously considered (Straus, 1982). The progressive decrease of carnivore activity highlighted by the reduction of carnivore modifications from the MP to the UP at Bacho Kiro Cave and Les Cottés fits with the pattern previously detected in some other sites in Europe from this time period (Discamps, 2014; Discamps et al., 2019; Rendu et al., 2019; Smith et al., 2021; Stiner & Kuhn, 2006). This possible change of relationship of carnivores to humans, from competitor to prey or source of raw material is emphasised by the appearance of human modifications on Ursidae remains during the IUP at Bacho Kiro Cave (alongside modifications on other carnivore species at Bacho Kiro Cave; (Smith et al., 2021)). Homo sapiens started to exploit carnivore remains more intensively as a raw material, notably illustrated by the increase in bone artefacts made from cave bear bones and teeth at Bacho Kiro Cave and other sites in southeast Europe and southwest Asia during the IUP (Bosch et al., 2019; Guadelli et al., 2011; Kuhn et al., 2009; Martisius et al., 2022; Stiner et al., 2013). Such specific needs in raw material can be investigated through skeletal part representation and carcass processing (Rendu et al., 2019). Furthermore, the higher percentage of carnivore traces in the Middle Palaeolithic layers at Bacho Kiro Cave and at Les Cottés attest to their repetitive use of the site correlated with possible short duration of human occupation (Hublin et al., 2020; Smith et al., 2021). The interaction between human groups and large carnivores seems to change during the MUPT and might indicate an increasing predatory pressure of human groups on their environment (Stiner & Kuhn, 2006) and/or a shorter duration of site occupation by Neanderthals compared to Late Pleistocene Homo sapiens.

ZooMS screening of fragmentary components of Palaeolithic bone assemblages should be systematically undertaken alongside the taphonomic analysis of the taxonomically unidentifiable specimens (see for example (Discamps, 2021)). In addition, the integration of the faunal data obtained from aDNA retrieved from the sediment of an archaeological site with the zooarchaeological and ZooMS analysis of palaeolithic faunal assemblages has the potential to provide a better understanding of the various episodes of occupation of a site or inform about the potential origin of the DNA preserved in the sediment.

Conclusion

The analysis of the morphologically unidentifiable component of Pleistocene bone assemblages offers an exciting new avenue for research. Our work on faunal assemblages from sites with occupational sequence that span the MUPT has highlighted inter- and intrasite differences between assemblages, taxa, layers and identification methods. We emphasise that the morphologically unidentifiable component of faunal assemblages does not necessarily reflect the morphologically identified component. Certain taxa are more readily identifiable based on morphology compared to others. Their bone elements show particular features allowing for their recognition even when fragmented (Morin et al., 2017a). This results in a discrepancy in the identification rate of differing taxa during the analysis of bone material. Taxonomic abundances are influenced by these methodological limits and any interpretation related to past human subsistence behaviour and hunting strategies can potentially be biased. Similar patterns might be expected in other monospecific faunal assemblages, and the assessment of morphologically unidentifiable bone fractions through ZooMS can reveal conditions that influence the variability of the results.

The integration of fragmentary bone components, identified through ZooMS or other biomolecular methods (Rüther et al., 2022), within a coherent zooarchaeological framework allows for a more exhaustive evaluation of the preserved bone assemblage, unlocking behavioural information based on skeletal part profiles, bone surface modifications and ecological indices. Our large-scale, non-targeted ZooMS studies across the MUPT at Bacho Kiro Cave, Les Cottés and La Ferrassie indicate an underestimated exploitation of the large ungulates such as *Bos/Bison* and Equidae, a progressive shift in prey selection from *Bos/Bison* to equids, a reduction in the frequency of site occupation by carnivores and an increase in their exploitation by Upper Palaeolithic *Homo sapiens* over the course of their progressive dispersal across Europe. This approach provides complementary data for assessing preserved bone remains, contributes to our understanding of bone assemblage formation, and represents a future path for Palaeolithic zooarchaeology.

References

- Banks, W. E., Antunes, N., Rigaud, S., & d'Errico, F. (2013). Ecological constraints on the first prehistoric farmers in Europe. In *Journal of Archaeological Science* (Vol. 40, Issue 6, pp. 2746–2753).
- Bartram, Jr., E., L., & Marean, C. W. (1999). Explaining the "Klasies Pattern": Kua Ethnoarchaeology, the Die Kelders Middle Stone Age Archaeofauna, Long Bone Fragmentation and Carnivore Ravaging. *Journal of Archaeological Science*, *26*(1), 9–29.

- Bastin, B., Leveque, F., & Pradel, L. (1976). Recognition of interstadial pollen spectra between the Mousterian and the Old Perigordian of the Grotte des Cottes (Vienne). Comptes Rendus Hebdomadaires Des Seances de l'Academie Des Sciences. Serie D: Sciences Naturelles.
- Behrensmeyer, A. K. (1978). Taphonomic and ecologic information from bone weathering. *Paleobiology*, *4*(2), 150–162.
- Berto, C., Krajcarz, M. T., Moskal-del Hoyo, M., Komar, M., Sinet-Mathiot, V., Zarzecka-Szubińska, K., Krajcarz, M., Szymanek, M., Wertz, K., Marciszak, A., & Others. (2021). Environment changes during Middle to Upper Palaeolithic transition in southern Poland (Central Europe). A multiproxy approach for the MIS 3 sequence of Koziarnia Cave (Kraków-Częstochowa Upland). *Journal of Archaeological Science: Reports*, 35, 102723.
- Binford, L. R. (1981). Bones: ancient men and modern myths. Academic Press.
- Blumenschine, R. J., Marean, C. W., & Capaldo, S. D. (1996). Blind Tests of Inter-analyst Correspondence and Accuracy in the Identification of Cut Marks, Percussion Marks, and Carnivore Tooth Marks on Bone Surfaces. *Journal of Archaeological Science*, *23*(4), 493–507.
- Bosch, M. D., Buck, L., & Stauss, A. (2019). Special issue: Personal ornaments in early prehistory location, location, location: Investigating perforation locations in Tritia gibbosula shells at Ksâr 'Akil (Lebanon) using micro-CT data.
- Brown, S., Douka, K., Collins, M. J., & Richter, K. K. (2021). On the standardization of ZooMS nomenclature. *Journal of Proteomics*, 235, 104041.
- Brown, S., Wang, N., Oertle, A., Kozlikin, M. B., Shunkov, M. V., Derevianko, A. P., Comeskey, D., Jope-Street, B., Harvey, V. L., Chowdhury, M. P., Buckley, M., Higham, T., & Douka, K. (2021). Zooarchaeology through the lens of collagen fingerprinting at Denisova Cave. *Scientific Reports*, *11*(1), 15457.
- Buckley, M., Collins, M., Thomas-Oates, J., & Wilson, J. C. (2009). Species identification by analysis of bone collagen using matrix-assisted laser desorption/ionisation time-of-flight mass spectrometry. *Rapid Communications in Mass Spectrometry: RCM*, *23*(23), 3843–3854.
- Buckley, M., Harvey, V. L., & Chamberlain, A. T. (2017). Species identification and decay assessment of Late Pleistocene fragmentary vertebrate remains from Pin Hole Cave (Creswell Crags, UK) using collagen *Boreas*.
- Castel. (2011). Archéozoologie de l'Aurignacien de l'Abri Castanet (Sergeac, Dordogne, France): les fouilles 1994-1998. *Revue de Paléobiologie*.
- Delagnes, A., & Rendu, W. (2011). Shifts in Neandertal mobility, technology and subsistence strategies in western France. *Journal of Archaeological Science*, *38*(8), 1771–1783.
- Delporte, H., & Delibrias, G. (1984). *Le grand abri de la Ferrassie: fouilles 1968-1973*. Ed. du Laboratoire de paléontologie humaine et de préhistoire.
- Dirrigl. (2002). Differential identifiability between chosen North American gallinaceous skeletons and the effect of differential survivorship. *Acta Zoologica Cracoviensia*. http://citeseerx.ist.psu.edu/viewdoc/download?doi=10.1.1.574.7664&rep=rep1&type=pdf
- Discamps, E. (2014). Ungulate biomass fluctuations endured by Middle and Early Upper Paleolithic societies (SW France, MIS 5-3): The contributions of modern analogs and cave hyena paleodemography. *Quaternary International: The Journal of the International Union for Quaternary Research*, 337, 64–79.
- Discamps, E. (2021). TIPZOO: a Touchscreen Interface for Palaeolithic Zooarchaeology. Towards making data entry and analysis easier, faster, and more reliable. *Peer Community Journal*, 1(e67). https://doi.org/10.24072/pcjournal.61

- Discamps, E., Bachellerie, F., Baillet, M., & Sitzia, L. (2019). The Use of Spatial Taphonomy for Interpreting Pleistocene Palimpsests: An Interdisciplinary Approach to the Châtelperronian and Carnivore Occupations at Cassenade (Dordogne, France). *Paleoanthropology*, 2019, 362–388.
- Discamps, E., Jaubert, J., & Bachellerie, F. (2011). Human choices and environmental constraints: deciphering the variability of large game procurement from Mousterian to Aurignacian times (MIS 5-3) in southwestern France. *Quaternary Science Reviews*, 30(19), 2755–2775.
- Domínguez-Rodrigo, M., Saladié, P., Cáceres, I., Huguet, R., Yravedra, J., Rodríguez-Hidalgo, A., Martín, P., Pineda, A., Martín, J., Gené, C., Aramendi, J., & Cobo-Sánchez, L. (2017). Use and abuse of cut mark analyses: The Rorschach effect. In *Journal of Archaeological Science* (Vol. 86, pp. 14–23). https://doi.org/10.1016/j.jas.2017.08.001
- Faith, J. T. (2007). Changes in reindeer body part representation at Grotte XVI, Dordogne, France. *Journal of Archaeological Science*, *34*(12), 2003–2011.
- Fewlass, H., Talamo, S., Wacker, L., Kromer, B., Tuna, T., Fagault, Y., Bard, E., McPherron, S. P., Aldeias, V., Maria, R., Martisius, N. L., Paskulin, L., Rezek, Z., Sinet-Mathiot, V., Sirakova, S., Smith, G. M., Spasov, R., Welker, F., Sirakov, N., ... Hublin, J.-J. (2020). A 14 C chronology for the Middle to Upper Palaeolithic transition at Bacho Kiro Cave, Bulgaria. *Nature Ecology & Evolution*, 1–8.
- Fisher, J. W. (1995). Bone surface modifications in zooarchaeology. *Journal of Archaeological Method and Theory*, *2*(1), 7–68.
- Garrod, D. A. E., Howe, B., & Gaul, J. H. (1939). Excavation in the Cave of Bacho Kiro, North-East Bulgaria. *Bulletin of the American School of Prehistoric Research. Cambridge, MA*, 15, 46–70.
- Gaudzinski, S., & Roebroeks, W. (2000). Adults only. Reindeer hunting at the middle palaeolithic site salzgitter lebenstedt, northern Germany. *Journal of Human Evolution*, 38(4), 497–521.
- Gaudzinski-Windheuser, S., Kindler, L., Pop, E., Roebroeks, W., & Smith, G. (2014). The Eemian Interglacial lake-landscape at Neumark-Nord (Germany) and its potential for our knowledge of hominin subsistence strategies. *Quaternary International: The Journal of the International Union for Quaternary Research*, 331, 31–38.
- Gaudzinski-Windheuser, S., & Niven, L. (2009). Hominin subsistence patterns during the Middle and Late Paleolithic in northwestern Europe. *The Evolution of Hominin Diets*.
- Gaudzinski-Windheuser, S., & Roebroeks, W. (2011). On Neanderthal subsistence in last interglacial forested environments in Northern Europe. *Lifeways, Subsistence and*
- Gibb, S., & Strimmer, K. (2012). MALDIquant: a versatile R package for the analysis of mass spectrometry data. *Bioinformatics*, 28(17), 2270–2271.
- Gobalet, K. W. (2001). A Critique of Faunal Analysis; Inconsistency among Experts in Blind Tests. *Journal of Archaeological Science*, *28*(4), 377–386.
- Grayson, D. K., & Delpech, F. (2002). Specialized Early Upper Palaeolithic Hunters in Southwestern France? *Journal of Archaeological Science*, *29*(12), 1439–1449.
- Grayson, D. K., & Delpech, F. (2008). The large mammals of Roc de Combe (Lot, France): The Châtelperronian and Aurignacian assemblages. *Journal of Anthropological Archaeology*, *27*(3), 338–362.
- Guadelli, A., Fernandez, P., Guadelli, J.-L., Miteva, V., & Sirakov, N. (2011). The Retouchers from the Gravettian Levels in Kozarnika Cave. *ARCHÆOPlus*, *5*, 155–162.

- Guérin, G., Frouin, M., Talamo, S., Aldeias, V., Bruxelles, L., Chiotti, L., Dibble, H. L., Goldberg, P., Hublin, J.-J., Jain, M., Lahaye, C., Madelaine, S., Maureille, B., McPherron, S. J. P., Mercier, N., Murray, A. S., Sandgathe, D., Steele, T. E., Thomsen, K. J., & Turq, A. (2015). A multi-method luminescence dating of the Palaeolithic sequence of La Ferrassie based on new excavations adjacent to the La Ferrassie 1 and 2 skeletons. *Journal of Archaeological Science*, *58*, 147–166.
- Hajdinjak, M., Mafessoni, F., Skov, L., Vernot, B., Hübner, A., Fu, Q., Essel, E., Nagel, S., Nickel, B., Richter, J., Moldovan, O. T., Constantin, S., Endarova, E., Zahariev, N., Spasov, R., Welker, F., Smith, G. M., Sinet-Mathiot, V., Paskulin, L., ... Pääbo, S. (2021). Initial Upper Palaeolithic humans in Europe had recent Neanderthal ancestry. *Nature*, 592(7853), 253–257.
- Higham, T., Douka, K., Wood, R., Ramsey, C. B., Brock, F., Basell, L., Camps, M., Arrizabalaga, A., Baena, J., Barroso-Ruíz, C., Bergman, C., Boitard, C., Boscato, P., Caparrós, M., Conard, N. J., Draily, C., Froment, A., Galván, B., Gambassini, P., ... Jacobi, R. (2014). The timing and spatiotemporal patterning of Neanderthal disappearance. *Nature*, 512(7514), 306–309.
- Hublin, J.-J. (2015). The modern human colonization of western Eurasia: when and where? *Quaternary Science Reviews*, *118*, 194–210.
- Hublin, J.-J., Sirakov, N., Aldeias, V., Bailey, S., Bard, E., Delvigne, V., Endarova, E., Fagault, Y., Fewlass, H., Hajdinjak, M., Kromer, B., Krumov, I., Marreiros, J., Martisius, N. L., Paskulin, L., Sinet-Mathiot, V., Meyer, M., Pääbo, S., Popov, V., ... Tsanova, T. (2020). Initial Upper Palaeolithic Homo sapiens from Bacho Kiro Cave, Bulgaria. *Nature*, 581(7808), 299–302.
- Jacobs, Z., Li, B., Jankowski, N., & Soressi, M. (2015). Testing of a single grain OSL chronology across the Middle to Upper Palaeolithic transition at Les Cottés (France). *Journal of Archaeological Science*, *54*, 110–122.
- Jaouen, K., Richards, M. P., Le Cabec, A., Welker, F., Rendu, W., Hublin, J.-J., Soressi, M., & Talamo, S. (2019). Exceptionally high δ15N values in collagen single amino acids confirm Neandertals as high-trophic level carnivores. *Proceedings of the National Academy of Sciences of the United States of America*, *116*(11), 4928–4933.
- Klein, R. G., Cruz-Uribe, K., & Milo, R. G. (1999). Skeletal Part Representation in Archaeofaunas: Comments on "Explaining the 'Klasies Pattern': Kua Ethnoarchaeology, the Die Kelders Middle Stone Age Archaeofauna, Long Bone Fragmentation and Carnivore Ravaging" by Bartram & Marean. *Journal of Archaeological Science*, *26*(9), 1225–1234.
- Kozłowski, J. K., & Ginter, B. (1982). *Excavation in the Bacho Kiro Cave (Bulgaria)*. Państwowe Wydawnictwo Naukowe.
- Kuhn, S. L., Stiner, M. C., Güleç, E., Özer, I., Yılmaz, H., Baykara, I., Açıkkol, A., Goldberg, P., Molina, K. M., Ünay, E., & Suata-Alpaslan, F. (2009). The early Upper Paleolithic occupations at Üçağızlı Cave (Hatay, Turkey). *Journal of Human Evolution*, *56*(2), 87–113.
- Lee Lyman, R. (1994). Vertebrate Taphonomy. Cambridge University Press.
- Lee Lyman, R., & Lyman, R. L. (1994). Vertebrate Taphonomy. Cambridge University Press.
- Lévêque, F. (1997). Le Passage du Paléolithique moyen au Paléolithique supérieur: Données stratigraphiques de quelques gisements sous-grotte du sud-ouest [The transition from middle to Upper Paleolithic: stratigraphie sequences of some south-west sites of France.]. *Quaternaire*, 8(2), 279–287.

- Lyman, R. L. (2002). Taxonomic identification of zooarchaeological remains. *The Review of Archaeology*, 23(2), 13–20.
- Marean, C. W. (1991). Measuring the post-depositional destruction of bone in archaeological assemblages. *Journal of Archaeological Science*, *18*(6), 677–694.
- Marean, C. W., & Assefa, Z. (1999). Zooarcheological evidence for the faunal exploitation behavior of Neandertals and early modern humans. *News, and Reviews*
- Marean, C. W., & Kim, S. Y. (1998). Mousterian large-mammal remains from kobeh cave behavioral implications for neanderthals and early modern humans. *Current Anthropology*, *39*(S1), S79–S114.
- Martisius, N. L., Spasov, R., Smith, G. M., Endarova, E., Sinet-Mathiot, V., Welker, F., Aldeias, V., Horta, P., Marreiros, J., Rezek, Z., McPherron, S. P., Sirakov, N., Sirakova, S., Tsanova, T., & Hublin, J.-J. (2022). Initial Upper Paleolithic bone technology and personal ornaments at Bacho Kiro Cave (Bulgaria). *Journal of Human Evolution*, *167*, 103198.
- Martisius, N. L., Welker, F., Dogandžić, T., Grote, M. N., Rendu, W., Sinet-Mathiot, V., Wilcke, A., McPherron, S. J. P., Soressi, M., & Steele, T. E. (2020). Non-destructive ZooMS identification reveals strategic bone tool raw material selection by Neandertals. *Scientific Reports*, *10*(1), 7746.
- Mellars, P. A. (2004). Reindeer specialization in the early Upper Palaeolithic: the evidence from south west France. *Journal of Archaeological Science*, *31*(5), 613–617.
- Morin. (2010). Taphonomic implications of the use of bone as fuel. Palethnologie.
- Morin, E. (2004). Late Pleistocene population interaction in western Europe and modern human origins: New insights based on the faunal remains from Saint-Césaire, southwestern France. University of Michigan Ann Arbor.
- Morin, E. (2012). Reassessing Paleolithic Subsistence: The Neandertal and Modern Human Foragers of Saint-Césaire. Cambridge University Press.
- Morin, E. (2020). Rethinking the emergence of bone grease procurement. *Journal of Anthropological Archaeology*, *59*, 101178.
- Morin, E., Ready, E., Boileau, A., Beauval, C., & Coumont, M.-P. (2017a). Problems of Identification and Quantification in Archaeozoological Analysis, Part I: Insights from a Blind Test. *Journal of Archaeological Method and Theory*, *24*(3), 886–937.
- Morin, E., Ready, E., Boileau, A., Beauval, C., & Coumont, M.-P. (2017b). Problems of Identification and Quantification in Archaeozoological Analysis, Part II: Presentation of an Alternative Counting Method. *Journal of Archaeological Method and Theory*, *24*(3), 938–973.
- Niven, L., Steele, T. E., Rendu, W., Mallye, J.-B., McPherron, S. P., Soressi, M., Jaubert, J., & Hublin, J.-J. (2012). Neandertal mobility and large-game hunting: The exploitation of reindeer during the Quina Mousterian at Chez-Pinaud Jonzac (Charente-Maritime, France). *Journal of Human Evolution*, *63*(4), 624–635.
- Oksanen, J., Blanchet, F. G., Friendly, M., Kindt, R., Legendre, P., McGlinn, D., Minchin, P. R., O'hara, R. B., Simpson, G. L., Solymos, P., & Others. (2019). Vegan: community ecology package (version 2.5-6). *The Comprehensive R Archive Network*.
- Olsen, S. L., & Shipman, P. (1988). Surface modification on bone: Trampling versus butchery. *Journal of Archaeological Science*, *15*(5), 535–553.
- Pederzani, S., Britton, K., Aldeias, V., Bourgon, N., Fewlass, H., Lauer, T., McPherron, S. P., Rezek, Z., Sirakov, N., Smith, G. M., Spasov, R., Tran, N.-H., Tsanova, T., & Hublin, J.-J. (2021). Subarctic climate for the earliest Homo sapiens in Europe. *Science Advances*, 7(39), eabi4642.
- Peyrony, D. (1934). La Ferrassie. Moustérien, Périgordien, Aurignacien. Préhistoire III.

- Pickering, T. R., Egeland, C. P., Schnell, A. G., Osborne, D. L., & Enk, J. (2006). Success in Identification of Experimentally Fragmented Limb Bone Shafts: Implications for Estimates of Skeletal Element Abundance in Archaeofaunas.
- Pothier Bouchard, G., Riel-Salvatore, J., Negrino, F., & Buckley, M. (2020). Archaeozoological, taphonomic and ZooMS insights into The Protoaurignacian faunal record from Riparo Bombrini. *Quaternary International: The Journal of the International Union for Quaternary Research*, *551*, 243–263.
- Pradel, L. (1967). La Grotte des Cottés, commune de Saint-Pierre-de-Maillé (Vienne); Moustérien—Périgordien—Aurignacien. Datation par le radiocarbone. *L'Anthropologie*, 71, 271–277.
- Prüfer, K., Posth, C., Yu, H., Stoessel, A., Spyrou, M. A., Deviese, T., Mattonai, M., Ribechini, E., Higham, T., Velemínský, P., Brůžek, J., & Krause, J. (2021). A genome sequence from a modern human skull over 45,000 years old from Zlatý kůň in Czechia. *Nature Ecology & Evolution*, *5*(6), 820–825.
- R Core Team, 2021. (n.d.). *R: A language and environment for statistical computing* [R Foundation for Statistical Computing].
- Rendu, W., Costamagno, S., Meignen, L., & Soulier, M.-C. (2012). Monospecific faunal spectra in Mousterian contexts: Implications for social behavior. *Quaternary International: The Journal of the International Union for Quaternary Research*, 247, 50–58.
- Rendu, W., Renou, S., Soulier, M.-C., Rigaud, S., Roussel, M., & Soressi, M. (2019). Subsistence strategy changes during the Middle to Upper Paleolithic transition reveals specific adaptations of Human Populations to their environment. *Scientific Reports*, *9*(1), 15817.
- Richards, M. P., Taylor, G., Steele, T., McPherron, S. P., Soressi, M., Jaubert, J., Orschiedt, J., Mallye, J. B., Rendu, W., & Hublin, J. J. (2008). Isotopic dietary analysis of a Neanderthal and associated fauna from the site of Jonzac (Charente-Maritime), France. *Journal of Human Evolution*, *55*(1), 179–185.
- RStudio Team. (2022). Rstudio: Integrated Development Environment for R. *RStudio*, *PBC*, *Boston*, *MA*. http://www.rstudio.com/
- Ruebens, K., Sinet-Mathiot, V., Talamo, S., Smith, G. M., Welker, F., Hublin, J.-J., & McPherron, S. P. (2022). The Late Middle Palaeolithic Occupation of Abri du Maras (Layer 1, Neronian, Southeast France): Integrating Lithic Analyses, ZooMS and Radiocarbon Dating to Reconstruct Neanderthal Hunting Behaviour. *Journal of Paleolithic Archaeology*, *5*(1), 4.
- Shannon, C. E. (1948). A mathematical theory of communication. *The Bell System Technical Journal*, *27*(3), 379–423.
- Sinet-Mathiot, V., Smith, G. M., Romandini, M., Wilcke, A., Peresani, M., Hublin, J.-J., & Welker, F. (2019). Combining ZooMS and zooarchaeology to study Late Pleistocene hominin behaviour at Fumane (Italy). *Scientific Reports*, *9*(1), 12350.
- Smith, G. M. (2015). Neanderthal megafaunal exploitation in Western Europe and its dietary implications: a contextual reassessment of La Cotte de St Brelade (Jersey). *Journal of Human Evolution*, 78, 181–201.
- Smith, G. M., Spasov, R., Martisius, N. L., Sinet-Mathiot, V., Aldeias, V., Rezek, Z., Ruebens, K., Pederzani, S., McPherron, S. P., Sirakova, S., Sirakov, N., Tsanova, T., & Hublin, J.-J. (2021). Subsistence behavior during the Initial Upper Paleolithic in Europe: Site use, dietary practice, and carnivore exploitation at Bacho Kiro Cave (Bulgaria). *Journal of Human Evolution*, 161, 103074.

- Soressi, M., Roussel, M., Rendu, W., Primault, J., Rigaud, S., Texier, P.-J., Richter, D., Talamo, S., Ploquin, F., Larmignat, B., Tavormina, C., & Hublin, J.-J. (2010). Les Cottés (Vienne). Nouveaux travaux sur l'un des gisements de référence pour la transition Paléolithique moyen/supérieur. *Préhistoire entre Vienne et Charente Hommes et sociétés du Paléolithique*, 221–234.
- Soulier, M.-C., & Costamagno, S. (2017). Let the cutmarks speak! Experimental butchery to reconstruct carcass processing. *Journal of Archaeological Science: Reports*, *11*, 782–802
- Steele, T. E. (2004). Variation in mortality profiles of red deer(Cervus elaphus) in Middle Palaeolithic assemblages from western Europe. *International Journal of Osteoarchaeology*, 14(34), 307–320.
- Steele, T. E. (2015). The contributions of animal bones from archaeological sites: the past and future of zooarchaeology. *Journal of Archaeological Science*, *56*, 168–176.
- Stiner, M. C. (1991a). The Faunal Remains From Grotta Guattari: A Taphonomic Perspective. *Current Anthropology*, 32(2), 103–117.
- Stiner, M. C. (1991b). Food procurement and transport by human and non-human predators. *Journal of Archaeological Science*, *18*(4), 455–482.
- Stiner, M. C. (1993). Modern Human Origins Faunal Perspectives. *Annual Review of Anthropology*, 22(1), 55–82.
- Stiner, M. C., & Kuhn, S. L. (1995). DiVerential Burning, Recrystallization, and Fragmentation of Archaeological Bone. *Journal of Archaeological Science*, 22, 223–237.
- Stiner, M. C., & Kuhn, S. L. (2006). Changes in the "Connectedness" and Resilience of Paleolithic Societies in Mediterranean Ecosystems. *Human Ecology*, *34*(5), 693–712.
- Stiner, M. C., Kuhn, S. L., & Güleç, E. (2013). Early upper paleolithic shell beads at Üçağızlı Cave I (Turkey): technology and the socioeconomic context of ornament life-histories. *Journal of Human Evolution*, 64(5), 380–398.
- Straus, L. G. (1982). Carnivores and Cave Sites in Cantabrian Spain. *Journal of Anthropological Research*, 38(1), 75–96.
- Strohalm, M., Kavan, D., Novák, P., Volný, M., & Havlícek, V. (2010). mMass 3: a cross-platform software environment for precise analysis of mass spectrometric data. *Analytical Chemistry*, 82(11), 4648–4651.
- Talamo, S., Aldeias, V., Goldberg, P., Chiotti, L., Dibble, H. L., Guérin, G., Hublin, J.-J., Madelaine, S., Maria, R., Sandgathe, D., Steele, T. E., Turq, A., & Mcpherron, S. J. P. (2020). The new 14 C chronology for the Palaeolithic site of La Ferrassie, France: the disappearance of Neanderthals and the arrival of Homo sapiens in France. *Journal of Quaternary Science*, 35(7), 961–973.
- Talamo, S., Soressi, M., Roussel, M., Richards, M., & Hublin, J.-J. (2012). A radiocarbon chronology for the complete Middle to Upper Palaeolithic transitional sequence of Les Cottés (France). *Journal of Archaeological Science*, *39*(1), 175–183.
- Turq, A., Dibble, H. L., Goldberg, P., McPherron, S. P., Sandgathe, D., Mercier, N., Bruxelles, L., Laville, D., & Madelaine, S. (2012). Reprise des fouilles dans la partie ouest du gisement de la Ferrassie, Savignac-de-Miremont, Dordogne: problématique et premiers résultats. 78.
- van Doorn, N. L., Hollund, H., & Collins, M. J. (2011). A novel and non-destructive approach for ZooMS analysis: ammonium bicarbonate buffer extraction. *Archaeological and Anthropological Sciences*, *3*(3), 281.

- van Doorn, N. L., Wilson, J., Hollund, H., Soressi, M., & Collins, M. J. (2012). Site-specific deamidation of glutamine: a new marker of bone collagen deterioration. *Rapid Communications in Mass Spectrometry: RCM*, *26*(19), 2319–2327.
- Welker, F., Hajdinjak, M., Talamo, S., Jaouen, K., Dannemann, M., David, F., Julien, M., Meyer, M., Kelso, J., Barnes, I., Brace, S., Kamminga, P., Fischer, R., Kessler, B. M., Stewart, J. R., Pääbo, S., Collins, M. J., & Hublin, J.-J. (2016). Palaeoproteomic evidence identifies archaic hominins associated with the Châtelperronian at the Grotte du Renne. *Proceedings of the National Academy of Sciences of the United States of America*, 113(40), 11162–11167.
- Welker, F., Soressi, M. A., Roussel, M., Riemsdijk, I. van, Hublin, J.-J., & Collins, M. J. (2017). Variations in glutamine deamidation for a Châtelperronian bone assemblage as measured by peptide mass fingerprinting of collagen. *STAR: Science & Technology of Archaeological Research*, *3*(1), 15–27.
- Welker, F., Soressi, M., Rendu, W., Hublin, J.-J., & Collins, M. (2015). Using ZooMS to identify fragmentary bone from the Late Middle/Early Upper Palaeolithic sequence of Les Cottés, France. *Journal of Archaeological Science*, *54*, 279–286.
- Wilson, J., van Doorn, N. L., & Collins, M. J. (2012). Assessing the extent of bone degradation using glutamine deamidation in collagen. *Analytical Chemistry*, *84*(21), 9041–9048.
- Yravedra, J., & Domínguez-Rodrigo, M. (2009). The shaft-based methodological approach to the quantification of long limb bones and its relevance to understanding hominid subsistence in the Pleistocene: application to four Palaeolithic sites. *Journal of Quaternary Science*, *24*(1), 85–96.

Acknowledgments

We would like to thank Harold Dibble for co-directing the excavation at La Ferrassie and for his precious contribution during the early stages of this project. We thank Jean-Jacques Cleyet Merle, Catherine Cretin, and Bernard Nicolas for facilitating access to the La Ferrassie fauna stored at the Musée National de Préhistoire (Les Eyzies, France). We thank Prof. Nikolay Spassov, the National Archaeological Institute and the National Museum of Natural History from the Bulgarian Academy of Sciences (Sofia, Bulgaria) and the Museum of History in Dryanovo for supporting the Bacho Kiro Cave fieldwork and storage of the faunal collection from Bacho Kiro Cave. Thanks to Jakob Hansen and Lindsey Paskulin for technical assistance during sampling. We also thank the IZI Fraunhofer (Leipzig, Germany), Stefan Kalkhof, and Johannes Schmidt for providing access to the MALDI-TOF MS instrument. Thanks to Karen Ruebens and members of the Welker group, Ragnheiður Diljá Ásmundsdóttir, Zandra Fagernäs, Jakob Hansen, Louise Le Meillour, Dorothea Mylopotamitaki, and Huan Xia for comments on a previous version of the manuscript.

Funding

This study was funded by the Max Planck Society. T.E.S. received travel support through University of California, Davis' Small Grants in Aid of Research. M.S. is funded by the Dutch Research council (NWO; VI.C.191.070). F.W. received funding from the European Research

Council (ERC) under the European Union's Horizon 2020 research and innovation program (grant agreement no. 948365). G.M.S. is funded by the European Union's Horizon 2020 research and innovation program under the Marie Sklodowska-Curie scheme (grant agreement No. 101027850). N.L.M. was funded by the National Science Foundation (NSF-SBE; Award ID: 2004818).

Authors' contributions

V.S.M., G.M.S. and F.W. designed the research. V.S.M. and F.W. performed the proteomic analysis. W.R., T.E.S., R.S., S.M., S.R., M.-C.S., and N.L.M. performed zooarchaeological analysis. V.A., E.E., P.G., S.J.P.M., Z.R., D.S., N.S., S.S., M.S., T.T., A.T. and J.-J.H. provided samples and archaeological context. V.S.M., G.M.S. and F.W. wrote the manuscript with contributions of all authors.

Supplementary information to:

Identifying the unidentified enhances insights into hominin subsistence strategies during the Middle to Upper Palaeolithic transition

Virginie Sinet-Mathiot^{1*}, William Rendu², Teresa E. Steele³, Rosen Spasov⁴, Stéphane Madelaine^{5,6}, Sylvain Renou⁷, Marie-Cécile Soulier⁸, Naomi L. Martisius⁹, Vera Aldeias¹⁰, Elena Endarova⁴, Paul Goldberg^{10,11,12}, Shannon J.P. McPherron¹, Zeljko Rezek¹³, Dennis Sandgathe¹⁴, Nikolay Sirakov¹⁵, Svoboda Sirakova¹⁵, Marie Soressi¹⁶, Tsenka Tsanova¹⁷, Alain Turq⁵, Jean-Jacques Hublin^{13, 1}, Frido Welker^{18*}, Geoff M. Smith^{19*}

- 1 Max Planck Institute for Evolutionary Anthropology, Leipzig, Germany.
- 2 ArchaeoZOOlogy in Siberia and Central Asia ZooSCAn, CNRS IAET SB RAS International Research Laboratory, IRL 2013, Institute of Archaeology SB RAS, Novosibirsk, Russia.
- 3 Department of Anthropology, University of California, Davis, Davis, CA, USA.
- 4 Archaeology Department, New Bulgarian University, Sofia, Bulgaria.
- 5 Musée national de Préhistoire, Les Eyzies, France.
- 6 CNRS UMR 5199 PACEA, Université de Bordeaux, Pessac, France.
- 7 HADÈS Agence Atlantique, Bordeaux, France.
- 8 CNRS UMR 5608 TRACES, Université de Toulouse-Jean Jaurès, Maison de la Recherche, Toulouse, France.
- 9 Department of Anthropology, The University of Tulsa, Tulsa, OK, USA
- 10 Interdisciplinary Center for Archaeology and the Evolution of Human Behaviour, Universidade do Algarve, Campus de Gambelas, 8005-139, Faro, Portugal
- 11 School of Earth, Atmospheric and Life Sciences, University of Wollongong, Australia
- 12 Institute for Archaeological Sciences, Eberhard Karls University of Tübingen, Tübingen, Germany.
- 13 Chaire de Paléoanthropologie, CIRB (UMR 7241 U1050), Collège de France, Paris, France.
- 14 Department of Archaeology, Simon Fraser University, Burnaby, British Columbia, Canada.
- 15 National Institute of Archaeology with Museum, Bulgarian Academy of Sciences, Sofia, Bulgaria.
- 16 Faculty of Archaeology, Leiden University, The Netherlands.
- 17 Department of Chemistry G. Ciamician, Alma Mater Studiorum, University of Bologna, Via Selmi 2, Bologna, Italy
- 18 Globe institute, University of Copenhagen, Copenhagen, Denmark.
- 19 School of Anthropology and Conservation, University of Kent, Canterbury, UK.

SI Table 1: Count of specimens identified up to subfamily or genus through both methods of identification, and the total amount of faunal specimens analysed by zooarchaeologists (including teeth) for each layer and its cultural attribution at Bacho Kiro Cave, Les Cottés and La Ferrassie.

	Layer	Cultural attribution	ZooMS	Morphology	Total fauna (including teeth)
	1	Initial Upper	776	1077	5631
Bacho Kiro	J	Palaeolithic	433	232	776
	K	Middle Palaeolithic	337	143	606
	US04upper	Aurignacian	70	630	1609
Les Cottés	US04lower	Aufigliacian	168	715	2003
Les Cottes	US06	Châtelperronian	217	166	477
	US08	Mousterian	220	397	1080
La Ferrassie	6	Châtelperronian	527	142	809

SI Table 2: Count of ZooMS samples analysed for this study from Bacho Kiro Cave, Les Cottés and La Ferrassie per extraction protocols, and total of taxonomically unidentified specimens through ZooMS. Les Cottés specimens from Welker et al., 2015 are not included in the table.

	Bacho Kiro Cave	Les Cottés	La Ferrassie
Total ZooMS samples	1,595	523	527
AmBic protocol	1,595	523	527
Acid demineralisation	1 (0.06%)	369 (58.11%)	70 (13.28%)
Total unidentified	53 (3.32%)	16 (2.52%)	9 (1.71%)

SI Table 3: Body size classes adopted at Bacho Kiro Cave, La Ferrassie and Les Cottés for ungulates and carnivores (modified from Morin 2012). Birds, leporids, fishes and rodents are excluded from this table. For ungulates, Size 1 = Small, Size 2 = Small/Medium, Size 3 = Medium-Large, Size 4 = Large, Size 5 = megafauna For carnivores Size 1 = small, Size 2 and 3 = medium, Size 3 = Large.

	Size classes									
Size 1	Size 2	Size 3	Size 4	Size 5						
wolf (Canis lupus)	hyena (Crocuta	cave lion (Panthera	rhinoceros (Stephanorhinus	mammoth (Mammuthus						
won (Canis Iupus)	spelaea)	leo spelaea)	hemeiotechus)	primigenius)						
red fox (Vulpes	reindeer (Rangifer	leopard (Panthera	giant deer (Megaloceros							
vulpes)	tarandus)	pardus)	giganteus)							
dhole (Cuon	wild ass (Equus	bear (Ursus	Bos/Bison (Bison priscus, Bos							
alpinus)	hydruntinus)	spelaeus, Ursus	primigenius),							
roe deer (Capreolus capreolus)		horse (Equus ferus)								
goat (Caprinae sp.)		red deer (Cervus elaphus)								
fallow deer (Dama dama)		Cervidae sp.								
ibex (Capra ibex)										
pig (Sus scrofa)										

SI Table 4: Wilcoxon-Mann-Whitney tests of the comparison of glutamine deamidation of the peptide COL1α1 508-519 between layers from Les Cottés and Bacho Kiro Cave. The adjusted p value (P.adj.signif) is the smallest familywise significance level at which a particular comparison will be declared statistically significant as part of the multiple comparison testing, and was considered to address here the statistical comparison. The adjusted p-value significance symbols correspond to the following cutpoints: <1e-04: "****", <0.001: "****", <0.05: "*", >0.05: "ns".

Site	group1	group2	statistic	р	p.adj	p.adj.signif
Les Cottés	US04LOWER	US04UPPER	819	0.51	0.51	ns
Les Cottés	US04LOWER	US06	3383	0.000762	0.004	**
Les Cottés	US04LOWER	US08	5041	0.049	0.197	ns
Les Cottés	US04UPPER	US06	1277.5	0.23	0.46	ns
Les Cottés	US04UPPER	US08	1689	0.085	0.256	ns
Les Cottés	US06	US08	10287	1.80E-08	1.08E-07	****
Bacho Kiro Cave	I	J	122911	8.19E-11	8.19E-11	****
Bacho Kiro Cave	I	K	115535	1.05E-81	3.15E-81	****
Bacho Kiro Cave	J	K	70140.5	3.18E-63	6.36E-63	****

Measurement	Site	Layer	group1	group2	statistic	р	p.adj	p.adj.signif
Ambic_P1105	Les Cottés	US04UPPER	Bos/Bison	Equidae	13	0.641	0.641	ns
Ambic_P1105	Les Cottés	US04UPPER	Bos/Bison	Rangifer	1.5	0.241	0.482	ns
Ambic_P1105	Les Cottés	US04UPPER	Equidae	Rangifer	23.5	0.147	0.441	ns
Ambic_P1105	Les Cottés	US04LOWER	Bos/Bison	Equidae	434	0.147	0.294	ns
Ambic_P1105	Les Cottés	US04LOWER	Bos/Bison	Rangifer	22	0.205	0.294	ns
Ambic_P1105	Les Cottés	US04LOWER	Equidae	Rangifer	64	0.013	0.038	*
Ambic_P1105	Les Cottés	US06	Bos/Bison	Equidae	883.5	0.481	0.84	ns
Ambic_P1105	Les Cottés	US06	Bos/Bison	Rangifer	1025.5	0.28	0.84	ns
Ambic_P1105	Les Cottés	US06	Equidae	Rangifer	414.5	0.28	0.84	ns
Ambic_P1105	Les Cottés	US08	Bos/Bison	Equidae	813.5	0.236	0.507	ns
Ambic_P1105	Les Cottés	US08	Bos/Bison	Rangifer	350	0.477	0.507	ns
Ambic_P1105	Les Cottés	US08	Equidae	Rangifer	44	0.169	0.507	ns
Ambic_P1105	Bacho Kiro Cave	I	Bos/Bison	Capra sp.	7067.5	0.175	0.875	ns
Ambic_P1105	Bacho Kiro Cave	I	Bos/Bison	Cervid/Saiga	1438	0.349	0.956	ns
Ambic_P1105	Bacho Kiro Cave	I	Bos/Bison	Equidae	8839	0.078	0.465	ns
Ambic_P1105	Bacho Kiro Cave	I	Bos/Bison	Ursidae	32807	3.70E-16	3.70E-15	***
Ambic_P1105	Bacho Kiro Cave	I	Capra sp.	Cervid/Saiga	331	0.239	0.956	ns
Ambic_P1105	Bacho Kiro Cave	I	Capra sp.	Equidae	2104.5	0.02	0.136	ns
Ambic_P1105	Bacho Kiro Cave	I	Capra sp.	Ursidae	7641	1.56E-10	1.40E-09	***
Ambic_P1105	Bacho Kiro Cave	ı	Cervid/Saiga	Equidae	241.5	0.786	0.956	ns
Ambic_P1105	Bacho Kiro Cave	I	Cervid/Saiga	Ursidae	911	0.268	0.956	ns
Ambic_P1105	Bacho Kiro Cave	I	Equidae	Ursidae	6099.5	0.001	0.009	**
Ambic_P1105	Bacho Kiro Cave	J	Bos/Bison	Capra sp.	1695.5	0.164	0.656	ns
Ambic_P1105	Bacho Kiro Cave	J	Bos/Bison	Cervid/Saiga	2696	4.76E-06	4.28E-05	***
Ambic_P1105	Bacho Kiro Cave	J	Bos/Bison	Equidae	1665.5	0.002	0.018	*
Ambic_P1105	Bacho Kiro Cave	J	Bos/Bison	Ursidae	12377	6.29E-10	6.29E-09	***
Ambic_P1105	Bacho Kiro Cave	J	Capra sp.	Cervid/Saiga	625.5	0.007	0.052	ns
Ambic_P1105	Bacho Kiro Cave	J	Capra sp.	Equidae	375.5	0.116	0.58	ns
Ambic_P1105	Bacho Kiro Cave	J	Capra sp.	Ursidae	2850	0.008	0.052	ns
Ambic_P1105	Bacho Kiro Cave	J	Cervid/Saiga	Equidae	286.5	0.19	0.656	ns
Ambic_P1105	Bacho Kiro Cave	J	Cervid/Saiga	Ursidae	2422.5	0.457	0.732	ns
Ambic_P1105	Bacho Kiro Cave	J	Equidae	Ursidae	1969.5	0.366	0.732	ns
Ambic_P1105	Bacho Kiro Cave	К	Bos/Bison	Capra sp.	1630.5	0.59	1	ns
Ambic_P1105	Bacho Kiro Cave	K	Bos/Bison	Cervid/Saiga	1727.5	0.55	1	ns
Ambic_P1105	Bacho Kiro Cave	K	Bos/Bison	Equidae	1380.5	0.032	0.318	ns
Ambic_P1105	Bacho Kiro Cave	K	Bos/Bison	Ursidae	1531.5	0.47	1	ns
Ambic_P1105	Bacho Kiro Cave	K	Capra sp.	Cervid/Saiga	750	0.771	1	ns
Ambic_P1105	Bacho Kiro Cave	K	Capra sp.	Equidae	569	0.219	1	ns
Ambic_P1105	Bacho Kiro Cave	K	Capra sp.	Ursidae	644	0.867	1	ns
Ambic_P1105	Bacho Kiro Cave	K	Cervid/Saiga	Equidae	597.5	0.227	1	ns
Ambic_P1105	Bacho Kiro Cave	K	Cervid/Saiga	Ursidae	671	0.934	1	ns
Ambic_P1105	Bacho Kiro Cave	K	Equidae	Ursidae	360	0.223	1	ns
Ambic_P1106	La Ferrassie	6	Bos/Bison	Cervid/Saiga	4380.5	0.008	0.042	*
Ambic_P1107	La Ferrassie	6	Bos/Bison	Equidae	2831.5	0.574	1	ns
Ambic_P1108	La Ferrassie	6	Bos/Bison	Rangifer	25867.5	3.66E-08	2.20E-07	****
Ambic_P1109	La Ferrassie	6	Cervid/Saiga	Equidae	234.5	0.152	0.456	ns
Ambic_P1110	La Ferrassie	6	Cervid/Saiga	Rangifer	2339.5	0.833	1	ns
Ambic_P1111	La Ferrassie	6	Equidae	Rangifer	2264	0.046	0.182	ns

SI Table 6: Faunal spectrum of the ZooMS and morphology component from US04 (Upper and Lower), US06 and US08 of Les Cottés.

Les Cottés ZooMS	US04 L	JPPER	US04 L	.OWER	US	06	US	08
Taxon	NISP	%NISP	NISP	%NISP	NISP	%NISP	NISP	%NISP
Canidae	0	0.00	0	0.00	1	0.46	0	0.00
Felidae	0	0.00	0	0.00	1	0.46	0	0.00
Ursidae	0	0.00	0	0.00	1	0.46	0	0.00
Elephantidae	1	1.43	9	5.36	7	3.23	0	0.00
Rhinocerotidae	2	2.86	5	2.98	13	5.99	1	0.45
Equidae	46	65.71	106	63.10	40	18.42	37	16.82
Cervid/Saiga	0	0.00	2	1.19	9	4.17	3	1.36
Rangifer tarandus	15	21.43	16	9.52	48	22.12	15	6.82
Bos/Bison	5	7.14	30	17.86	86	39.63	163	74.09
Capra sp.	0	0.00	0	0.00	1	0.46	1	0.45
Caprinae (not capra sp.)	0	0.00	0	0.00	1	0.46	0	0.00
Suidae	0	0.00	0	0.00	1	0.46		
Bovidae	0	0.00	0	0.00	1	0.46	0	0.00
Bovidae/Cervidae	0	0.00	0	0.00	1	0.46	0	0.00
Capra sp./Rangifer	1	1.43	0	0.00	5	2.30	0	0.00
Caprinae	0	0.00	0	0.00	1	0.46	0	0.00
Total	70	100.00	168	100.00	217	100.00	220	100.00
Les Cottés Morphology	US04 L	JPPER	US04 L	.OWER	US06		US08	
Taxon	NISP	%NISP	NISP	%NISP	NISP	%NISP	NISP	%NISP
Lagomorpha	2	0.32	2	0.28	0	0.00	0	0.00
Canidae	2	0.32	4	0.56	0	0.00	4	1.01
Canidae (not Vulpes vulpes)	3	0.48	1	0.14	0	0.00	0	0.00
Elephantidae	4	0.64	0	0.00	4	2.41	4	1.01
Rhinocerotidae	0	0.00	1	0.14	0	0.00	2	0.50
Equidae	69	10.95	156	21.82	22	13.25	40	10.07
Cervid/Saiga	0	0.00	0	0.00	1	0.60	3	0.75
Rangifer tarandus	524	83.17	499	69.79	101	60.85	178	44.83
Bos/Bison	25	3.97	51	7.13	37	22.29	166	41.83
Capra sp.	1	0.16	0	0.00	1	0.60	0	0.00
Suidae	0	0.00	1	0.14	0	0.00	0	0.00
Total	630	100.00	715	100.00	166	100.00	397	100.00

SI Table 7: Faunal spectrum of the ZooMS and morphology component from Layers I, J and K of Bacho Kiro Cave.

Bacho Kiro Cave ZooMS	I		J		К	
Taxon	NISP	%NISP	NISP	%NISP	NISP	%NISP
Canidae	0	0.00	2	0.46	0	0.00
Felinae	0	0.00	3	0.69	1	0.30
Vulpes vulpes	0	0.00	0	0.00	3	0.89
Ursidae	223	28.74	174	40.12	46	13.69
Elephantidae	0	0.00	2	0.46	7	2.08
Rhinocerotidae	0	0.00	2	0.46	6	1.79
Equidae	84	10.82	25	5.76	31	9.23
Cervid/Saiga	12	1.55	37	8.63	50	14.88
Bos/Bison	357	46.01	117	26.96	111	33.04
Capra sp.	69	8.89	27	6.32	46	13.69
Caprinae (not C <i>apra</i> sp.)	2	0.26	3	0.69	1	0.30
Caprinae	2	0.26	6	1.38	13	3.87
Castor fiber	0	0.00	0	0.00	1	0.30
Felinae/Ursidae	4	0.52	26	5.99	6	1.69
Hyaenidae/Pantherinae/Mustelidae	8	1.03	0	0.00	5	1.38
Cervid/Saiga/Caprinae/Capreolus capreolus	0	0.00	1	0.23	2	0.60
Bovidae/Cervidae	1	0.13	0	0.00	0	0.00
Bovidae/Rangifer	3	0.39	0	0.00	0	0.00
Caprinae/ <i>Rangifer</i>	0	0.00	5	1.15	6	1.69
Capra sp./Rangifer	11	1.42	3	0.69	2	0.60
Total	776	100.00	433	100.00	337	100.00
Bacho Kiro Cave Morphology	I		J		K	
l=- '						
Taxon	NISP	%NISP	NISP	%NISP	NISP	%NISP
Canis sp.	NISP 5	%NISP 0.46	NISP 0	%NISP 0.00	NISP 0	%NISP 0.00
Canis sp. Canis lupus	5 12	0.46 1.11			0 4	
Canis sp.	5	0.46	0	0.00	0	0.00
Canis sp. Canis lupus	5 12	0.46 1.11	0 4	0.00 1.72	0 4	0.00 2.80
Canis sp. Canis lupus Crocuta spelaea	5 12 21	0.46 1.11 1.95	0 4 7	0.00 1.72 3.02	0 4 1	0.00 2.80 0.70
Canis sp. Canis lupus Crocuta spelaea Cuon alpinus	5 12 21 0	0.46 1.11 1.95 0.00	0 4 7 1	0.00 1.72 3.02 0.43	0 4 1 0	0.00 2.80 0.70 0.00
Canis sp. Canis lupus Crocuta spelaea Cuon alpinus Felidae	5 12 21 0 0	0.46 1.11 1.95 0.00 0.00	0 4 7 1	0.00 1.72 3.02 0.43 0.43	0 4 1 0	0.00 2.80 0.70 0.00 0.00
Canis sp. Canis lupus Crocuta spelaea Cuon alpinus Felidae Gulo gulo	5 12 21 0 0	0.46 1.11 1.95 0.00 0.00	0 4 7 1 1	0.00 1.72 3.02 0.43 0.43	0 4 1 0 0	0.00 2.80 0.70 0.00 0.00 0.00
Canis sp. Canis lupus Crocuta spelaea Cuon alpinus Felidae Gulo gulo Hyaena sp.	5 12 21 0 0 1	0.46 1.11 1.95 0.00 0.00 0.09 0.19	0 4 7 1 1 1	0.00 1.72 3.02 0.43 0.43 0.43	0 4 1 0 0 0	0.00 2.80 0.70 0.00 0.00 0.00
Canis sp. Canis lupus Crocuta spelaea Cuon alpinus Felidae Gulo gulo Hyaena sp. Panthera leo spelaeus	5 12 21 0 0 1 2	0.46 1.11 1.95 0.00 0.00 0.09 0.19	0 4 7 1 1 4	0.00 1.72 3.02 0.43 0.43 0.43 1.72 0.00	0 4 1 0 0 0 0	0.00 2.80 0.70 0.00 0.00 0.00 0.00
Canis sp. Canis lupus Crocuta spelaea Cuon alpinus Felidae Gulo gulo Hyaena sp. Panthera leo spelaeus Panthera pardus	5 12 21 0 0 1 2 5	0.46 1.11 1.95 0.00 0.00 0.09 0.19 0.46 0.09	0 4 7 1 1 4 0	0.00 1.72 3.02 0.43 0.43 0.43 1.72 0.00 0.43	0 4 1 0 0 0 0	0.00 2.80 0.70 0.00 0.00 0.00 0.00 0.00 3.50
Canis sp. Canis lupus Crocuta spelaea Cuon alpinus Felidae Gulo gulo Hyaena sp. Panthera leo spelaeus Panthera pardus Ursidae	5 12 21 0 0 1 2 5 1 263	0.46 1.11 1.95 0.00 0.09 0.19 0.46 0.09 24.42	0 4 7 1 1 4 0 1	0.00 1.72 3.02 0.43 0.43 1.72 0.00 0.43 66.38	0 4 1 0 0 0 0 0 0 5 38	0.00 2.80 0.70 0.00 0.00 0.00 0.00 3.50 26.57
Canis sp. Canis lupus Crocuta spelaea Cuon alpinus Felidae Gulo gulo Hyaena sp. Panthera leo spelaeus Panthera pardus Ursidae Vulpes vulpes	5 12 21 0 0 1 2 5 1 263 4	0.46 1.11 1.95 0.00 0.09 0.19 0.46 0.09 24.42 0.37	0 4 7 1 1 4 0 1 154	0.00 1.72 3.02 0.43 0.43 1.72 0.00 0.43 66.38 0.86	0 4 1 0 0 0 0 0 0 5 38	0.00 2.80 0.70 0.00 0.00 0.00 0.00 3.50 26.57
Canis sp. Canis lupus Crocuta spelaea Cuon alpinus Felidae Gulo gulo Hyaena sp. Panthera leo spelaeus Panthera pardus Ursidae Vulpes vulpes Mammuthus Primigenius	5 12 21 0 0 1 2 5 1 263 4	0.46 1.11 1.95 0.00 0.09 0.19 0.46 0.09 24.42 0.37 0.00	0 4 7 1 1 4 0 1 154 2	0.00 1.72 3.02 0.43 0.43 1.72 0.00 0.43 66.38 0.86 0.00	0 4 1 0 0 0 0 0 5 38 1	0.00 2.80 0.70 0.00 0.00 0.00 0.00 3.50 26.57 0.70
Canis sp. Canis lupus Crocuta spelaea Cuon alpinus Felidae Gulo gulo Hyaena sp. Panthera leo spelaeus Panthera pardus Ursidae Vulpes vulpes Mammuthus Primigenius Stephanorhinus hemiotechus	5 12 21 0 0 1 2 5 1 263 4 0	0.46 1.11 1.95 0.00 0.09 0.19 0.46 0.09 24.42 0.37 0.00	0 4 7 1 1 4 0 1 154 2	0.00 1.72 3.02 0.43 0.43 1.72 0.00 0.43 66.38 0.86 0.00 0.86	0 4 1 0 0 0 0 0 5 38 1 1	0.00 2.80 0.70 0.00 0.00 0.00 0.00 3.50 26.57 0.70 0.00
Canis sp. Canis lupus Crocuta spelaea Cuon alpinus Felidae Gulo gulo Hyaena sp. Panthera leo spelaeus Panthera pardus Ursidae Vulpes vulpes Mammuthus Primigenius Stephanorhinus hemiotechus Rhinoceros sp.	5 12 21 0 0 1 2 5 1 263 4 0 0	0.46 1.11 1.95 0.00 0.09 0.19 0.46 0.09 24.42 0.37 0.00 0.00	0 4 7 1 1 4 0 1 154 2 0	0.00 1.72 3.02 0.43 0.43 1.72 0.00 0.43 66.38 0.86 0.00 0.86 0.00	0 4 1 0 0 0 0 0 5 38 1 1 0	0.00 2.80 0.70 0.00 0.00 0.00 0.00 3.50 26.57 0.70 0.00 0.00
Canis sp. Canis lupus Crocuta spelaea Cuon alpinus Felidae Gulo gulo Hyaena sp. Panthera leo spelaeus Panthera pardus Ursidae Vulpes vulpes Mammuthus Primigenius Stephanorhinus hemiotechus Rhinoceros sp. Equidae	5 12 21 0 0 1 2 5 1 263 4 0 0 0	0.46 1.11 1.95 0.00 0.09 0.19 0.46 0.09 24.42 0.37 0.00 0.19 6.87	0 4 7 1 1 4 0 1 154 2 0 2	0.00 1.72 3.02 0.43 0.43 1.72 0.00 0.43 66.38 0.86 0.00 0.86 0.00 3.45	0 4 1 0 0 0 0 0 5 38 1 1 0 0	0.00 2.80 0.70 0.00 0.00 0.00 0.00 3.50 26.57 0.70 0.70 0.00 7.69
Canis sp. Canis lupus Crocuta spelaea Cuon alpinus Felidae Gulo gulo Hyaena sp. Panthera leo spelaeus Panthera pardus Ursidae Vulpes vulpes Mammuthus Primigenius Stephanorhinus hemiotechus Rhinoceros sp. Equidae Cervid/Saiga	5 12 21 0 0 1 2 5 1 263 4 0 0 2 74 309	0.46 1.11 1.95 0.00 0.09 0.19 0.46 0.09 24.42 0.37 0.00 0.00 0.19 6.87 28.69	0 4 7 1 1 4 0 1 154 2 0 2 0 8 15	0.00 1.72 3.02 0.43 0.43 1.72 0.00 0.43 66.38 0.86 0.00 0.86 0.00 3.45 6.465517	0 4 1 0 0 0 0 0 5 38 1 1 0 0 0	0.00 2.80 0.70 0.00 0.00 0.00 0.00 3.50 26.57 0.70 0.00 0.00 7.69 15.38
Canis sp. Canis lupus Crocuta spelaea Cuon alpinus Felidae Gulo gulo Hyaena sp. Panthera leo spelaeus Panthera pardus Ursidae Vulpes vulpes Mammuthus Primigenius Stephanorhinus hemiotechus Rhinoceros sp. Equidae Cervid/Saiga Bos/Bison	5 12 21 0 0 1 2 5 1 263 4 0 0 2 74 309 278	0.46 1.11 1.95 0.00 0.09 0.19 0.46 0.09 24.42 0.37 0.00 0.19 6.87 28.69 25.81	0 4 7 1 1 4 0 1 154 2 0 2 0 8 15 21	0.00 1.72 3.02 0.43 0.43 1.72 0.00 0.43 66.38 0.86 0.00 0.86 0.00 3.45 6.465517 9.05	0 4 1 0 0 0 0 0 5 38 1 1 0 0 0	0.00 2.80 0.70 0.00 0.00 0.00 0.00 3.50 26.57 0.70 0.00 7.69 15.38 26.57 13.99
Canis sp. Canis lupus Crocuta spelaea Cuon alpinus Felidae Gulo gulo Hyaena sp. Panthera leo spelaeus Panthera pardus Ursidae Vulpes vulpes Mammuthus Primigenius Stephanorhinus hemiotechus Rhinoceros sp. Equidae Cervid/Saiga Bos/Bison Capra sp.	5 12 21 0 0 1 2 5 1 263 4 0 0 2 74 309 278 92	0.46 1.11 1.95 0.00 0.09 0.19 0.46 0.09 24.42 0.37 0.00 0.19 6.87 28.69 25.81 8.54	0 4 7 1 1 4 0 1 154 2 0 2 0 8 15 21	0.00 1.72 3.02 0.43 0.43 1.72 0.00 0.43 66.38 0.86 0.00 0.86 0.00 3.45 6.465517 9.05 4.31	0 4 1 0 0 0 0 0 5 38 1 1 0 0 0 11 22 38 20	0.00 2.80 0.70 0.00 0.00 0.00 0.00 3.50 26.57 0.70 0.00 7.69 15.38 26.57
Canis sp. Canis lupus Crocuta spelaea Cuon alpinus Felidae Gulo gulo Hyaena sp. Panthera leo spelaeus Panthera pardus Ursidae Vulpes vulpes Mammuthus Primigenius Stephanorhinus hemiotechus Rhinoceros sp. Equidae Cervid/Saiga Bos/Bison Capra sp. Rupicapra rupicapra	5 12 21 0 0 1 2 5 1 263 4 0 0 2 74 309 278 92	0.46 1.11 1.95 0.00 0.09 0.19 0.46 0.09 24.42 0.37 0.00 0.19 6.87 28.69 25.81 8.54 0.09	0 4 7 1 1 4 0 1 154 2 0 2 0 8 15 21 10	0.00 1.72 3.02 0.43 0.43 1.72 0.00 0.43 66.38 0.86 0.00 0.86 0.00 3.45 6.465517 9.05 4.31 0.43	0 4 1 0 0 0 0 0 5 38 1 1 0 0 0 11 22 38 20	0.00 2.80 0.70 0.00 0.00 0.00 0.00 3.50 26.57 0.70 0.70 0.00 7.69 15.38 26.57 13.99 0.00

SI Table 8: Faunal spectrum of the ZooMS and morphology component from layer 6 at La Ferrassie.

La Ferrassie	Zoo	MS	Morph	nology
Taxon	NISP	%NISP	NISP	%NISP
Canidae	1	0.19	0	0.00
Mustelidae/Hyaenidae/Pantherinae	1	0.19	0	0.00
Ursidae	3	0.58	0	0.00
Elephantidae	1	0.19	0	0.00
Rhinocerotidae	6	1.16	0	0.00
Equidae	25	4.83	5	3.52
Cervid/Saiga	30	5.79	9	6.34
Capreolus capreolus	1	0.19	2	1.41
Rangifer tarandus	179	34.56	80	56.34
Bos/Bison	259	50.00	9	6.34
Capra sp.	3	0.58	0	0.00
Leporidae	0	0.00	1	0.70
Suidae	2	0.39	1	0.70
Caprinae/Muskox/Rangifer	1	0.19	0	0.00
Caprinae/Rangifer	6	1.16	0	0.00
Cervus/ <i>Rangifer</i>	0	0.00	35	24.65
Total	518	100.00	142	100.00

SI Table 9: Ecological diversity indices for each component (morphology and ZooMS) and the combination of both (morphology + ZooMS) of La Ferrassie (LF), Bacho Kiro Cave (BK) and Les Cottés (CTS). The table includes values of the Shannon-Wiener Index (H), Pielou's Evenness (J), NISP (number of identified specimens), NTAXA (number of taxa) and confidence intervals for the Shannon's index.

Site	Layer	Method of Identification	Shannon- Wiener Index	Evenness	NISP	NTAXA	Shannon Index 2.5%	Shannon Index 97.5%
BK	I	Morphology	1.687	0.679	1077	15	1.635	1.729
BK	I	ZooMS	1.307	0.672	755	10	1.248	1.36
BK	I	Morphology+ZooMS	1.628	0.655	1832	15	1.589	1.66
BK	J	Morphology	1.276	0.554	232	13	1.103	1.416
BK	J	ZooMS	1.473	0.614	393	14	1.363	1.549
BK	J	Morphology+ZooMS	1.475	0.575	625	16	1.372	1.553
BK	K	Morphology	1.827	0.793	143	13	1.662	1.916
BK	K	ZooMS	1.793	0.721	308	15	1.674	1.872
BK	K	Morphology+ZooMS	1.842	0.698	451	17	1.742	1.904
LF	Layer 6	Morphology	1.266	0.609	142	11	1.057	1.399
LF	Layer 6	ZooMS	1.209	0.487	511	15	1.106	1.278
LF	Layer 6	Morphology+ZooMS	1.381	0.523	653	17	1.288	1.449
CTS	US04UPPER	Morphology	0.628	0.302	630	11	0.536	0.706
CTS	US04UPPER	ZooMS	0.938	0.583	67	8	0.679	1.123
CTS	US04UPPER	Morphology+ZooMS	0.746	0.339	697	12	0.662	0.82
CTS	US04LOWER	Morphology	0.845	0.406	715	11	0.774	0.905
CTS	US04LOWER	ZooMS	1.136	0.634	168	9	0.965	1.269
CTS	US04LOWER	Morphology+ZooMS	1.042	0.453	883	13	0.973	1.092
CTS	US06	Morphology	1.056	0.589	166	9	0.917	1.171
CTS	US06	ZooMS	1.595	0.642	209	15	1.432	1.702
CTS	US06	Morphology+ZooMS	1.454	0.585	375	15	1.34	1.53
CTS	US08	Morphology	1.112	0.571	397	10	1.009	1.185
CTS	US08	ZooMS	0.813	0.454	220	9	0.671	0.932
CTS	US08	Morphology+ZooMS	1.105	0.532	617	11	1.031	1.167

SI Table 10: Proportions (%NISP) of the dominant taxa within the ZooMS and morphology components per layers of Les Cottés and La Ferrassie. Numbers in brackets indicate the NISP for each category.

La Ferrassie		ZooMS	Morph
Bos/Bison		53% (259)	9% (9)
Rangifer tarandus		36% (179)	78% (80)
Les Cottés			
Bos/Bison	US04 UPPER	5% (3)	4% (25)
	US04 LOWER	17% (25)	7% (51)
	US06	49% (81)	23% (37)
	US08	76% (152)	43% (166)
	US04 UPPER	23% (14)	85% (524)
Panaifor tarandus	US04 LOWER	11% (16)	71% (499)
Rangifer tarandus	US06	29% (48)	63% (101)
	US08	7% (13)	46% (178)
	US04 UPPER	72% (43)	11% (69)
Equidos	US04 LOWER	71% (102)	22% (156)
Equidae	US06	22% (37)	14% (22)
	US08	17% (34)	10% (40)

SI Table 11: Wilcoxon-Mann-Whitney tests of the comparison of bone length distribution between taxa and layers at Bacho Kiro Cave. The adjusted p-value significance symbols correspond to the following cutpoints: <1e-04: "****", <0.001: "***", <0.01: "**", <0.05: "*", >0.05: ns".

Method of Identification	Layer	Measurement	group1	group2	statistic	р	p.adj	p.adj.signif
Morphology	I	BONE_LENGTH	Bos/Bison	Capra sp.	21838.5	2.43E-23	2.43E-22	****
Morphology	I	BONE_LENGTH	Bos/Bison	Cervid/Saiga	47846	0.009	0.027	*
Morphology	I	BONE_LENGTH	Bos/Bison	Equidae	11694.5	0.07	0.141	ns
Morphology	I	BONE_LENGTH	Bos/Bison	Ursidae	49553.5	8.58E-13	6.86E-12	****
Morphology	1	BONE_LENGTH	Capra sp.	Cervid/Saiga	5853.5	8.05E-18	7.24E-17	****
Morphology	1	BONE_LENGTH	Capra sp.	Equidae	1435.5	1.05E-10	7.35E-10	****
Morphology	1	BONE_LENGTH	Capra sp.	Ursidae	7946	5.14E-07	3.08E-06	***
Morphology	I	BONE_LENGTH	Cervid/Saiga	Equidae	11468.5	0.863	0.863	ns
Morphology	1	BONE_LENGTH	Cervid/Saiga	Ursidae	49698.5	1.31E-06	6.55E-06	***
Morphology	I	BONE_LENGTH	Equidae	Ursidae	11929.5	0.003	0.012	*
ZooMS	I	BONE_LENGTH	Bos/Bison	Capra sp.	12239	0.293	1	ns
ZooMS	I	BONE_LENGTH	Bos/Bison	Cervid/Saiga	1341.5	0.593	1	ns
ZooMS	ı	BONE LENGTH	Bos/Bison	Equidae	14313.5	0.3	1	ns
ZooMS	I	BONE_LENGTH	Bos/Bison	Ursidae	33623	0.508	1	ns
ZooMS	I	BONE LENGTH	Capra sp.	Cervid/Saiga	248	0.362	1	ns
ZooMS	ı	BONE LENGTH	Capra sp.	Equidae	2701		1	ns
ZooMS	ı	BONE_LENGTH	Capra sp.	Ursidae	6257.5			ns
ZooMS	ı	BONE LENGTH	Cervid/Saiga	Equidae	431			ns
ZooMS	i	BONE LENGTH	Cervid/Saiga	Ursidae	1028.5			ns
ZooMS	i	BONE LENGTH	Equidae	Ursidae	7420			ns
Morphology	j	BONE LENGTH	Bos/Bison	Capra sp.	201			**
Morphology	J	BONE LENGTH	Bos/Bison	Cervid/Saiga	184			ns
Morphology	J	BONE_LENGTH	Bos/Bison	Equidae	107			ns
Morphology	J	BONE LENGTH	Bos/Bison	Ursidae	2570.5			***
Morphology	J	BONE_LENGTH	Capra sp.	Cervid/Saiga	60		0.000121	ns
	J		Capra sp.	Equidae	24			
Morphology Morphology	J	BONE_LENGTH		Ursidae	635			ns
Morphology	J	BONE_LENGTH	Capra sp.					ns
Morphology	J	BONE_LENGTH	Cervid/Saiga	Equidae	42			ns
Morphology		BONE_LENGTH	Cervid/Saiga	Ursidae	1000			ns
Morphology	J	BONE_LENGTH	Equidae	Ursidae	751	0.298		ns
ZooMS	J	BONE_LENGTH	Bos/Bison	Capra sp.	1152.5			ns
ZooMS	J	BONE_LENGTH	Bos/Bison	Cervid/Saiga	1666.5			ns
ZooMS	J	BONE_LENGTH	Bos/Bison	Equidae	1546			ns
ZooMS	J	BONE_LENGTH	Bos/Bison	Ursidae	8932			ns
ZooMS	J	BONE_LENGTH	Capra sp.	Cervid/Saiga	506			ns
ZooMS	J	BONE_LENGTH	Capra sp.	Equidae	466			ns
ZooMS	J	BONE_LENGTH	Capra sp.	Ursidae	2681			ns
ZooMS	J	BONE_LENGTH	Cervid/Saiga	Equidae	473.5			ns
ZooMS	J	BONE_LENGTH	Cervid/Saiga	Ursidae	2754			ns
ZooMS	J	BONE_LENGTH	Equidae	Ursidae	1734.5		0.714	ns
Morphology	K	BONE_LENGTH	Bos/Bison	Capra sp.	510	0.033	0.266	ns
Morphology	K	BONE_LENGTH	Bos/Bison	Cervid/Saiga	365			
Morphology	K	BONE_LENGTH	Bos/Bison	Equidae	161	0.259	1	ns
Morphology	K	BONE_LENGTH	Bos/Bison	Ursidae	843	0.212	1	ns
Morphology	K	BONE_LENGTH	Capra sp.	Cervid/Saiga	120	0.011	0.1	ns
Morphology	K	BONE_LENGTH	Capra sp.	Equidae	39	0.003	0.025	*
Morphology	K	BONE_LENGTH	Capra sp.	Ursidae	333.5	0.452	1	ns
Morphology	K	BONE_LENGTH	Cervid/Saiga	Equidae	110	0.693	1	ns
Morphology	K	BONE_LENGTH	Cervid/Saiga	Ursidae	541	0.06	0.419	ns
Morphology	K	BONE_LENGTH	Equidae	Ursidae	276	0.112	0.672	ns
ZooMS	K	BONE_LENGTH	Bos/Bison	Capra sp.	1520.5	0.934	1	ns
ZooMS	K	BONE_LENGTH	Bos/Bison	Cervid/Saiga	1276	0.3	1	ns
ZooMS	K	BONE_LENGTH	Bos/Bison	Equidae	1025.5	0.706	1	ns
ZooMS	K	BONE_LENGTH	Bos/Bison	Ursidae	1488			ns
ZooMS	K	BONE_LENGTH	Capra sp.	Cervid/Saiga	564			ns
ZooMS	K	BONE LENGTH	Capra sp.	Equidae	465			ns
ZooMS	K	BONE_LENGTH	Capra sp.	Ursidae	657			ns
ZooMS	K	BONE_LENGTH	Cervid/Saiga	Equidae	486			ns
ZooMS	K	BONE_LENGTH	Cervid/Saiga	Ursidae	697			ns
LOUIVIO	15	DOTAL_FEMOLIA	Con vita, Saiga	Ursidae	037	0.223	1	115

SI Table 12: Wilcoxon-Mann-Whitney tests of the comparison of bone length distribution between taxa and layers at Les Cottés. The adjusted p-value significance symbols correspond to the following cutpoints: <1e-04: "****", <0.001: "***", <0.01: "***", <0.05: "*", >0.05: "ns".

Method of								
Identification	Layer	Measurement	group1	group2	statistic	р	p.adj	p.adj.signif
Morphology	US04UPPER	Bone length	Bos/Bison	Equidae	982.5	0.306	0.306	ns
Morphology	US04UPPER	Bone length	Bos/Bison	Rangifer	8961	0.002	0.004	**
Morphology	US04UPPER	Bone length	Equidae	Rangifer	23096	0.000176	0.000528	***
Morphology	US04LOWER	Bone length	Bos/Bison	Equidae	3611.5	0.294	0.588	ns
Morphology	US04LOWER	Bone length	Bos/Bison	Rangifer	13259.5	0.638	0.638	ns
Morphology	US04LOWER	Bone length	Equidae	Rangifer	44674	0.009	0.027	*
Morphology	US06	Bone length	Bos/Bison	Equidae	339.5	0.193	0.386	ns
Morphology	US06	Bone length	Bos/Bison	Rangifer	1959.5	0.731	0.731	ns
Morphology	US06	Bone length	Equidae	Rangifer	1473	0.056	0.169	ns
Morphology	US08	Bone length	Bos/Bison	Equidae	3055.5	0.25	0.25	ns
Morphology	US08	Bone length	Bos/Bison	Rangifer	21367.5	2.94E-09	8.82E-09	****
Morphology	US08	Bone length	Equidae	Rangifer	5333.5	2.83E-06	5.66E-06	****
ZooMS	US04UPPER	Bone length	Bos/Bison	Equidae	43	0.057	0.17	ns
ZooMS	US04UPPER	Bone length	Bos/Bison	Rangifer	10	0.429	0.67	ns
ZooMS	US04UPPER	Bone length	Equidae	Rangifer	139	0.335	0.67	ns
ZooMS	US04LOWER	Bone length	Bos/Bison	Equidae	1228.5	0.169	0.507	ns
ZooMS	US04LOWER	Bone length	Bos/Bison	Rangifer	119.5	0.222	0.507	ns
ZooMS	US04LOWER	Bone length	Equidae	Rangifer	390	0.702	0.702	ns
ZooMS	US06	Bone length	Bos/Bison	Equidae	694	0.622	1	ns
ZooMS	US06	Bone length	Bos/Bison	Rangifer	569.5	0.981	1	ns
ZooMS	US06	Bone length	Equidae	Rangifer	242	0.829	1	ns
ZooMS	US08	Bone length	Bos/Bison	Equidae	2031	0.725	1	ns
ZooMS	US08	Bone length	Bos/Bison	Rangifer	681.5	0.411	1	ns
ZooMS	US08	Bone length	Equidae	Rangifer	137.5	0.947	1	ns

SI Table 13: Wilcoxon-Mann-Whitney tests of the comparison of bone length distribution between method of identification, taxa and layers at Les Cottés. The adjusted p-value significance symbols correspond to the following cutpoints: <1e-04: "***", <0.001: "***", <0.05: "*", >0.05: "ns".

Layer	Taxon	Measurement	group1	group2	statistic	р	p.signif
US04LOWER	Bos/Bison	Bone length	Morphology	ZooMS	534	0.543	ns
US04LOWER	Equidae	Bone length	Morphology	ZooMS	8049.5	0.0686	ns
US04LOWER	Rangifer	Bone length	Morphology	ZooMS	2159	0.7	ns
US04UPPER	Bos/Bison	Bone length	Morphology	ZooMS	101.5	0.032	*
US04UPPER	Equidae	Bone length	Morphology	ZooMS	1564.5	0.0566	ns
US04UPPER	Rangifer	Bone length	Morphology	ZooMS	1815.5	0.515	ns
US06	Bos/Bison	Bone length	Morphology	ZooMS	919.5	0.523	ns
US06	Equidae	Bone length	Morphology	ZooMS	333	0.229	ns
US06	Rangifer	Bone length	Morphology	ZooMS	975.5	0.523	ns
US08	Bos/Bison	Bone length	Morphology	ZooMS	13575	0.00202	**
US08	Equidae	Bone length	Morphology	ZooMS	838.5	0.00471	**
US08	Rangifer	Bone length	Morphology	ZooMS	715	0.538	ns

SI Table 14: Wilcoxon-Mann-Whitney tests of the comparison of bone length distribution between taxa at La Ferrassie. The adjusted p-value significance symbols correspond to the following cutpoints: <1e-04: "****", <0.001: "***", <0.01: "**", <0.05: "*", >0.05: "ns".

Method of							
Identification	Measurement	group1	group2	statistic	р	p.adj	p.adj.signif
ZooMS	BONE_LENGTH	Bos/Bison	Cervid/Saiga	2412	0.127	0.381	ns
ZooMS	BONE_LENGTH	Bos/Bison	Equidae	3529.5	0.02	0.098	ns
ZooMS	BONE_LENGTH	Bos/Bison	Rangifer	22524	0.92	0.92	ns
ZooMS	BONE_LENGTH	Cervid/Saiga	Equidae	415	0.008	0.047	*
ZooMS	BONE_LENGTH	Cervid/Saiga	Rangifer	2803.5	0.13	0.381	ns
ZooMS	BONE_LENGTH	Equidae	Rangifer	1577.5	0.032	0.128	ns

SI Table 15: Percentage of specimens displaying low weathering (stage 0-2) or high weathering (3-5) based on the study by Behrensmeyer (1978) for the dominant taxa in layers I, J and K at Bacho Kiro Cave.

Bacho Kiro Cave		Low weathering			High weathering		
		I	J	K	I	J	K
Bos/Bison	ZooMS	100 (333)	97.43 (114)	100 (83)	0 (0)	2.56 (3)	0 (0)
	Morphology	98.92 (275)	95.24 (20)	100 (38)	1.08 (3)	4.76 (1)	0 (0)
Capra sp.	ZooMS	100 (68)	100 (27)	100 (37)	0 (0)	0 (0)	0 (0)
	Morphology	100 (93)	100 (11)	100 (20)	0 (0)	0 (0)	0 (0)
Cervid/Saiga	ZooMS	100 (9)	100 (32)	100 (35)	0 (0)	0 (0)	0 (0)
	Morphology	99.35 (304)	100 (13)	100 (22)	0.65 (2)	0 (0)	0 (0)
Equidae	ZooMS	100 (80)	96.00 (24)	100 (26)	0 (0)	4.00 (1)	0 (0)
	Morphology	100 (74)	100 (8)	100 (11)	0 (0)	0 (0)	0 (0)
Ursidae	ZooMS	100 (209)	98.28 (171)	100 (34)	0 (0)	1.72 (3)	0 (0)
	Morphology	99.24 (261)	100 (154)	100 (38)	0.76 (2)	0 (0)	0 (0)

SI Table 16: Percentage of specimens displaying low weathering (stage 0-2) or high weathering (3-5) based on the study by Behrensmeyer (1978) for the dominant taxa at La Ferrassie.

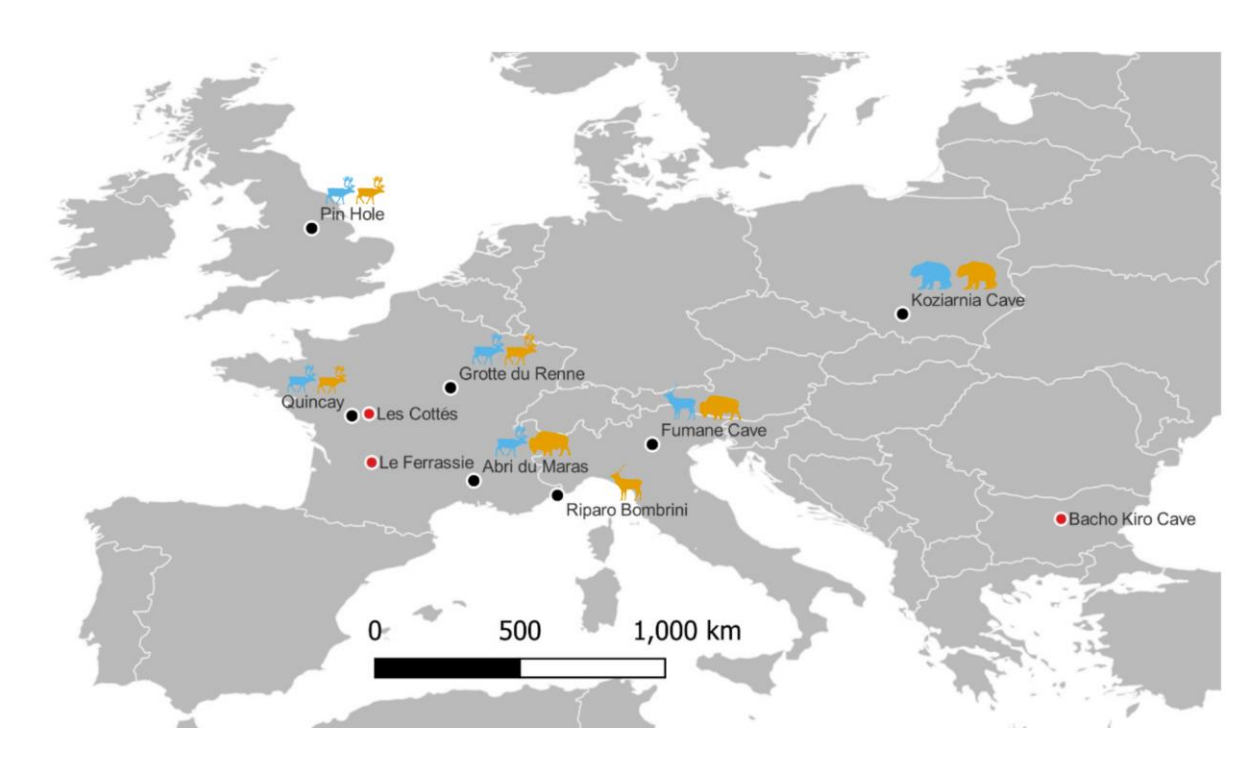
La Ferrassie		Low weathering	High weathering	
Bos/Bison	ZooMS	98.23% (222)	1.77% (4)	
	Morphology	100% (4)	0 (0)	
Cervid/ <i>Saiga</i>	ZooMS	94.74% (18)	5.26% (1)	
	Morphology	100% (3)	0 (0)	
Equidae	ZooMS	100% (23)	0 (0)	
	Morphology	100% (2)	0 (0)	
Rangifer	ZooMS	99.30% (141)	0.70% (1)	
	Morphology	100% (46)	0 (0)	

SI Table 17: Number of specimens identified as carnivore (ZooMS or Morphology) showing anthropogenic bone surface modifications at Bacho Kiro Cave and Les Cottés.

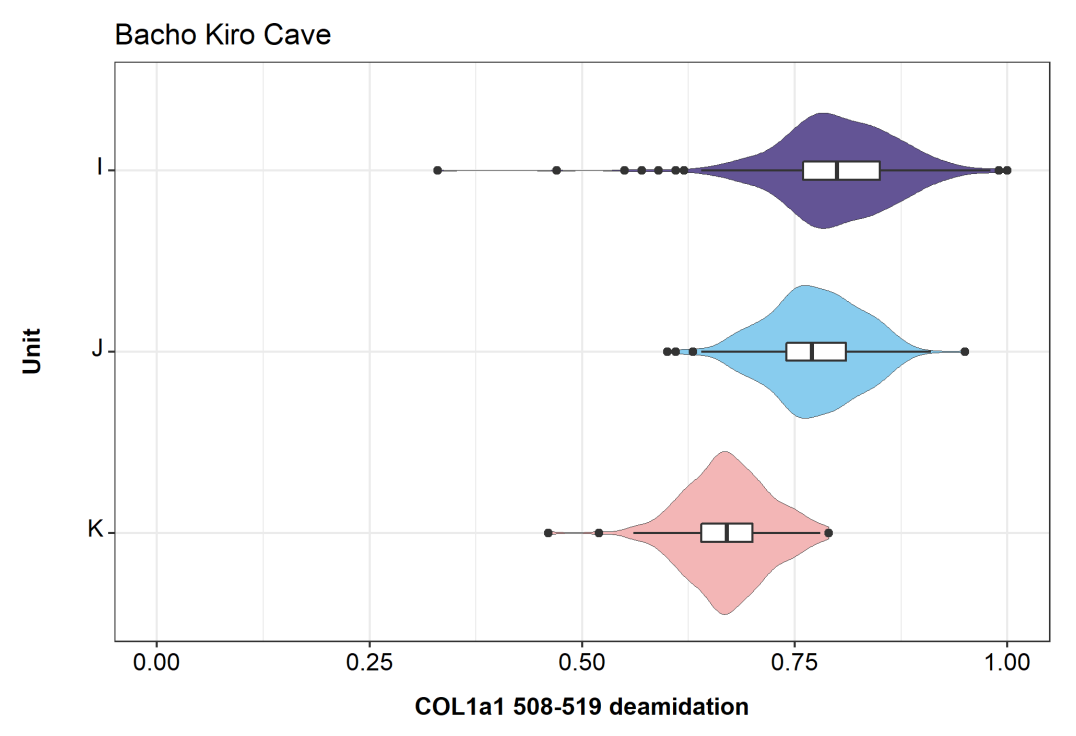
	Method of			
Site	Identification	Layer	Taxon	NISP
Bacho Kiro Cave	Morphology	I	Canis lupus	3
Bacho Kiro Cave	Morphology	I	Crocuta spelaea	3
Bacho Kiro Cave	Morphology	I	Panthera (leo) spelaea	1
Bacho Kiro Cave	Morphology	I	Ursidae	42
Bacho Kiro Cave	Morphology	I	Vulpes vulpes	1
Bacho Kiro Cave	Morphology	J	Crocuta spelaea	1
Bacho Kiro Cave	Morphology	J	Ursidae	1
Bacho Kiro Cave	Morphology	K	Panthera pardus	2
Bacho Kiro Cave	ZooMS	I	Hyaenidae/Pantherinae/Mustelidae	1
Bacho Kiro Cave	ZooMS	I	Ursidae	25
Bacho Kiro Cave	ZooMS	J	Felinae/Ursidae	2
Bacho Kiro Cave	ZooMS	J	Ursidae	13
Les Cottés	Morphology	US04UPPER	Canidae	1
Les Cottés	Morphology	US08	Canidae	1

SI Table 18: Percentages of the identified axial bone elements among methods of identification at Bacho Kiro Cave (morphology and ZooMS).

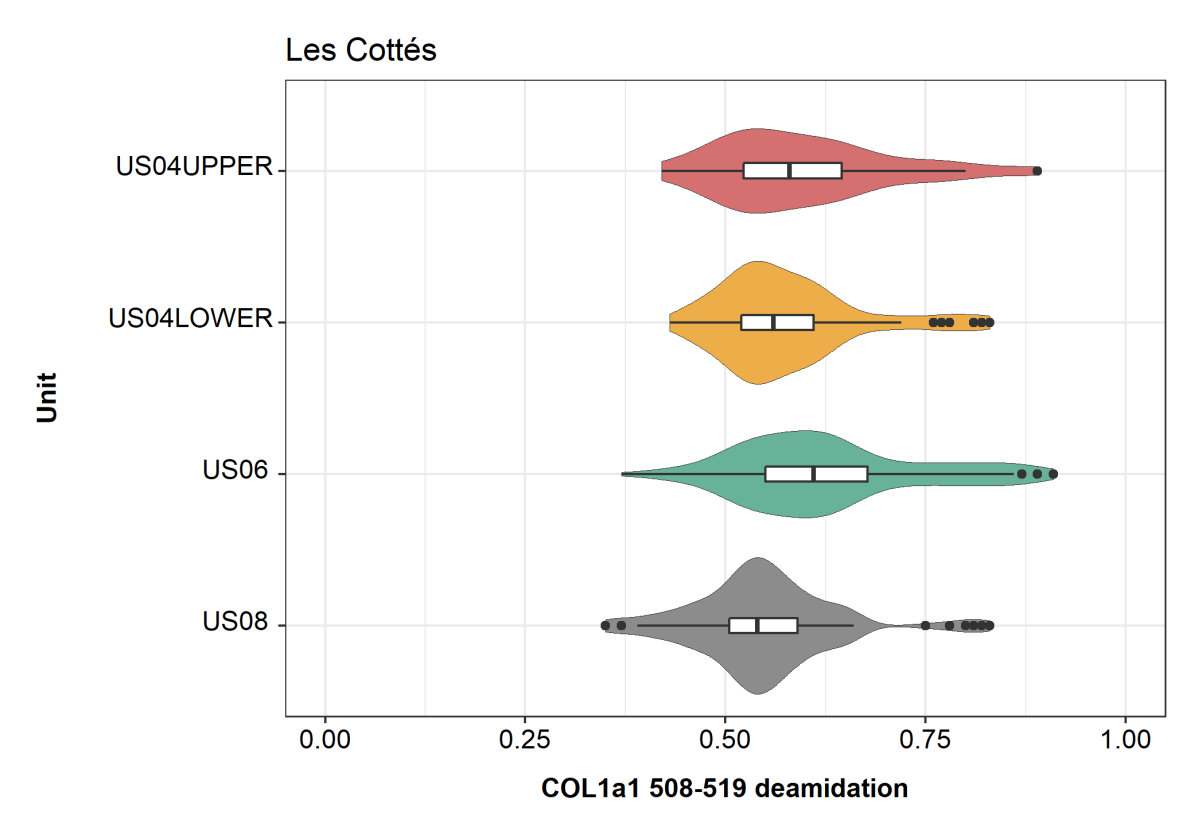
Skeletal Elements	Method of Identification	NISP	%NISP
Acetabulum	Morphology	6	100
Atlas	Morphology	3	100
Axis	Morphology	4	80
Ischium	Morphology	4	100
Rib	Morphology	36	18.85
Scapula	Morphology	9	75
Vertebrae Caudal	Morphology	1	100
Vertebrae Cervical	Morphology	8	72.73
Vertebrae Lumbar	Morphology	3	75
Vertebrae Thoracic	Morphology	10	100
Axis	ZooMS	1	20
Ilium	ZooMS	1	100
Rib	ZooMS	155	81.15
Scapula	ZooMS	3	25
Sternabrae	ZooMS	1	100
Vertebrae Cervical	ZooMS	3	27.27
Vertebrae Indeterminate	ZooMS	28	100
Vertebrae Lumbar	ZooMS	1	25



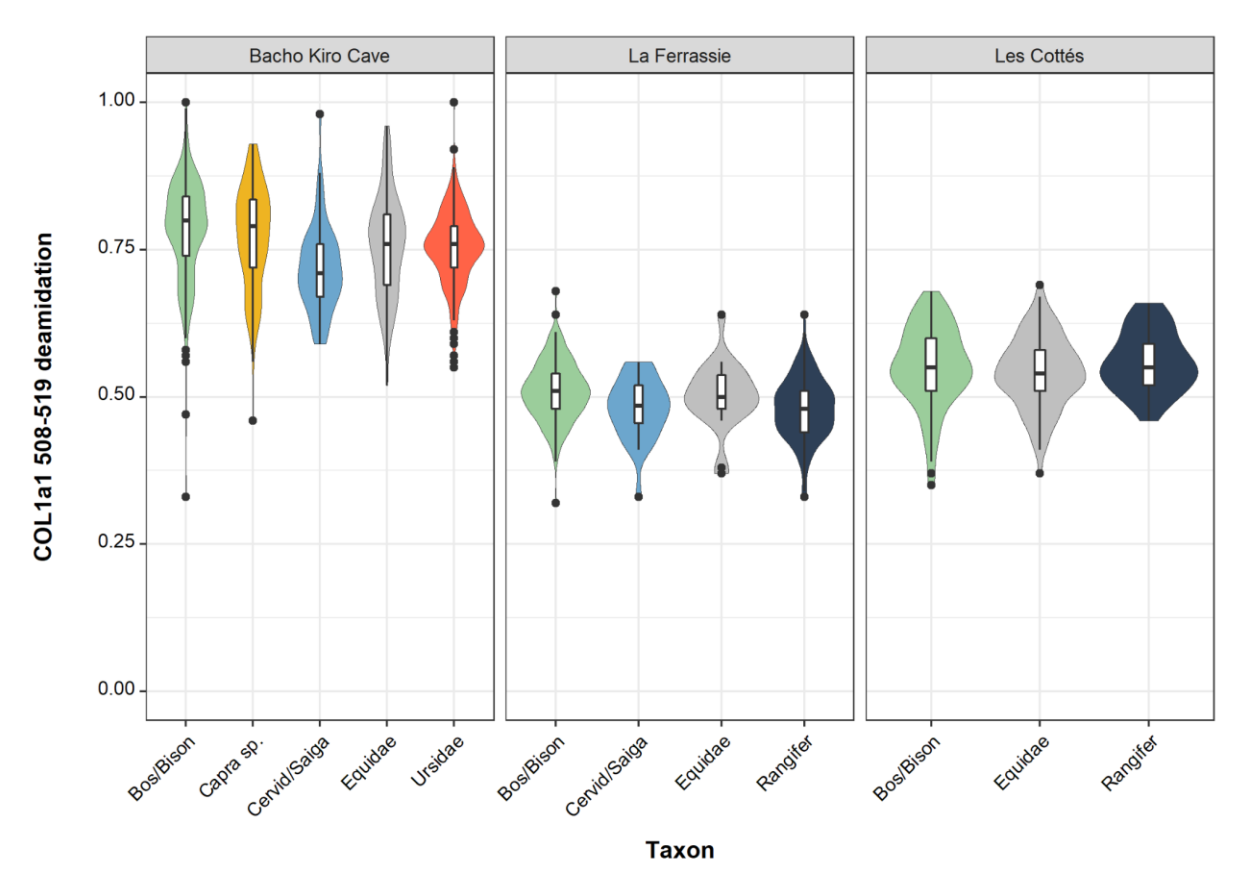
SI Figure 1: Site location of Bacho Kiro Cave, Les Cottés and La Ferrassie (red dots) and other published european non-targeted ZooMS studies with zooarchaeological data available for the same archaeological layers. For each site (Pin Hole Cave (UK)(Buckley et al., 2017), Quinçay (France)(Welker et al., 2017), Grotte du Renne (France)(Welker et al., 2016), Abri du Maras (France)(Ruebens et al., 2022), Fumane Cave (Italy)(Sinet-Mathiot et al., 2019), Riparo Bombrini(Pothier Bouchard et al., 2020) and Koziarnia Cave (Poland)(Berto et al., 2021)), animal silhouettes (phylopic.org) indicate the dominant taxa in each component (ZooMS: orange and morphology: blue), although the complete faunal spectrum of each sites includes various taxa. The morphology component from Riparo Bombrini is not illustrated on the map as it is represented by a low NISP (<20 morphologically identified specimens).



SI Figure 2: Peptide deamidation (all taxa combined) obtained for layers I, J and K at Bacho Kiro Cave. Sample sizes for each layer are K (n = 219), J (n = 349) and I (n = 561).



SI Figure 3: Peptide deamidation (all taxa combined) obtained for US04 Upper, US04 Lower, US06 and US08 at Les Cottés. Sample sizes for each layer are US08 (n = 115), US06 (n = 126), US04LOWER (n = 75) and US04UPPER (n = 24).



SI Figure 4: Peptide deamidation of the dominant taxa for all studied layers at Bacho Kiro Cave, Les Cottés and La Ferrassie.

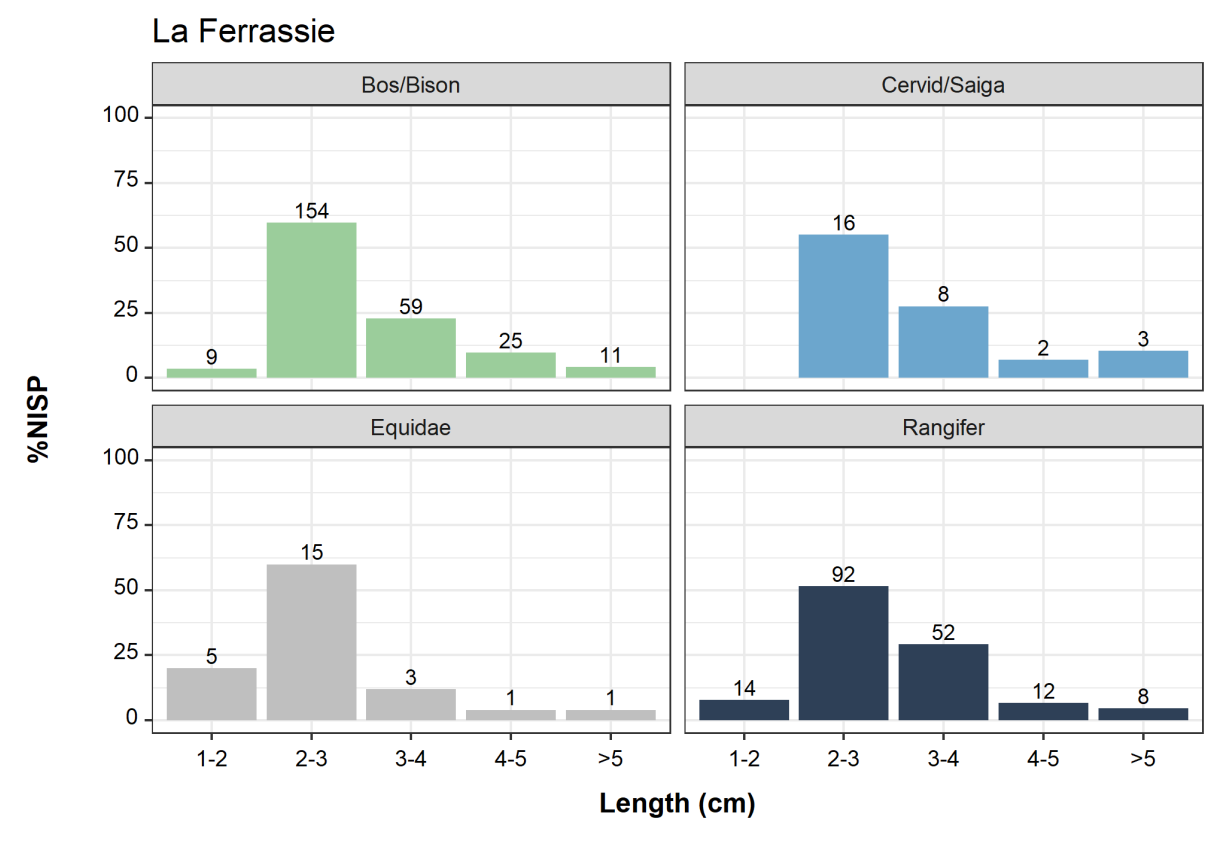
Bacho Kiro Cave Bos/Bison Capra sp. Cervid/Saiga Equidae Ursidae 28 >5 -29 43 4-5 -36 13 84 49 3-4 -2-3 183 39 13 36 16 >5 26 4-5 23 31 3-4 38 13 13 54 9 50 2-3 >5 -10 18 12 10 10 4-5 -3-4 -2-3 -40% 0% 40% 40% 0% 40% 40% 0% 40% 40% 0% 40% 40% 0% 40%

SI Figure 5: Bone length distribution of the dominant taxa within the ZooMS (orange) and the Morphology (blue) dataset for Layers I, J and K at Bacho Kiro Cave. Numbers on the bars are the NISP for each size class.

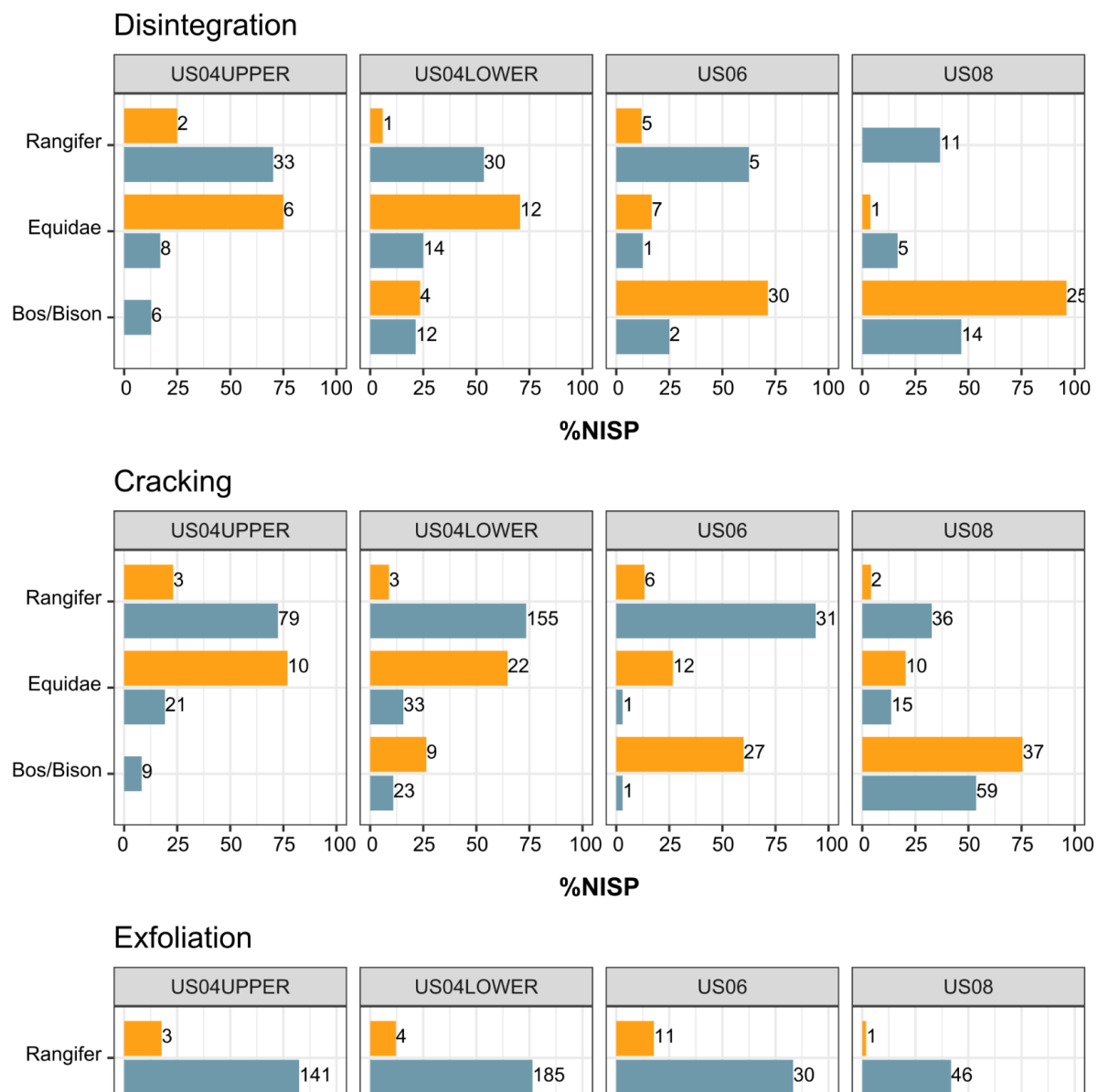
%NISP

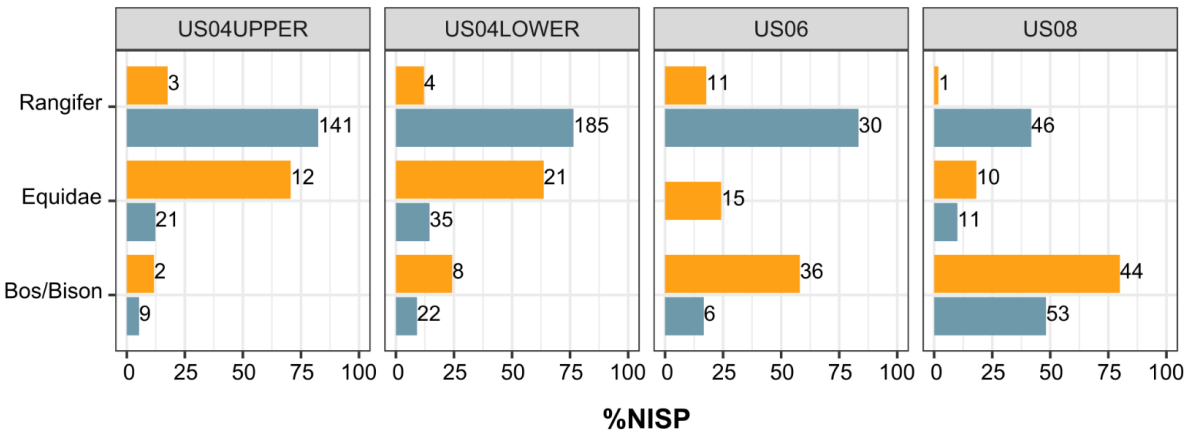
Les Cottés Bos/Bison Rangifer Equidae 11 26 88 14 US04UPPER >5 -4-5 13 13 131 3-4 -12 13 9 137 2-3 - 2 103 **US04LOWER** 15 3 3 >5 -10 18 15 67 4-5 -33 3-4 -Length (cm) 28 39 137 2-3 -10 5 >5 -4-5 6 US06 5 3-4 -23 6 11 36 20 2-3 -38 24 >5 -9 31 26 4-5 US08 3-4 -29 61 2-3 -50% 100% 50% 50% 100% 50% 100% 50% 0% 0% 0% 50% %NISP

SI Figure 6: Bone length distribution of the dominant taxa within the ZooMS (orange) and the Morphology (blue) dataset for US04 (Upper and Lower), US06 and US08 at Les Cottés. Numbers on the bars are the NISP for each size class.



SI Figure 7: Bone length distribution of the dominant taxa within the ZooMS dataset at La Ferrassie. Numbers on the bars are the NISP for each size class.



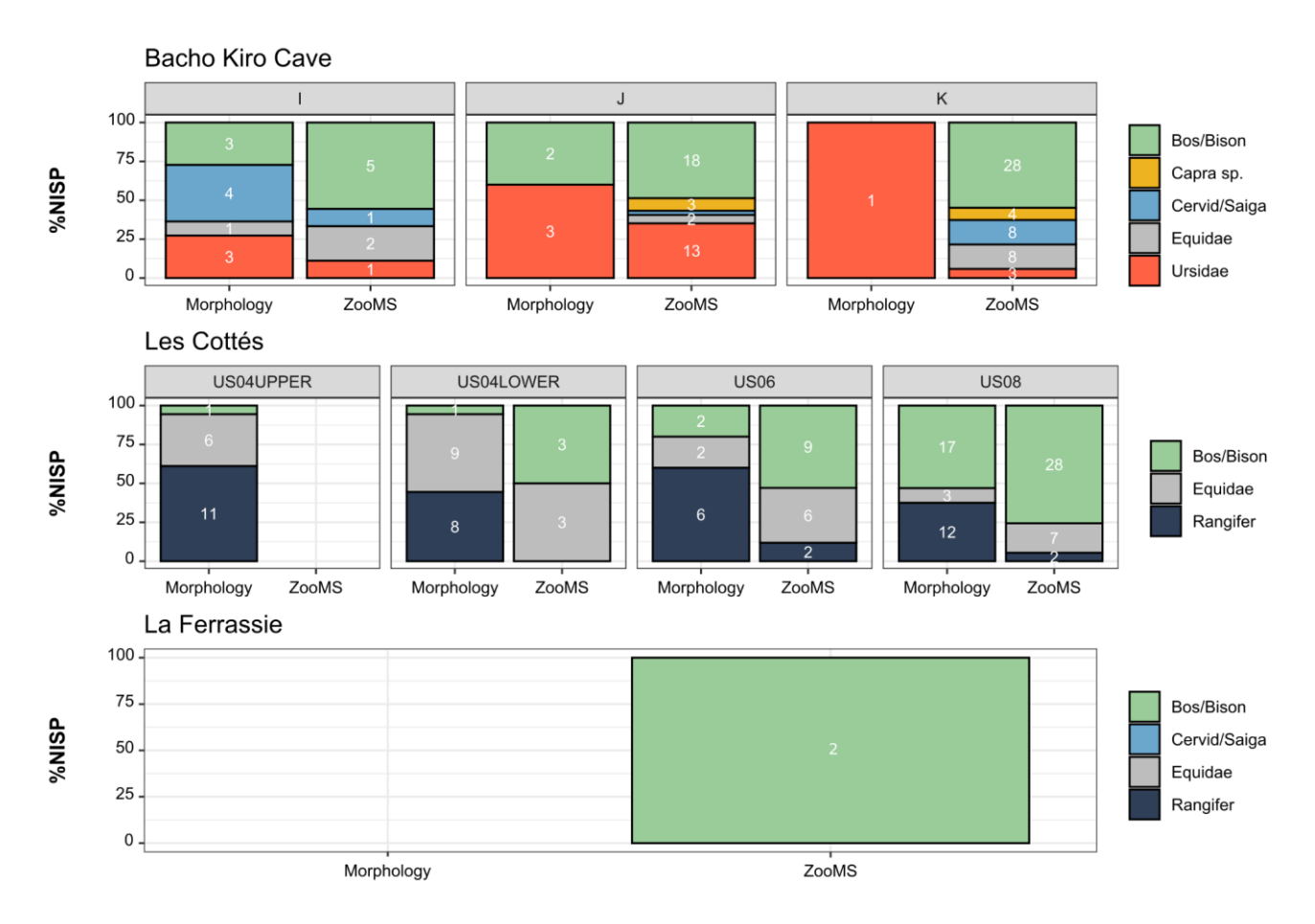


SI Figure 8: Percentage of disintegration, cracking and exfoliation on dominant taxa specimens in ZooMS (orange) and Morphology (blue) datasets from US04, US06 and US08 at Les Cottés. Numbers on the bars are the NISP.

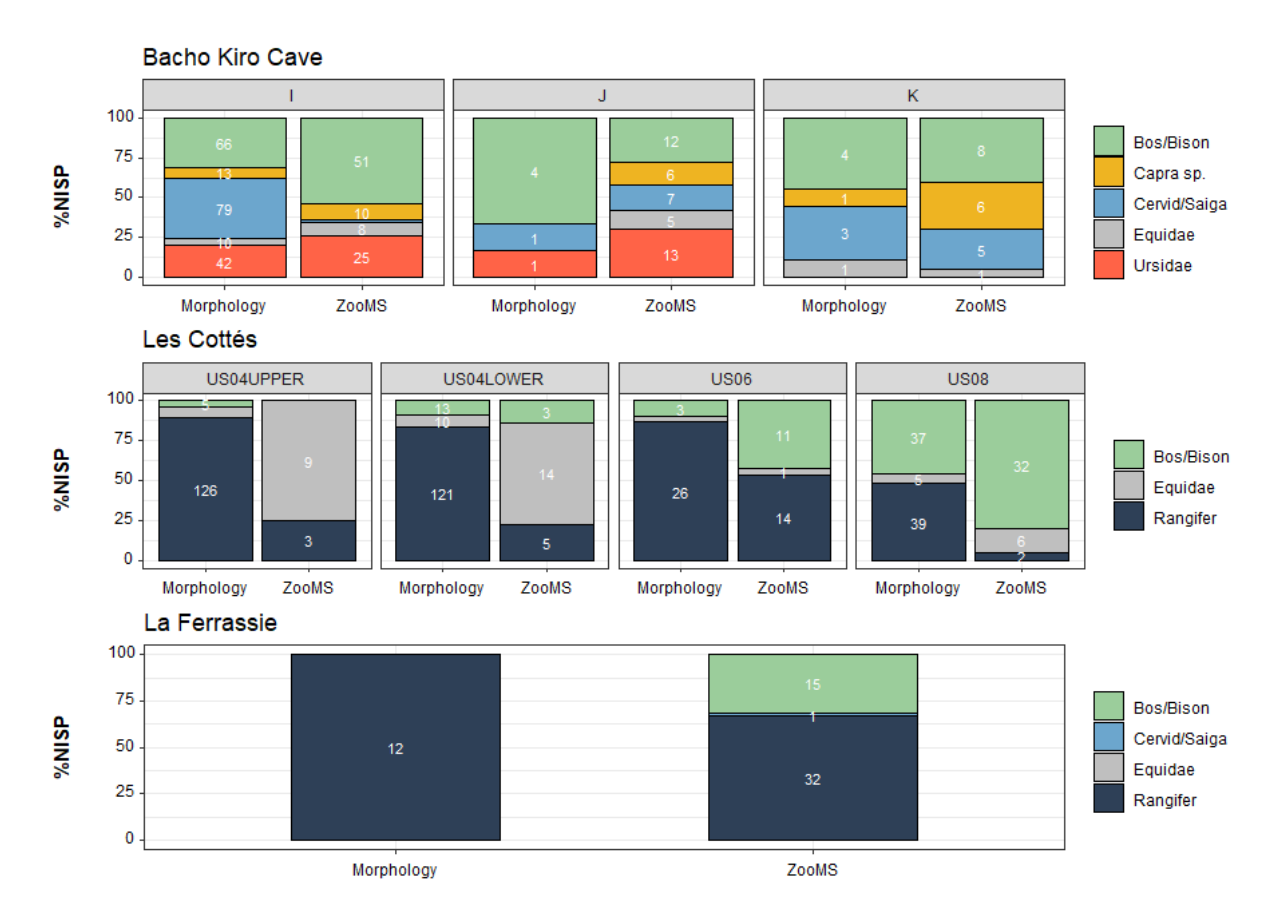
Readability - ZooMS US04UPPER US04LOWER US06 US08 100 75. 50 - Rangife Rangifer 25 . %NISP 0 -Readability - Morphology US04UPPER US04LOWER US06 US08 100 -75 50 - Rangifer Bos/Bisor Rangifer Bos/Bisor Bos/Biso Bos/Biso 25 . %NISP 75-100% 50-75% 25-50% 0-25%

Les Cottés

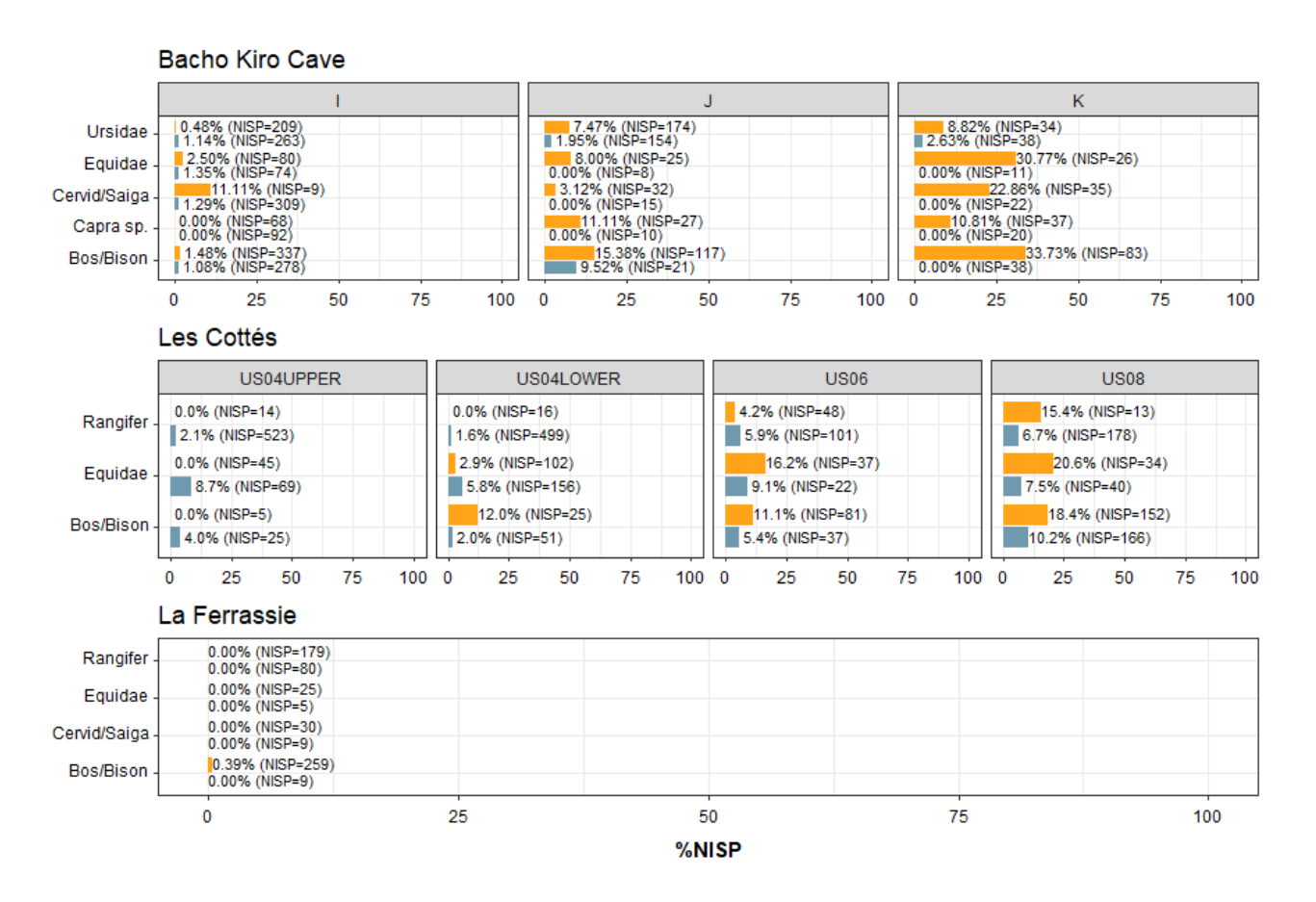
SI Figure 9: Percentage of readable bone surfaces (75-100% meaning 75-100% of the bone surface of the specimen is readable) for each dominant taxa from ZooMS and Morphology datasets from US04, US06 and US08 at Les Cottés.



SI Figure 10: Percentages of carnivore modifications on the dominant taxa within each method of identification and layers at Bacho Kiro Cave, Les Cottés and La Ferrassie. Numbers on the bars are the NISP of specimens showing carnivore modifications.

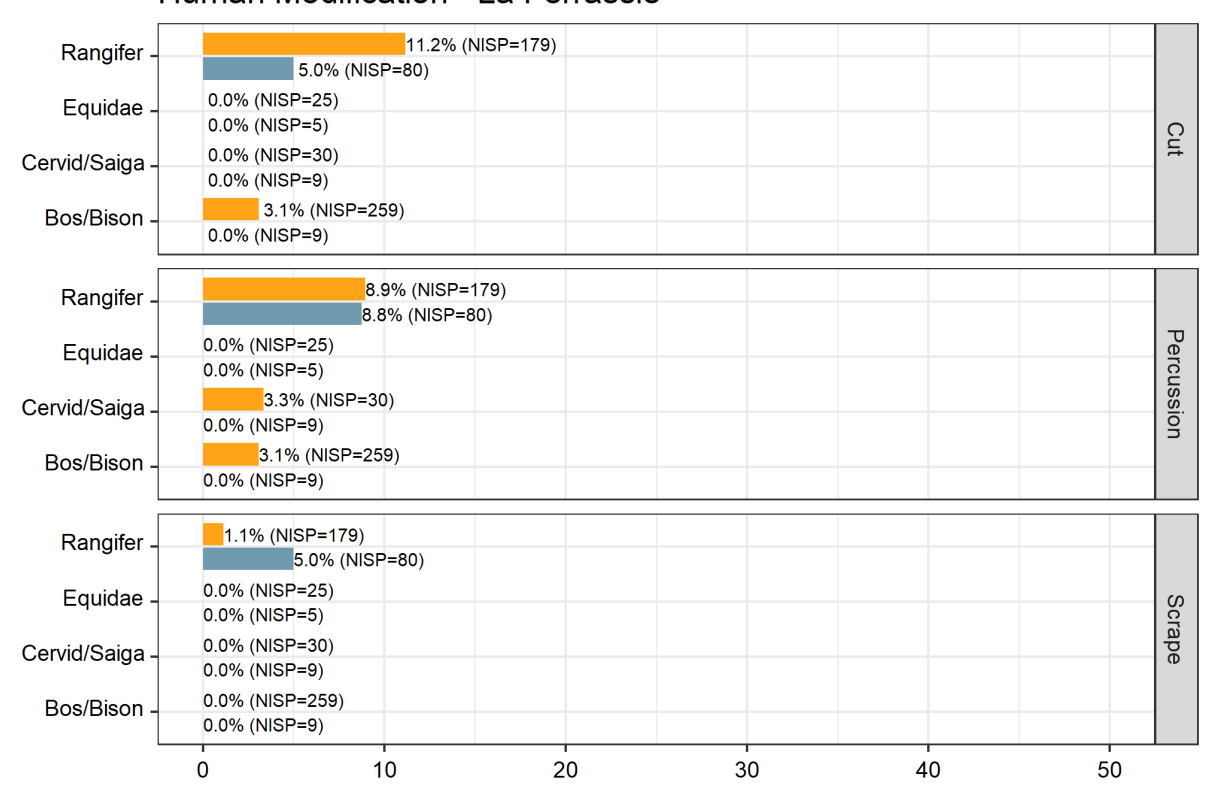


SI Figure 11: Percentages of anthropogenic modifications on the dominant taxa within each method of identification and layers at Bacho Kiro Cave, Les Cottés and La Ferrassie. Numbers on the bars are the NISP of specimens showing carnivore modifications.



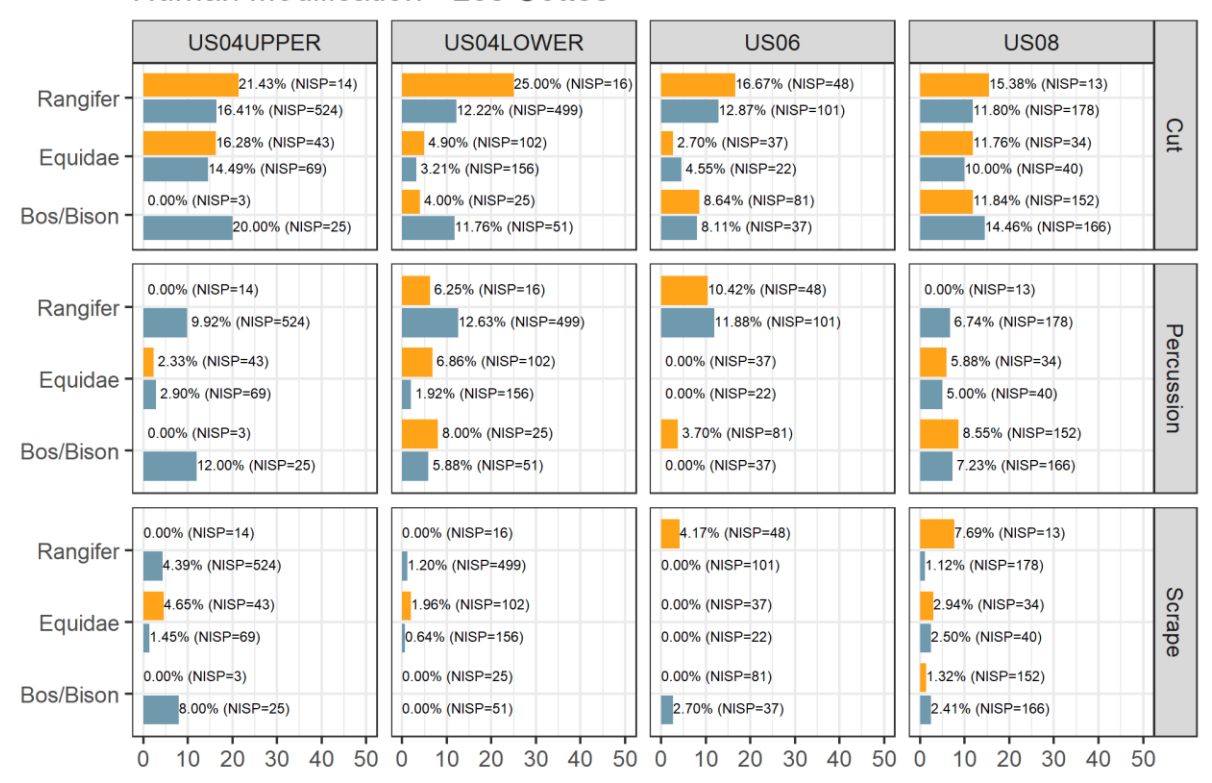
SI Figure 12: Percentages of carnivore modifications within the ZooMS (orange) and morphology (blue) datasets on the dominant taxa at Bacho Kiro Cave, Les Cottés and La Ferrassie. Numbers on the bars are the %NISP and total NISP of specimens identified for the taxon.

Human Modification - La Ferrassie



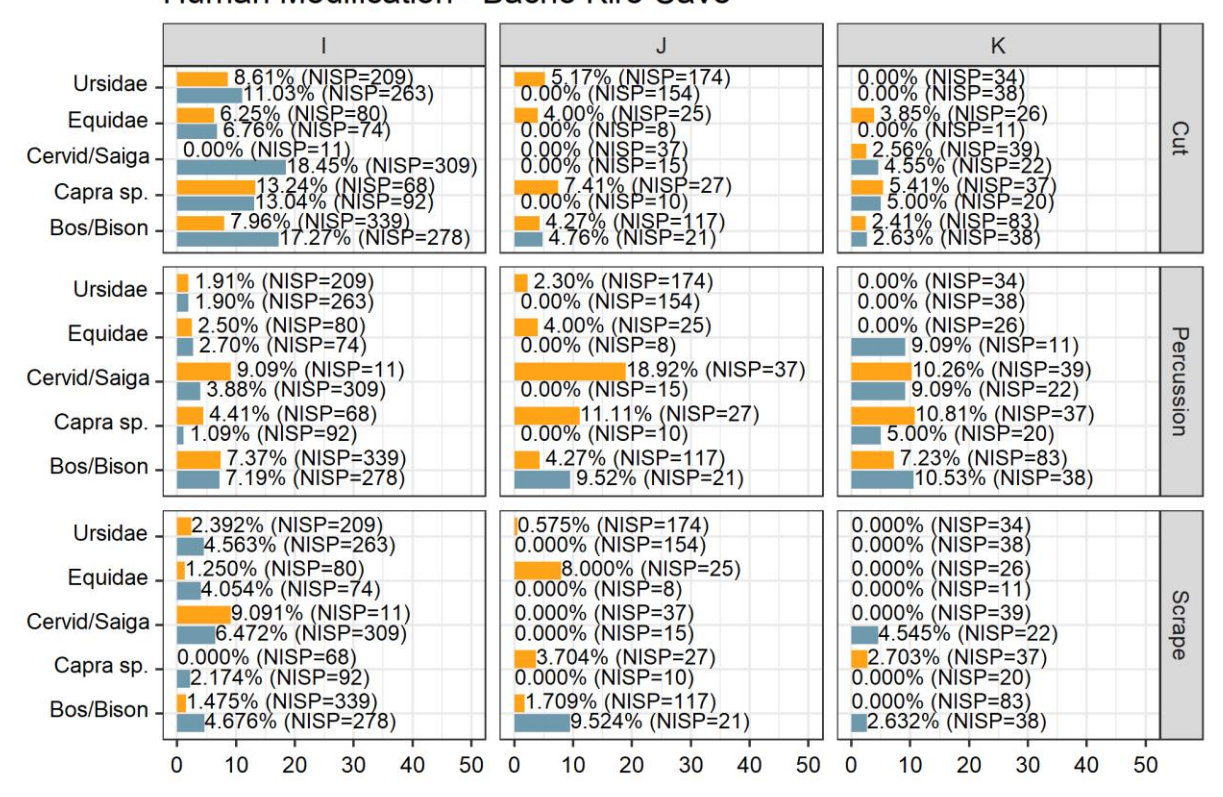
SI Figure 13: Percentage of specimens with human bone surface modifications (cut marks, percussion and scraping traces) across dominant taxa within ZooMS (orange) and Morphology (blue) datasets at La Ferrassie. Numbers on the bars are the %NISP and total NISP of specimens identified for the taxon.

Human Modification - Les Cottés

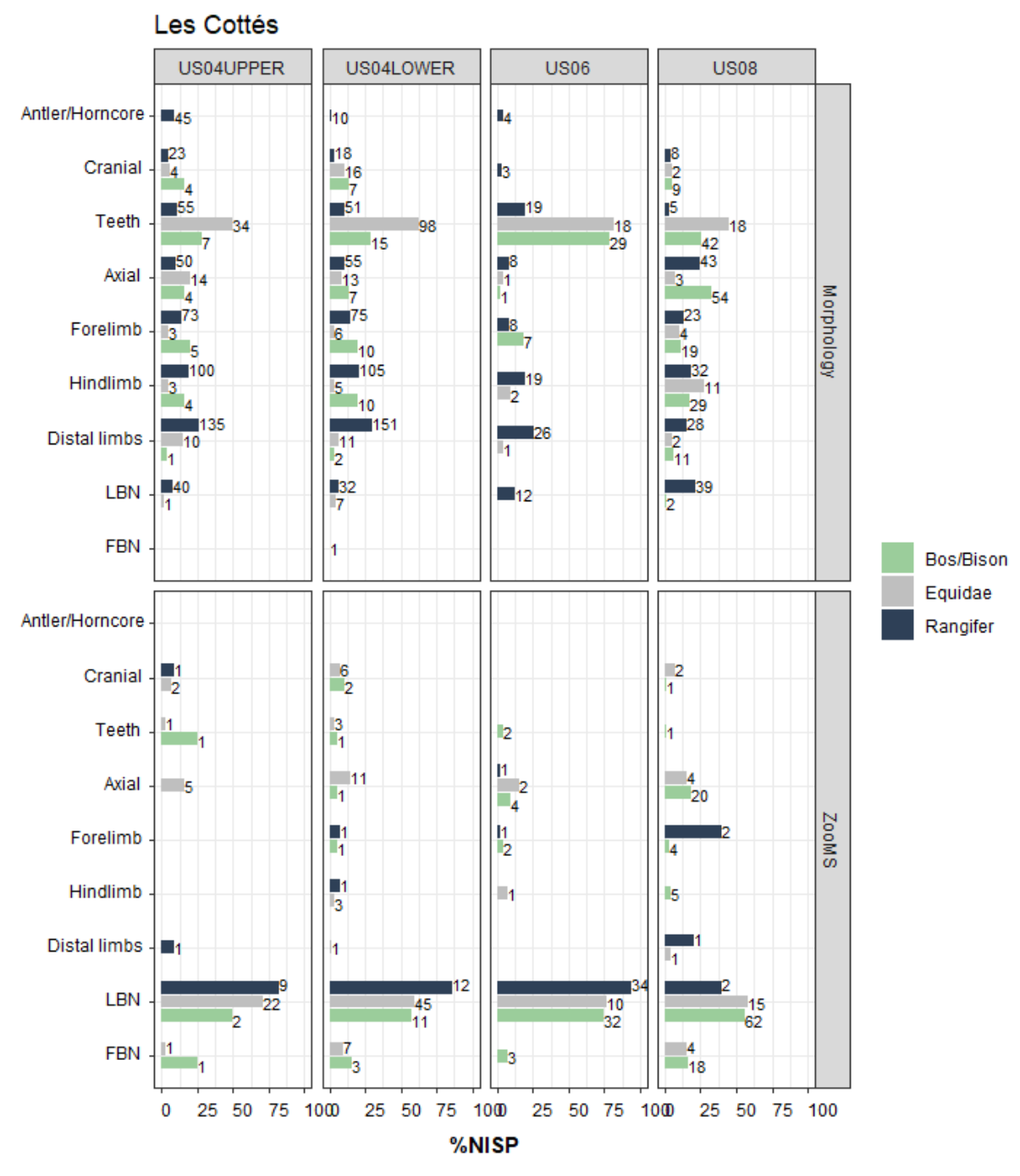


SI Figure 14: Percentage of specimens with human bone surface modifications (cut marks, percussion and scraping traces) across dominant taxa within ZooMS (orange) and Morphology (blue) datasets from US04 Lower, US06 and US08 at Les Cottés. Numbers on the bars are the %NISP and total NISP of specimens identified for the taxon.

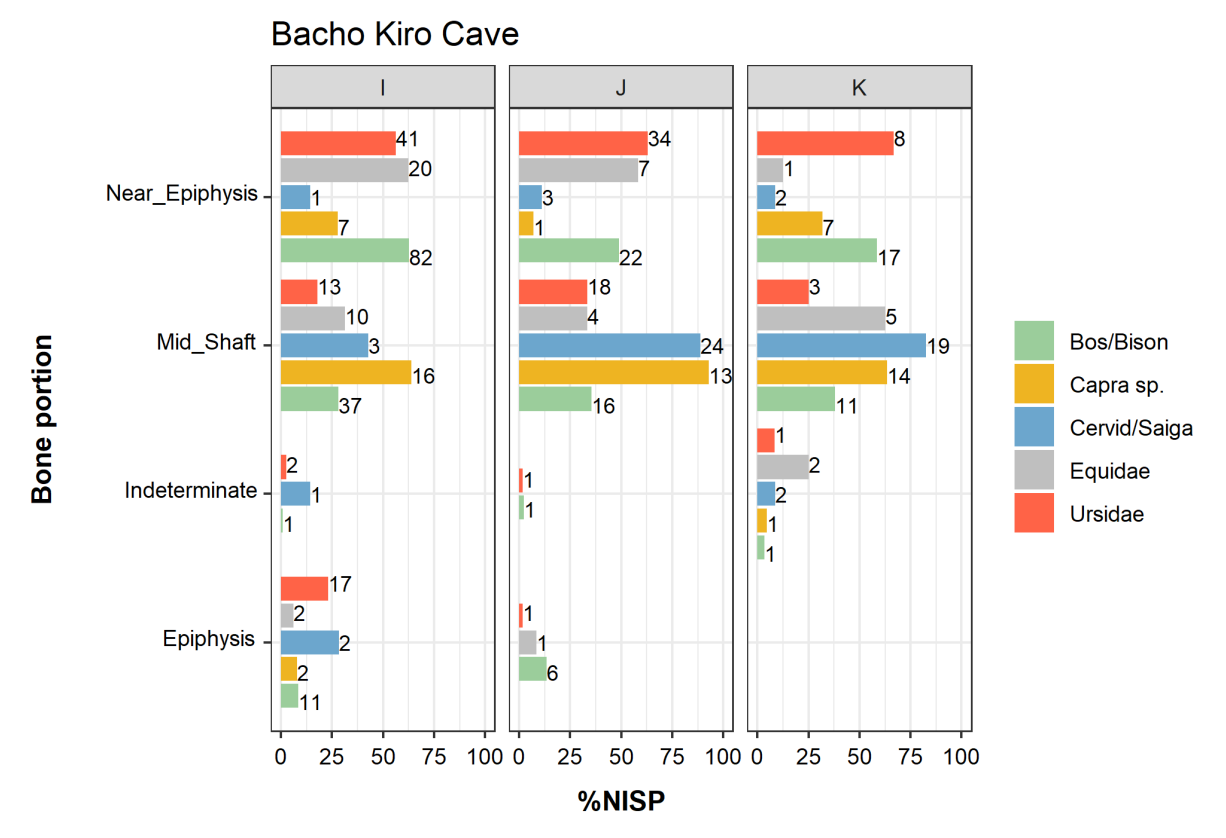
Human Modification - Bacho Kiro Cave



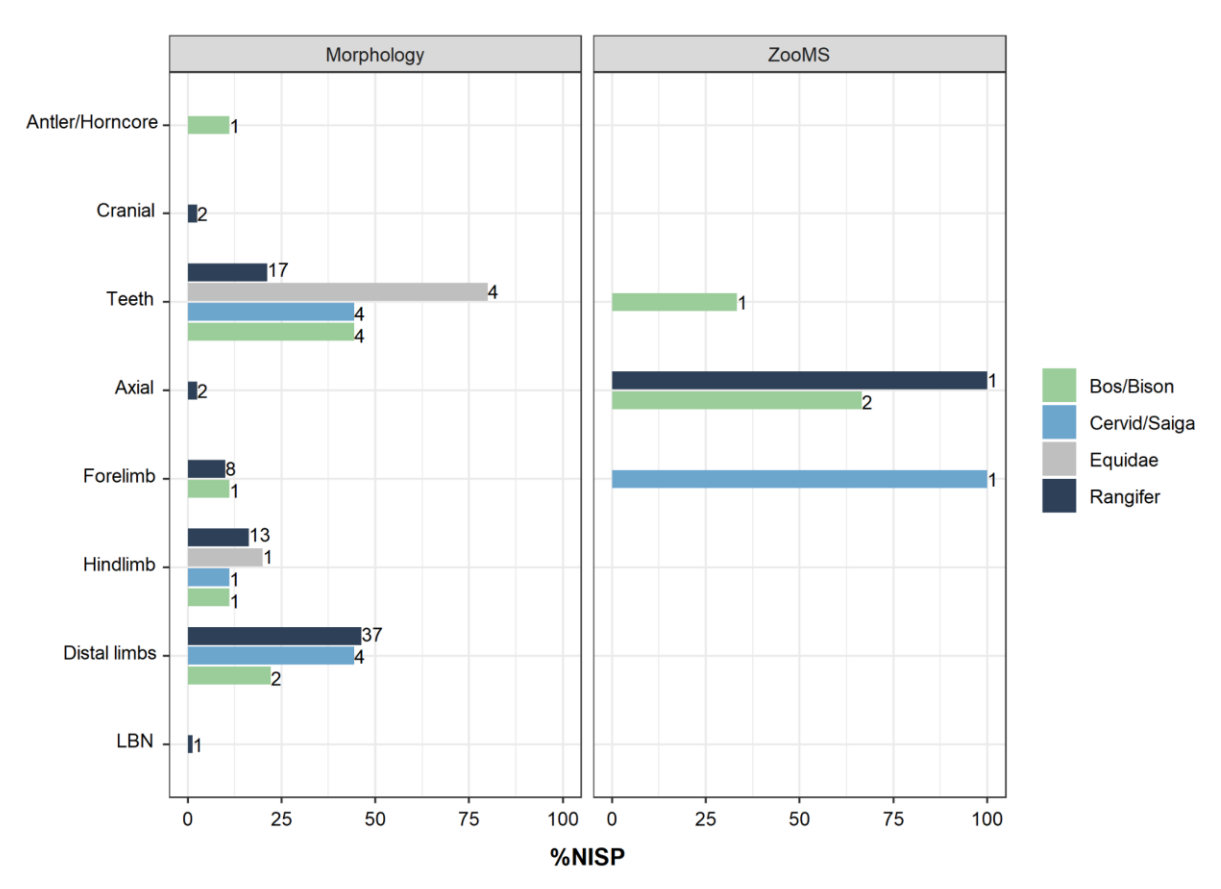
SI Figure 15: Percentage of specimens with human bone surface modifications (cut marks, percussion and anvil marks, and scraping traces) across dominant taxa among ZooMS (orange) and Morphology (blue) datasets from Layer I, J and K at Bacho Kiro Cave. Numbers on the bars are the %NISP and total NISP of specimens identified for the taxon.



SI Figure 16: Skeletal distribution of the bone specimens identified through morphology (top) and ZooMS (bottom) from the dominant taxa at Les Cottés. Numbers on the bars give the total NISP for each body part, layers and ID-method. Unidentified body parts (NID) were excluded from the plot. LBN: Long Bone fragment, FBN: Flat Bone fragment.



SI Figure 17: Distribution of the bone portions (Epiphysis, Near Epiphysis, Mid Shaft or Indeterminate) among the long bones (LBN) from the ZooMS component, between taxa and layers at Bacho Kiro Cave. Numbers on the bars of the graph correspond to the NISP for each category.



SI Figure 18: Skeletal distribution of the bone specimens identified through morphology (left) and ZooMS (right) from the dominant taxa at the site of La Ferrassie. Numbers within the bars give the total NISP for each body part and ID-method. Unidentified body parts (NID) were excluded from the plot. LBN: Long Bone fragment.

References

Berto, C., Krajcarz, M. T., Moskal-del Hoyo, M., Komar, M., Sinet-Mathiot, V., Zarzecka-Szubińska, K., Krajcarz, M., Szymanek, M., Wertz, K., Marciszak, A., & Others. (2021). Environment changes during Middle to Upper Palaeolithic transition in southern Poland (Central Europe). A multiproxy approach for the MIS 3 sequence of Koziarnia Cave (Kraków-Częstochowa Upland). *Journal of Archaeological Science: Reports*, 35, 102723.

Buckley, M., Harvey, V. L., & Chamberlain, A. T. (2017). Species identification and decay assessment of Late Pleistocene fragmentary vertebrate remains from Pin Hole Cave (Creswell Crags, UK) using collagen fingerprinting. Boreas.

Ruebens, K., Sinet-Mathiot, V., Talamo, S., Smith, G. M., Welker, F., Hublin, J.-J., & McPherron, S. P. (2022). The Late Middle Palaeolithic Occupation of Abri du Maras (Layer 1, Neronian, Southeast France): Integrating Lithic Analyses, ZooMS and Radiocarbon Dating to Reconstruct Neanderthal Hunting Behaviour. Journal of Paleolithic Archaeology, 5(1), 4.

Pothier Bouchard, G., Riel-Salvatore, J., Negrino, F., & Buckley, M. (2020). Archaeozoological, taphonomic and ZooMS insights into The Protoaurignacian faunal record from Riparo Bombrini. *Quaternary International: The Journal of the International Union for Quaternary Research*, *551*, 243–263.

- Sinet-Mathiot, V., Smith, G. M., Romandini, M., Wilcke, A., Peresani, M., Hublin, J.-J., & Welker, F. (2019). Combining ZooMS and zooarchaeology to study Late Pleistocene hominin behaviour at Fumane (Italy). *Scientific Reports*, *9*(1), 12350.
- Welker, F., Hajdinjak, M., Talamo, S., Jaouen, K., Dannemann, M., David, F., Julien, M., Meyer, M., Kelso, J., Barnes, I., Brace, S., Kamminga, P., Fischer, R., Kessler, B. M., Stewart, J. R., Pääbo, S., Collins, M. J., & Hublin, J.-J. (2016). Palaeoproteomic evidence identifies archaic hominins associated with the Châtelperronian at the Grotte du Renne. *Proceedings of the National Academy of Sciences of the United States of America*, 113(40), 11162–11167.
- Welker, F., Soressi, M. A., Roussel, M., Riemsdijk, I. van, Hublin, J.-J., & Collins, M. J. (2017). Variations in glutamine deamidation for a Châtelperronian bone assemblage as measured by peptide mass fingerprinting of collagen. *STAR: Science & Technology of Archaeological Research*, *3*(1), 15–27.
- Welker, F., Soressi, M., Rendu, W., Hublin, J.-J., & Collins, M. (2015). Using ZooMS to identify fragmentary bone from the Late Middle/Early Upper Palaeolithic sequence of Les Cottés, France. *Journal of Archaeological Science*, *54*, 279–286.